Development and Validation Trace Geosmin and 2-MIB Detection in Seawater: Application to Zeolite and Photocatalytic Treatment in Marine RAS Water

A thesis submitted in fulfilment

of the requirements for the degree

of

Master of Engineering

at

The University of Waikato

by

Gulmira Kasseneva

THE UNIVERSITY OF
WAIKATO
Te Whare Wānanga o Waikato

2026

Abstract

Taste and odour compounds such as geosmin (GSM) and 2-methylisoborneol (2-MIB) are a major challenge in marine recirculating aquaculture systems (RAS) because they are occur at trace ng/L levels in the water, accumulate in fish flesh and cause strong earthy off-flavours that reduce customer satisfaction and perceived product quality, while remaining difficult to remove and to measure reliably. This thesis addresses a combined analytical and treatment gap by developing and validating a GC-MS method for trace-level GSM and 2-MIB detection in seawater and applying it to evaluate zeolite-based adsorption and photocatalytic treatment options in marine RAS water.

A headspace solid-phase microextraction GC-MS (HS-SPME-GC-MS) method was developed, optimized and validated for artificial and real seawater matrices with a target detection limit below 10 ng/L. The final conditions used SIM mode, an internal standard, 3 g NaCl in 10 mL samples, 60°C and 30 min incubation, and 15 min extraction, achieving linear calibration with $R^2 > 0.99$ and limits of detection below 10 ng/L for both compounds. Systematic experiments revealed that matrix composition, organic content, competitive sorption on the fibre, incomplete SPME enrichment and analyte instability all significantly affected performance.

Using the validated method, batch experiments in artificial seawater at 1000 ng/L compared powder zeolite-Y, an immobilized TiO_2-zeolite coating with and without UV, and UV alone. Powder zeolite-Y achieved rapid and near-complete removal (about 95% for 2-MIB and 99% for GSM, with capacities ~ 7.5 ng/mg), while the TiO_2-zeolite coating with UV initially gave ~97-98% removal but declined on reuse.

Overall, the work shows that trace-level GSM and 2-MIB in seawater are challenging to manage because of low concentrations, volatility and SPME limitations, but that a carefully controlled HS-SPME-GC-MS method combined with zeolite-based adsorption provides a practical basis for monitoring and reducing these off-flavour compounds in marine RAS water.

Acknowledgment

I would like to express my thanks to supervisors, Mark Lay and Chanelle Gavin, for giving me the chance to carry out this research and for their guidance, encouragement, and feedback throughout my master's studies. I am also very grateful to the laboratory technical officer, Steven Wu, and the advanced technical officer, Jenny Stockdill, for their practical support, expertise, and patience in helping me with experimental setup, sample preparation, and instrument troubleshooting. Special thanks go to Simon Muncaster for arranging and providing the samples that were essential for this work. I would also like to acknowledge the wider faculty and administrative staff of the Engineering School and Library for their assistance, resources, and a supportive research environment. Finally, I am also especially grateful to my family and friends for their unwavering support, understanding, and encouragement, which made it possible for me to complete this thesis.

Authorship

I confirm that I am the sole author of this thesis and that it is based on my own original research. It does not include any material that has been previously published or written by another person.

This thesis involved the use of AI based tools, including Perplexity and Grammarly, to support the writing process. These tools were used particularly for improving clarity, refining grammar and exploring ways to articulate complex ideas.

All conceptual contributions, experiments, analysis and interpretations are the author's own work, and all necessary steps were taken to maintain University academic integrity.

Table of Contents

List of Figures

List of Tables

Chapter 1

1.1 Background

Aquaculture currently supplies close to half of all fish consumed globally, with demand expected to grow as wild stocks decline (*Home | Plant Production and Protection | Food and Agriculture Organization of the United Nations*, n.d.). Land-based Recirculating Aquaculture Systems (RAS) have developed as a sustainable production model, continuously treating and reusing water to reduce consumption and enable controlled growth year-round (Davidson et al., 2014).

New Zealand has committed to expanding this sector as part of its blue economy strategy. Currently, land-based recirculating aquaculture systems in New Zealand are limited in scale and are mainly used in research and early commercial applications (e.g. NIWA's operational kingfish facility in Northland) with government-backed investment plans extending through 2035 (*Aquaculture Plan Key to Economic Growth | Beehive.Govt.Nz*, n.d.).

1.2 Off-Flavours in RAS: Geosmin and 2-MIB

A critical water quality problem in RAS is the build-up of geosmin (GSM) and 2-methylisoborneol (2-MIB). These trace-level secondary metabolites are produced by actinobacteria and cyanobacteria on biofilter surfaces (Abd El-Hack et al., 2022; Lawton et al., 2003). Both compounds impart a strong earthy or musty off-flavour to fish flesh at concentrations in the low ng/L range, rendering products commercially unacceptable before any physical deterioration is visible.

The standard industry practice for managing off-flavours in RAS is depuration, which means moving fish to fresh, odour-free water and not feeding them for about ten days before harvest. This approach is costly, delays product delivery, raises animal welfare concerns due to feed withdrawal (Davidson et al., 2024), and does not remove geosmin and 2-MIB from the recirculating water itself (Lindholm-Lehto & Vielma, 2019). Currently there is no widely adopted, efficient purpose-designed geosmin and 2-MIB removal method for operating RAS reported in the literature (Davidson et al., 2014), and eliminating geosmin (Wee et al., 2015) and 2-MIB from water remains technically challenging due to its detection at extremely low concentrations. Consequently, treatment and control solutions for these compounds are being actively investigated worldwide.

1.3 Human Detection Thresholds and Target Concentration

While there are no established standards for geosmin and 2-MIB limit concentrations for RAS systems, published sensory studies report odour detection thresholds for geosmin in drinking water ranging from 3.8 to 9.5 ng/L, and for 2-MIB between 15 and 45 ng/L. Concentrations below 10 ng/L and 15 ng/L, respectively, generally considered acceptable (Howgate, 2004; Polak & Provasi, 1992; Tucker, 2000; Young et al., 1996). This aligns with regulatory monitoring thresholds in Australia (*Australian Drinking Water Guidelines | NHMRC*, n.d.) and South Korea (Kim et al., 2015), and on this basis 10 ng/L was selected as the target trace-level concentration for this study.

1.4 Treatment Approaches: State of Knowledge and Gaps

Ozonation, activated carbon, and UV photolysis have demonstrated effective GSM and MIB removal, ozone-peroxide achieving 93% and 77% removal of GSM and MIB respectively in a RAS (Azaria et al., 2021), and powdered activated carbon up to 90% for both compounds (Yan, 2016). However, these results are predominantly based on freshwater systems, and performance in seawater, where higher ionic strength alters oxidation chemistry and reduces adsorption capacity, is largely unknown. Commercial hybrid systems exist but are patent-protected, their data unpublished, and their costs prohibitive for independent evaluation (Davidson et al., 2014).

This research focuses on two accessible treatment alternatives identified through a thorough literature review. The first is powdered zeolite Y, a low-cost microporous adsorbent that has been shown to have promising adsorption of GSM and 2-MIB in drinking water and freshwater (Ellis & Korth, 1993) aquaculture, but has not been systematically evaluated in seawater matrices. The second is UV photocatalysis using an immobilized zeolite-TiO_2 composite coating, which combines zeolite's adsorptive capacity with the ability of TiO_2 photocatalysis to generate hydroxyl radicals for oxidative degradation (Lawton et al., 2003; Wee et al., 2015). To isolate individual contributions, this work compares four conditions: powder zeolite only, UV only, composite coating without UV and composite coating with UV.

1.5 Analytical Detection: Gaps in Published Methods

GC-MS with headspace SPME pre-concentration is the established technique for trace-level GSM and MIB analysis, achieving detection limits of 1-10 ng/L under optimized conditions (L. Wang et al., 2025; You, 2012). However, all published validated methods were developed for freshwater or drinking water. Seawater significantly alters headspace partitioning and SPME fibre efficiency. Prior University of Waikato work showed salt addition alone reduced peak areas by up to 40% (Yan, 2016). Additional challenges include analyte adsorption onto sampling equipment, vaporization under storage and handling, and the absence of any published data about SPME fibre enrichment in high-salinity matrices. Because no complete, validated GC-MS method for trace-level GSM and MIB in seawater is available in the published literature, the performance of treatment methods in saline matrices cannot be reliably quantified. This creates a circular research gap: treatment efficacy studies cannot be robustly conducted without a seawater-validated analytical method, yet the need for the method is driven by the treatment research objective. Therefore, the primary objective of the thesis is to develop and validate the detection method which can be applied to quantify treatment efficiencies.

1.6 Research Objectives

The main aim of the study is to develop and apply a GC-MS-based analytical and treatment assessment framework for GSM and MIB in marine RAS seawater. The objectives are:

- To develop, optimize and validate a GC-MS method for quantifying GSM and MIB in marine water matrix at target concentration identified from literature review, with key instrument and SPME extraction parameters.

- To test method performance in real seawater samples with a focus on seawater-specific matrix effects and analyte stability relevant to routine monitoring.
- To comparatively evaluate GSM and MIB removal under four laboratory-scale conditions (zeolite-TiO_2 composite with UV, powder zeolite alone, UV alone, and composite without UV) and to identify the most promising treatment option for RAS.

1.7 Thesis Structure

This thesis is organized into five chapters. Following this introduction, Chapter 2 presents a literature review covering aquaculture and RAS development, the occurrence and impacts of GSM and MIB, analytical detection methods, and treatment strategies reported in the literature. Chapter 3 describes the materials and methods used in this research, including seawater preparation, GC-MS and SPME configurations, and the experimental setups for zeolite adsorption and immobilized zeolite-TiO_2 composite UV photocatalysis. Chapter 4 presents the results and discussion, integrating method development and validation data, treatment performance, and a critical analysis of the limitations and practical challenges of the developed analytical method and treatment approaches. Chapter 5 summarizes the main conclusions and provides recommendations for future work, including methodological improvements and considerations for scaling the treatment options to marine RAS applications.

Chapter 2

This chapter reviews the existing literature relevant to this study. It begins with an overview of aquaculture globally and in New Zealand, recirculating aquaculture systems (RAS) and associated water quality challenges. Then the occurrence, sources, and sensory impact of geosmin and 2-MIB in aquaculture systems are discussed, followed by a review of analytical methods used for their detection, with a focus on GC-MS and SPME extraction techniques. Finally, current treatment approaches for geosmin and 2-MIB removal, including adsorption and photocatalysis, are examined.

2.1. Aquaculture

2.1.1 Aquaculture Globally

Protein is an essential component of food ingredients consumed by humans. Median protein intake in American population ranges from 13.4% to 16.0% of the calories consumed (*National Health and Nutrition Examination Survey - an Overview | ScienceDirect Topics*, n.d.).

Over the years, aquaculture has been recognized as a major source of sustainable protein globally (Little & MacKenzie, 2023). Aquatic products are an important source of high-quality protein, are rich in polyunsaturated fatty acids, and offer substantial nutritional value. Moderate consumption can reduce the risk of diabetes in adults and benefit the development of infants and young children. Aquatic products are also a vital component of a balanced diet (Zhao et al., 2025).

Aquaculture is playing a crucial role in contributing to food security and human nutrition; this is especially important with anticipated global population growth (Ahmed & Turchini, 2021). Aquaculture is the mostly rapidly growing food production

industry in the world, and production has increased by over 600% since 1990 (*Home | Plant Production and Protection | Food and Agriculture Organization of the United Nations*, n.d.). Global demand for aquatic foods has grown steadily over the past several decades, with consumption rising faster than population growth. Per-person intake has roughly doubled since the 1960s, increasing from about 10 kg per year to just over 20 kg by 2019. Looking ahead, factors such as higher incomes, expanding urban populations, better handling and storage after harvest, and shifts in dietary preferences are expected to drive aquatic food consumption to levels around 15% higher by 2030 (Ruben et al., 2025).

2.1.2 New Zealand aquaculture

For New Zealand, aquaculture is a key part of economic wealth. It is concentrated in several key regions, with the Marlborough Sounds, Coromandel Peninsula, Northland, and Tasman and Golden Bay. It has the potential to boost New Zealand's economy, contribute to the job market, and support regional communities. The Aquaculture Development Plan for 2025-2030 estimates that this industry will grow to $3 billion by 2035. Currently, the industry's revenue is over $760 million, and it employs over 3,000 people. According to Oceans and Fisheries, Regional Development and Resources Minister H. S. Jones, aquaculture is a primary industry crucial to the nation's prosperity and demonstrates the Coalition Government's commitment to delivering a bigger and better aquaculture sector for New Zealand (*Aquaculture Plan Key to Economic Growth | Beehive.Govt.Nz*, n.d.).

Optimizing the sustainable production of seafood in aquaculture is a main part of what NIWA (the National Institute of Water and Atmospheric Research) does, and their research will play a great role in helping the government reach its ambitious target (*Our Mission | Earth Sciences New Zealand | NIWA*, n.d.).

Given the environmental concerns and the susceptibility of fish production to climate change and other environmental factors, one favoured adaptation strategy is the use of Recirculating Aquaculture Systems (RAS) (Ahmed et al., 2019). RAS enables raising fish indoors on land in controlled environments, reducing straightforward interfaces between production and the environment.

Recirculating Aquaculture Systems form the technological basis of the present study and are discussed in detail in the following section.

2.2 RAS

RAS are environmentally friendly, water-efficient and rigorous farming systems that are highly productive. They do not cause negative environmental impacts like habitat damage, water body pollution, eutrophication, biotic reduction, or environmental interruptions involving biodiversity due to escape of captive fish and exotic species. Additionally, they help prevent both infection outbreaks and the spread of parasites (Ahmed & Turchini, 2021).

2.2.1 Fundamental principles of RAS operation and production

RAS are fish farms that are located onshore, and often indoors, where fish are kept in tanks within a managed condition. Water is filtered to remove waste before being recirculated, using mechanical, biological filtration, sterilization, and oxygenation (Figure 1) (Ahmed & Turchini, 2021). Although setups vary in sophistication and efficiency, most RAS reuse over 90% of the wastewater (Badiola et al., 2018; D. R. Murray, 2014). They offer prospects to improve waste management, minimize water use, and enable nutrient reuse (Martins et al., 2010; D. R. Murray, 2014). While originally developed for fresh and warm water species like channel catfish, striped bass,

and tilapia, RAS can be adapted for brackish, marine, and cold-water species (Helfrich & Libey, n.d.). By separating fish production from the sea environment, RAS can be an alternative to conventional net-pen aquaculture (Ahmed & Turchini, 2021). RAS also creates appropriate settings for sensitive fish species (Zhang et al., 2011).

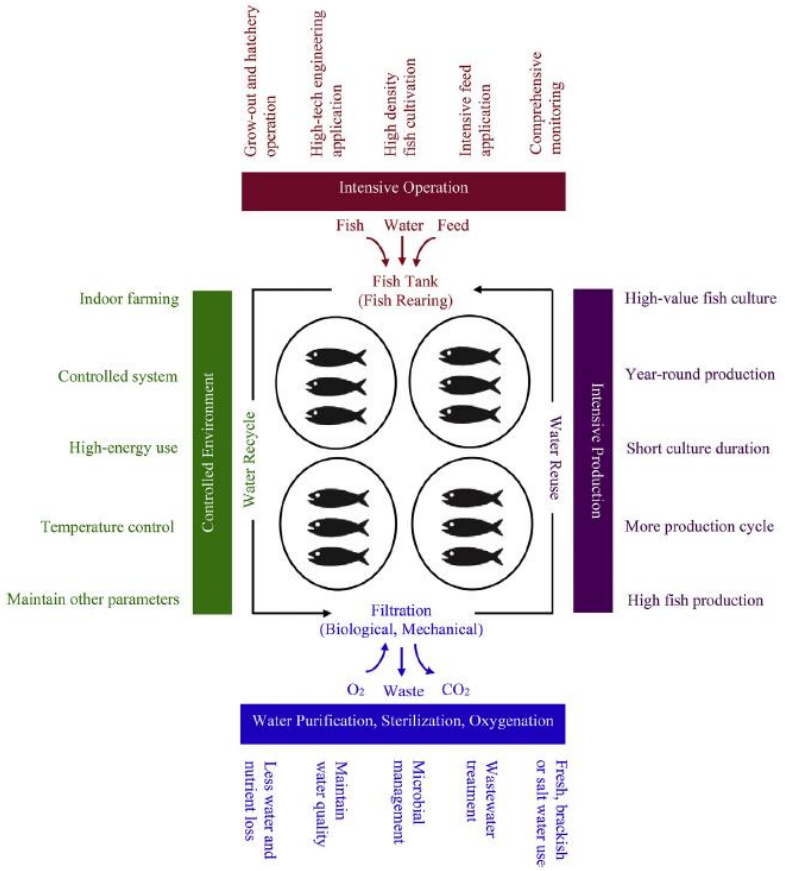

Figure 1 A generalized form of RAS for fish production (Ahmed & Turchini, 2021).

Although capable of producing various seafood, they are mainly used for highly valuable fish such as barramundi, catfish, eel, perch, prawn, salmon, seabass, seabream, shrimp, sturgeon, trout, and tuna - often stocked densely with production running year-round to cover operational costs (Dalsgaard et al., 2013; Martins et al., 2010; D. R. Murray, 2014). Other species like arctic char, clarias, halibut, pangasius, tilapia, and turbot are also common in RAS (Badiola et al., 2018; Summerfelt & Vinci, 2008). Species selection is usually driven by market demand for profitability (Badiola et al.,

2017) and depends on rapid growing, hardy fish suited for RAS systems (Badiola et al., 2018).

2.2.1.1 RAS Components

As shown in the figure below, a typical RAS system consists of a primary water intake for fresh water and one or more fish tanks. The first step in RAS water treatment is sedimentation, which removes settleable solids such as fish faeces, uneaten feed, and bacterial flocs. The water then flows to mechanical filtration, such as sand filtration, to remove what has not been removed by sedimentation (Molleda, 2007). Next, the water flows to a nitrification biofilter to oxidize ammonia emitted by the fish into nitrate. An aerator or low-head oxygenator is used to separate carbon dioxide produced by the fish and to add oxygen needed by the fish and nitrifying bacteria. Auxiliary facilities could be added if required, depending on water quality to enhance the performance of the RAS or to monitor and control physicochemical parameters in the system. For example, this could include UV disinfection, ozonation, pH regulation, heat exchange, or denitrification. The specific design of these functional components differs between the different technology providers (Balami, 2021).

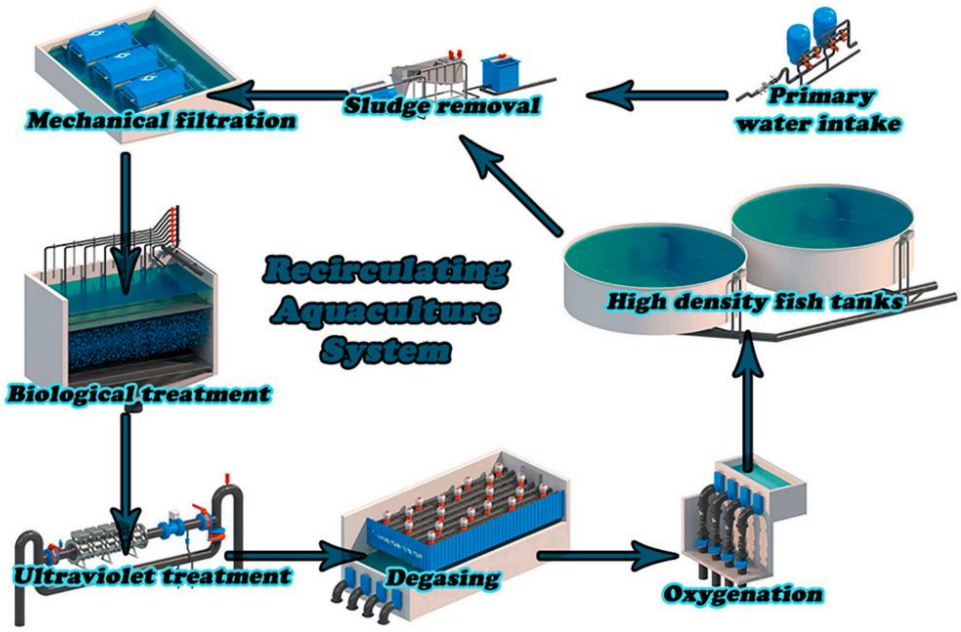

Figure 2 Recirculating aquaculture system (RAS) components (Abd El-Hack et al., 2022).

2.2.1.2 RAS Advantages and disadvantages

An indoor fish farming in RAS has several major advantages over conventional aquaculture (Gupta et al., 2024):

1) It is suitable for areas with limited water resources as it treats and recycles water, thus requiring much less water than in flow-through system.

2) Due to high stocking density, it requires significantly less surface area.

3) Water parameters such as temperature, dissolved oxygen, carbon dioxide (CO_2), total ammonia nitrogen, and nitrate levels can be maintained; thus, water quality is controlled in the RAS.

4) Its environmental biosecurity is increased with better-controlled feed water quality.

In addition, there are numerous environmental advantages such as better waste management opportunities, power use for heat exchange, lowered CO_2 emissions with logistics improvement, biological pollution prevention from escapees, and recycling

nutrients. All these advantages make RAS a more sustainable and eco-friendly alternative for fish farming (Gupta et al., 2024).

The establishment of functional RAS operations requires significant capital investment for the equipment, infrastructure, feed water and wastewater treatment systems, engineering, construction, and management. Also skilled and knowledgeable workforce is paramount. (Balami, 2021). In one Atlantic salmon comparison, the modeled land-based closed containment RAS needed about US$54 million in capital versus US$30 million for the open net-pen system (Y. Liu et al., 2016).

Furthermore, one key challenge is disease prevention and treatment, as the same water is recirculated continuously. Accumulated organic matter from uneaten feed and fish waste fosters microbial growth that deteriorates water quality which is another potential cause of the infections and health issues of the fish (Aich et al., 2020). Even after water is reused, pathogens remaining in the biofilm can impact the fish's health and cause potential risk to public health (Dalsgaard et al., 2013).

2.2.2. RAS in NZ

The first commercial-scale RAS in New Zealand is the latest development at the NIWA Northland Aquaculture Centre. This system is designed to demonstrate sustainable, high-density (over 100 kg/m^3) finfish (yellowtail kingfish) production while minimizing environmental impact through advanced water treatment and recirculation. The system is flexible and can be customized for different species and locations (*Recirculating Aquaculture Systems | Earth Sciences New Zealand | NIWA*, n.d.).

Geosmin and 2-MIB accumulation has been identified as a key water quality challenge in RAS environments, including the NIWA facility, as these compounds impart earthy and musty off-flavours to fish flesh even at trace concentrations. The following section reviews the nature, sources, and behaviour of these compounds in aquaculture systems.

2.3. Geosmin and 2-MIB

Unpleasant tastes and odours, known as off-flavours in aquaculture products, significantly affect market demand and customer acceptance in the industry (Tucker, 2000). The most common off-flavour is a musty, earthy smell caused by geosmin and 2-methylisoborneol (2-MIB) (Abd El-Hack et al., 2022; Suffet et al., 1999). Off-flavours result from the existence of specific metabolites, including aliphatic hydrocarbons, sulfur compounds, aldehydes, ketones, and especially geosmin and 2-MIB (Jüttner, 1988). These compounds are generated by various species of streptomyces or actinobacteria (Gerber & Lechevalier, 1965), cyanobacteria, and myxobacteria (Dickschat et al., 2005). Other microorganisms like fungi (Smith et al., 2008) and the amoeboid protist *Vannella* spp. (Hayes et al., 1991) can also produce geosmin and 2-MIB. As mentioned by Lindholm-Lehto and Vielma (2019) the main sources of earthy-musty substances in RAS are the biological membranes in the biofilters and bio-floc or biofilm in the tanks, as the RAS environment is rich in nutrients and the biofilm is an ideal place for bacterial growth. Chemical arrangements of these compounds are illustrated in Figure 3 below.

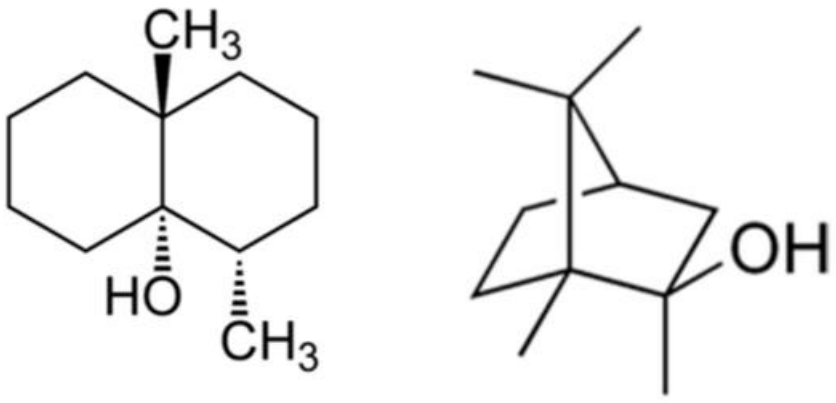

Figure 3 Chemical assembly of geosmin (GSM, left) and 2-methylisoborneol (2-MIB, right) (Zorzi et al., 2023).

Geosmin and 2-MIB are tertiary alcohols and both exist as (+) and (−) enantiomers. The reason for odour issues is the biological production of the naturally occurring (−) compounds (Jüttner & Watson, 2007). "Both compounds are highly potent in impairing flavour, with geosmin described as having a muddy and earthy smell, while 2-MIB is characterized by musty, camphor-like, mouldy, and basement-like odours" (Suffet et al., 1999). Both are absorbed from water into the fish through gills, skin, and intestinal tract by fatty flesh, with the gills being the main method of uptake (Howgate, 2004). Being lipophilic these compounds accumulate in fat-rich tissues (Persson et al., 2007) until an equilibrium state is achieved between the water phase and the fish. The primary factors influencing the concentration of substances in fish flesh are their levels in water and the duration of exposure, as well as specific variables such as fish species (notably fat content), water temperature, size, and age of the fish (Howgate, 2004; Percival et al., 2008).

Although the economic impact from these off-flavours is considered as the major challenge for commercial aquaculture production globally, they do not affect fish health and growth (Tucker, 2000).

2.3.1 Sources of GSM and 2-MIB and factors affecting their presence in aquaculture

GSM and 2-MIB are generated as by-products of growth and metabolism in cyanobacteria and certain actinomycetes and are also formed in small amounts by green algae, diatoms, fungi, and slime moulds, as shown in Figure 4.

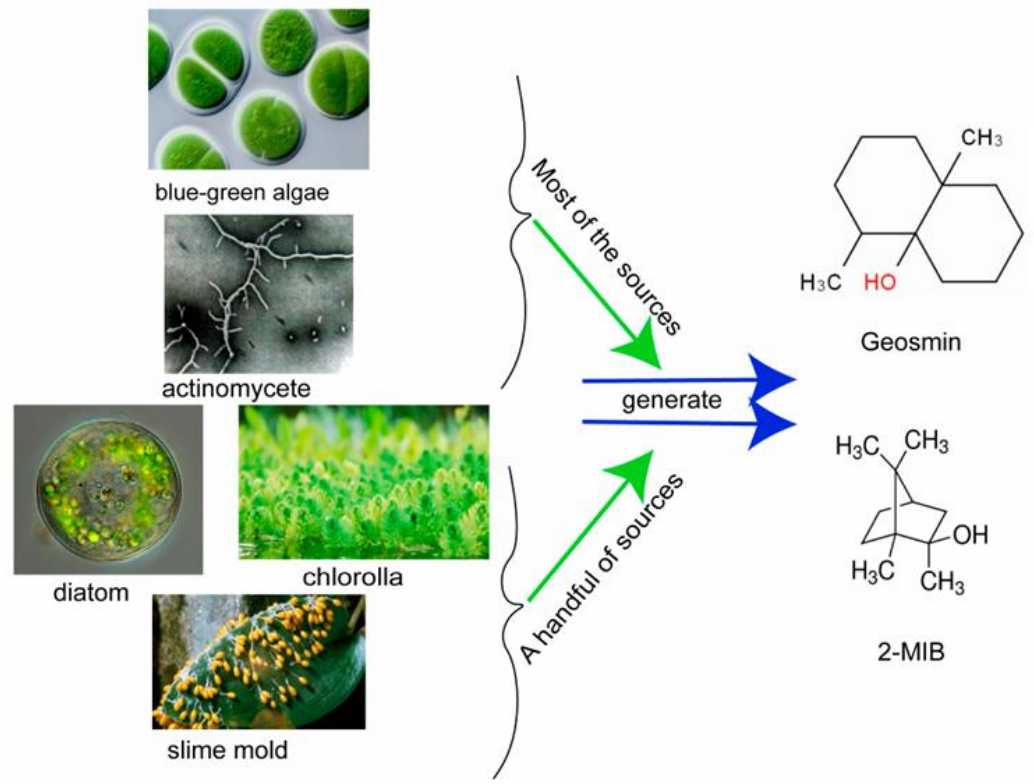

Figure 4 GSM and 2-MIB producers (M. Wang et al., 2025).

In traditional pond farming systems, odour compounds are often associated with actinomycetes and cyanobacteria activity. Especially in nutrient-rich and well-lit outdoor ponds, cyanobacterial proliferation may lead to the formation of GSM and 2-MIB. In RAS, the formation of biofilm provides an ideal environment for actinomycetes to grow due to the abundance of nutrients in the aquaculture water. Actinomycetes were reported as the main producers of odorous compounds in RAS (Abd El-Hack et al., 2022) during non-algae bloom (M. Wang et al., 2025). Furthermore, factors such as phosphates (Oh et al., 2017), nitrates (Clercin & Druschel, 2019), and dissolved oxygen (Jiadong et al., 2009) in the system have been confirmed to have significant effects on the formation of GSM and 2-MIB.

The occurrence of off-flavours is closely linked to water quality. The biomass of earthy and musty substances (EMS) producers in RASs can be controlled by adjusting the proportion of nutrients in water by physical, chemical, or biological methods.

2.3.2 Concentrations of Geosmin and 2-MIB

Geosmin odour detection threshold in water was 3.8 ng/L by humans while another study determined it to be 5 ng/L (Srinivasan & Sorial, 2011; Young et al., 1996), while (Polak & Provasi, 1992) identified the odour limits for (-) geosmin as 9.5 ng/L.

The odour human detection level for 2-MIB in water was greater, between 15 and 45 ng/L (Tucker, 2000; Young et al., 1996). This indicates a three- to four-fold deviation in reported limit values for geosmin compared with 2-MIB (Howgate, 2004). Such difference is understandable, given that sensory evaluation is subjective and different studies may have employed varying methods to determine thresholds. Generally, geosmin levels below 10 ng/L and 2-MIB levels below 15 ng/L are considered not problematic (Howgate, 2004).

Beyond aquaculture, GSM and 2-MIB are recognized as drinking water contaminants where cyanobacterial blooms affect surface supplies. The Australian Drinking Water Guidelines (ADWG) set an operational trigger of 10 ng/L for both compounds at the treatment plant outlet, requiring activated carbon dosing above this level (*Australian Drinking Water Guidelines | NHMRC*, n.d.). South Korea, where seasonal blooms in the Han and Nakdong rivers cause recurring taste-and-odour incidents, applies a monitoring recommendation of 20 ng/L (Kim et al., 2015). Based on the evidence above and given that no established universal standard exists for RAS water systems, 10 ng/L was selected as the minimum trace-level concentration detectable by most humans and was therefore adopted as the analytical threshold of interest in this study.

The reason of the widely different levels are operational variations and sampling time within the production period (Azaria & Van Rijn, 2018). It was also observed that concentrations of GSM and 2-MIB in the water are not consistently correlated with the concentrations detected in the fish tissue, as shown in the Table below.

Given their lipophilic nature, extremely low odour thresholds, and tendency to accumulate in fish tissue, the accurate detection and quantification of GSM and 2-MIB in both water and fish flesh requires specialized analytical methods, which are reviewed in the following section.

Table 1 Average concentrations of geosmin and 2-MIB in culture water and fish in RAS (Azaria & Van Rijn, 2018).

Fish species	**Culture water (ng/L)**		**Fish fillet (µg/kg)**		**Reference**
	GSM	2-MIB	GSM	2-MIB	
Hybrid Tilapia	10-75	40-175	N/A	N/A	(Guttman & van Rijn, 2008)
Rainbow trout	1-3	1-14	0.05-0.38	0.01-0.05	(Schrader et al., 2010)
Arctic char	30.5	1	0.7	0.008	(Houle et al., 2011)
Rainbow trout	6.6-36.1	3.2-28.5	0.1-2.4	0.01-0.55	(Petersen et al., 2011)
Atlantic salmon	7-29	132 ± 13.2	0.2-0.3	0.09 ± 0.03	(Burr et al., 2012)
Rainbow trout	5-70	1-7	0.07-0.37	0.01-0.03	(Schrader et al., 2013)
Rainbow trout	2-15	Not detected	3-5	Not detected	(Sarker et al., 2014)
European whitefish (*Coregonus lavaretus*)	128	94	32	24	(Lindholm-Lehto & Vielma, 2019)

2.4. Analytical Methods for the Identification of Geosmin and 2-MIB in Water

Since geosmin (GSM) and 2-methylisoborneol (2-MIB) have human odour threshold at extremely low concentrations – in the part-per-trillion (ng/L), analytical methods must be both highly sensitive (able to detect very small amounts) and selective (able to distinguish GSM and 2-MIB from thousands of other compounds in a water matrix). To achieve this, a two-step process is almost always required: first, the compounds must be extracted and concentrated from the water sample, and second, they must be separated and identified. This section reviews the common analytical methods used for extraction, separation, and detection of GSM and 2-MIB, including the current industry standard: gas chromatography coupled with mass spectrometry (GC-MS).

2.4.1 Extraction Techniques

Because GSM and 2-MIB occur at trace levels, chromatographic detection methods are almost always combined with a preliminary extraction and concentration step. The following subsections describe the main pre-treatment techniques that have been developed and applied over the past five decades.

2.4.1.1 Closed-Loop Stripping Analysis

Over the past 50 years, multiple pre-concentration methods have been developed for the extraction of geosmin and 2-MIB. Closed-Loop Stripping Analysis (CLSA) is the oldest and most established of these, purging volatile compounds from a water sample by bubbling an inert gas (e.g., helium) through it. The purged compounds are trapped onto a solid adsorbent such as activated carbon, then washed off the trap with a small volume of a strong organic solvent such as dichloromethane, yielding a concentrated extract ready for analysis (Krasner et al., 1983). While effective, CLSA can be time-

consuming (up to 2 hours), requires careful solvent handling, and demands a large sample volume. Despite its robustness, good sensitivity, and excellent recovery, the method lost popularity after the 1990s and was replaced by faster, simpler pre-conditioning approaches (Bristow et al., 2019).

2.4.1.2 Purge and Trap

Similar in principle to CLSA, Purge and Trap (P&T) systems automatically purge volatiles from a liquid sample and trap them on an adsorbent cartridge. The key difference is that the trap is then heated rapidly to desorb the compounds directly onto the capillary column of the GC, making it a fully automated and highly sensitive online technique (Brown et al., 2007).

2.4.1.3 Liquid-liquid Extraction

Liquid-liquid Extraction (LLE) is another well-established method and successfully applied for taste and odour components. For GSM and 2-MIB analysis in water, continuous liquid-liquid extraction (CLLE) and LLE and liquid-liquid micro extractions (LLME) have been used. However, these methods were found to be impractical, time-consuming and labour intensive, and they require large amount of environmentally unfriendly solvents, such as methanol, hexane or dichloromethane limiting their use in modern routine analysis (Bristow et al., 2019).

2,4.1.4 Solid Phase Micro Extraction

Solid phase microextraction (SPME) was originally developed by Belardi and Pawliszyn. It is a straightforward and cost-effective technique that has become widely used for analyzing volatile and semi-volatile compounds in various matrices such as food, water, and environmental samples. It is commonly applied to detect compounds like GSM and 2-MIB (Bristow et al., 2019; Burr et al., 2012; Petersen et al., 2011).

SPME is a modern, solvent-free, and widely used versatile method. This method was created to handle the limitations of LLE and Solid Phase Extraction (SPE) in terms of solvent use. Moreover, SPME is not only a simple, easily automated, and fast extraction method, but it also combines analytical steps such as extraction, concentration, and sample introduction into a single solvent-free process. It requires only a small sample volume and can be carried out either manually or automatically (Bristow et al., 2019). The method consists of a fibre coated with a stationary phase: a liquid polymer, solid sorbent, or a combination of both. The analyte is adsorbed from the headspace or directly from the water sample onto the fibre coating and then desorbed into the hot injector port of a gas chromatograph (GC). The heat desorbs the compounds from the fibre and into the GC system for analysis (Lloyd et al., 1998). The extraction efficiency depends on the partitioning of analytes between the gaseous and aqueous phases, as well as the equilibrium established between the fibre coating and the gas phase (Lindholm-Lehto & Vielma, 2019).

Headspace solid phase microextraction is capable of extremely high sensitivity, often reaching detection levels below 1 ng/L, yet many studies offer little insight into how results fluctuate from one day to the next. Wang (2008) demonstrated that combining SPME with CI-MS/MS can achieve detection limits of 0.46 ng/L for 2-MIB and 0.20 ng/L for geosmin. Despite this, the method continues to face issues with variable recoveries, which are influenced by factors such as equilibration time, extraction duration, fibre positioning during both adsorption and desorption, and the overall condition of the fibre. SPME recovery of geosmin and 2-MIB varies substantially depending on sample matrix and extraction conditions. Practical performance metrics such as limits of quantification (LOQ) are still not well documented in many publications (Manickum & John, 2012).

Fibre conditioning time and temperature are important for good SPME performance. The fibre is heated in the GC injector to remove residual contaminants, reduce carryover, and keep a stable baseline. The exact conditioning temperature (usually close to or higher than the analytes' boiling point) and time (about 5-10 minutes) depend on the fibre coating and target compounds (Juck & Technologies, n.d.).

Matrix effects in water can significantly reduce SPE cartridge efficiency, as competing compounds may bind to the sorbent and hinder the adsorption and subsequent elution of geosmin (Bristow et al., 2019).

Extraction temperature is a critical parameter in SPME, as it influences analyte mass-transfer rates, the extent of water vapour on the fibre, and the partitioning behaviour of analytes between the sample and the fibre coating (Bristow et al., 2019).

The following fibre coatings are commercially available: carboxen/ polydimethylsiloxane (CAR/PDMS), divinylbenzene/carboxen/ polydimethylsiloxane (DVB/CAR/PDMS), divinylbenzene (DVB), polyacrylate (PA), and polydimethylsiloxane/divinylbenzene (PDMS/DVB) (Bristow et al., 2019; (Sesha) Pochiraju et al., 2021). In 1995, Brand was the first to use a PDMS fibre for geosmin and 2-MIB extraction, achieving detection levels of 100-200 ng/L (Lloyd et al., 1998; McCallum et al., 1998). DVB/CAR/PDMS SPME fibre was used in this research.

2.4.2 Detection and Quantification methods

2.4.2.1 Gas Chromatography - Mass Spectrometry

After extraction and concentration, the extract contains many co-extracted compounds. To specifically identify and quantify GSM and 2-MIB, they must be separated from this complex mixture. This is achieved using gas chromatography (GC) followed by detection with mass spectrometry (MS) as illustrated on Figure below. The combination

GC-MS - is recognized as the most widely applied technique for detecting and quantifying chemical compounds in complex matrices. It offers high sensitivity, allowing for the detection of trace levels of volatile organic compounds in water (Bristow et al., 2019).

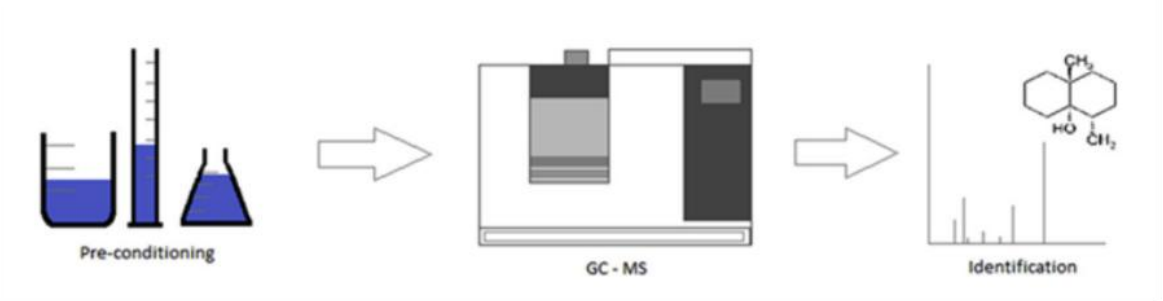

Figure 5 Illustrative sketch of a typical GC-MS analysis pathway for geosmin analysis (Bristow et al., 2019).

The combination of GC and MS is powerful (L. Wang et al., 2025) because it provides two independent levels of identification:

1. Retention time: The compound must elute at the expected time characteristic of GSM or 2-MIB.
2. Mass spectrum: The fragmentation pattern of the compound at that retention time must match the known spectral fingerprint of GSM or 2-MIB.

This dual confirmation makes GC-MS a highly reliable and definitive technique for quantifying these compounds at very low levels, often around 1 ng/L (L. Wang et al., 2025).

Detection is primarily carried out using a mass spectrometer with electron ionization (EI), which produces characteristic fragment ions for quantification in selected ion monitoring (SIM) mode. EI is a robust and straightforward ionization technique, but it is also one of the more aggressive methods: it generates broad fragmentation and a relatively low molecular ion peak, which can complicate identification when the analyte

is not well separated from the sample matrix (Bristow et al., 2019). Contaminants can increase background noise and hinder both identification and quantification. Additionally, EI is generally inefficient in the ion source, producing roughly one ion per thousand molecules. For these reasons, alternative ionization methods that are gentler - causing less fragmentation while remaining more efficient - may offer advantages for geosmin analysis (Bristow et al., 2019).

A summary of published analytical procedures for geosmin and 2-MIB, including pre-treatment method, chromatographic conditions, LOD, and LOQ, is provided in the Table below.

Table 2 Examples of analytical procedures, covering sample pre-treatment, analytical technique, chromatographic conditions, and the associated limits of detection (LOD) and quantification (LOQ) (Lindholm-Lehto & Vielma, 2019).

Sample type	Pretreatment	Method of analysis	Results	References
RAS water for Tilapia *Oreochromis niloticus* ×Oreochromis *aureus* 25 ml in 40 ml vial	SPME (incubation for 65°C for 10 min. preheating, PA	GC-FID (280°C) splitless mode (30 m x 0.25 mm, 0.25 µm MDN–5 fused silica capillary, He 1 ml/min, 60°C for 0.5 min → 100°C at 30°C/min → 185°C at 20°C/min → 250°C at 40°C /min for 2.3 min)	GSM 10 75 ng/L, MIB 50–170 ng/L	Guttman and van Rijn (2008)
RAS water (20 ml, 6 g NaCl) Brook trout *Salvelinus fontinalis*, Rainbow trout *O. mykiss*	SPME (65 µm PDMS-DVB fibre, 35 min in 40°C water bath)	GC–MS (DB–17 ms column, splitless mode, He 2 ml/min, 60°C for 2 min → 132°C, 4°C/min for 1 min → 250°C, 20°C/min for 5 min, SIM mode)	GSM and MIB detected	Auffret et al. (2011)
Rainbow trout *O. mykiss* 20 g fish, 25 ml water, internal standard RAS water 40 ml, NaCl	Water: SPME (2 cm 30/50 µm DVB/CAR/PDMS) 60°C water bath, stirred for 15 min Fish: Purge 30 s, 13,500 rpm, 50°C water bath, 100 ml N_2/min. for 60 min Tenax TA trap	GC-MS (30 m x 0.2 mm, 0.25 µm Rtx–5 ms, He 1.2 ml/min splitless mode, 45°C for 3 min →30°C/min → 250°C at 100°C/min → 300°C for 2 min)	LOD for GSM and MIB 0.2 ng/L	Petersen et al. (2011)
Water (0.6 ml, 0,3 g NaCl) Atlantic salmon *S. salar* fillet and skin (20 g, 0,6 ml distillate)	SPME (100 µm PDMS, 40°C 20 min preheating, shaken for 10 min)	GC–MS (30 m x 0.25 mm, 0.25 µm DB–5 capillary column, 60°C for 0.5 min → 30°C/min to 100°C, 20°C/min → 300°C for 2 min., SIM mode)	GSM 94,2 ± 29, 2 ng/kg, MIB 15 ± 2 ng/kg GSM 1–29 ng L^{-1}, MIB 132 ± 13 ng/L	Burr et al. (2012)
Atlantic salmon *S. salar* fillet 1 g, 1 ml saturated NaCl (aq)	Stir bar (1,000 rpm, 2 hr, 21°C), thermal desorption	GC–MS (30 m x 0.25 mm, 0.25 µm DB–5 ms fused-silica column, 50°C for 1 min → 25°C/min. 150°C for 1 min and to 280°C for 0.8 min., He 1.2 ml/min, internal standard of 2-isopropyl–3-methoxy-pyrazine, Scan mode	GSM 105–400 ng/kg MIB 141–800 ng/kg	Davidson et al. (2014)
Drinking water 40 ml in 60 ml vial, NaCl	HS–SPME (30/50 µm DVB/CAR/PDMS, 65°C, 30 min)	GC–MS-MS ion trap (30 m x 0.25 mm, 0.5 µm VF–5 ms capillary column, splitless mode, He 1 ml/min. 40°C for 5 min → 160°C 8°C/min → 260°C 20°C/min. SIM and Scan modes)	LOD: MIB 0,5 ng/L, GSM 0,2 ng/L GSM 0,2–2,1 ng/L, MIB nd–6,5 ng/L	Peng et al. (2014)

2.4.2.2 Quantification

To determine the exact concentration of GSM and 2-MIB in a sample, internal standard calibration is used. A known amount of a structurally similar but non-native compound (the internal standard) is added to the water sample at the very beginning of the extraction process (McCallum et al., 1998). By comparing the instrument response (peak area) of GSM and 2-MIB to the response of the internal standard using a pre-established calibration curve, the exact concentration in the original sample can be

calculated - accounting for any losses incurred during sample preparation (Petersen et al., 2011).

The reliable monitoring of geosmin and 2-MIB in water requires sophisticated analytical methods. While several extraction techniques are available, including CLS, SPME, and P&T, the final separation and detection almost universally rely on GC-MS. This combination provides the necessary sensitivity, selectivity, and confirmatory power to quantify these potent taste and odour compounds at the trace levels relevant to drinking water quality and consumer satisfaction. The continued refinement of these methods, particularly towards automation and solvent-free techniques like SPME, remains an important focus in environmental analytical chemistry.

2.4.3 Limitations of the method

The trace-level concentrations at which GSM and 2-MIB must be detected, combined with the complex matrix of real water samples, make their analysis particularly challenging. SPME fibres present multiple technical challenges for volatile organic compounds (VOC) and taste-and-odour analysis, including competitive sorption effects, variable fibre performance, mechanical fragility, and poor sensorial representativeness. The primary issue is that different SPME fibre types exhibit significant performance trade-offs. Tuduri et al. (2002) found that equilibration times and sensitivity vary considerably across fibre types - PDMS showed the shortest equilibration time (5 min) but poorest sensitivity, while PDMS/CAR showed the longest extraction time but greatest sensitivity. Critically, Tuduri et al. (2002) also identified competitive sorption on adsorptive fibres (PDMS/DVB and PDMS/CAR) as a major calibration problem affecting quantitative analysis.

VOC extraction by SPME is reduced in multicomponent mixtures compared to individual compounds due to competitive adsorption on the fibre surface. Multiple

studies demonstrate this effect. Tuduri et al. (2002) observed that competitive sorption on adsorptive fibres "can lead to SPME calibration problems." Murray (2001) found that higher molecular weight compounds displace lower molecular weight compounds by competing for active sites on the fibre, resulting in irregular analytical responses. Tuduri et al. (2002) quantified this effect: acetone showed a linear range of 3-60 μg/m³ in dynamic mode within a mixture, but this extended to 5-300 μg/m³ when analyzed as an isolated compound. Górecki et al. (1999) similarly documented displacement of compounds with low distribution ratios by those with high distribution ratios (i.e. affinity). SPME is therefore typically considered a non-exhaustive extraction technique, meaning that only part of the analyte is extracted and the distribution of analyte mass across the sampled phases must be taken into account (Ouyang & Pawliszyn, 2008).

Beyond extraction efficiency, Rega et al. (2003) demonstrated that SPME extracts poorly represent original odour profiles, with DVB/CAR/PDMS fibres performing best only at the shortest exposure times. Additionally, Müller et al. (2006) noted that commercial SPME fibres suffer from weak mechanical strength and high cost, limiting their deployment in field settings.

More recent work has explored advanced fibre coatings to address these limitations. Kremser et al. (2016) found that the robotic autosampler platform (PAL) SPME Arrow device offered significantly enhanced sensitivity over conventional SPME fibres, along with better robustness and stability, attributed to the larger sorbent volume increasing analyte uptake. Wei et al., (2019) reported the carbon metal organic frameworks (MOF-74-C) coatings showed “1.1-16.0 times larger” extraction efficiency than commercial fibers with detection limits “below” odor thresholds.

While robust analytical methods are essential for monitoring GSM and 2-MIB concentrations, detection alone is insufficient - effective water quality management in

RAS ultimately requires strategies to remove or degrade these compounds. The treatment methods developed for this purpose are reviewed in the following section.

2.5. GSM and 2-MIB Treatment

Abd El-Hack et al. (2022) suggest that the removal of geosmin from aquaculture water can typically be achieved by chemical, physical, and biological methods. Often used as disinfection units, ozone, UV irradiation, or chlorine, are found to be ineffective in geosmin elimination. However, Kutchera et al. (2009) found that UV/VUV (vacuum UV) radiation proved to be more effective in the degradation of off-flavour components such as geosmin and 2-MIB. According to Cook and Newcombe (2004) and Paulino et al. (2023), powdered activated carbon (PAC) and granular activated carbon (GAC) can efficiently remove musty-earthy taste and odour, but their effectiveness was reduced in the presence of other organic substances. Biological methods are considered as less expensive than chemical or physical methods but such industry-scale applications are not available (Ho et al., 2007).

2.5.1 Activated Carbon

Srinivasan and Sorial et al. (2011) stated that PAC is the most effective and commonly used practice in water treatment to manage odorants, and the major challenge in using it is the high concentration of organic contaminants, which have a competitive advantage in adsorption and therefore require higher dosages of PAC. This leads to another issue, which is the formation of excessive sludge and increasing operational cost. GAC filtration can be effective when it is customized and made selective to the particular target compounds; however, its efficiency is still influenced by natural organic compounds (NOCs). The carbon adsorption effectiveness is influenced by

factors such as adsorbent properties and water quality, for example pore size distribution, surface characteristics, and the presence of natural organic matter (NOM) (Srinivasan & Sorial, 2011). Paulino et al. (2023) reported that natural organic matter (NOM) can substantially reduce the adsorption capacity of granular activated carbon, with up to an order-of-magnitude lower uptake of geosmin and 2-MIB in natural waters containing 2.0–12.0 mg/L dissolved organic carbon (DOC) compared with single-solute solutions, under both equilibrium and non-equilibrium conditions (Figure below).

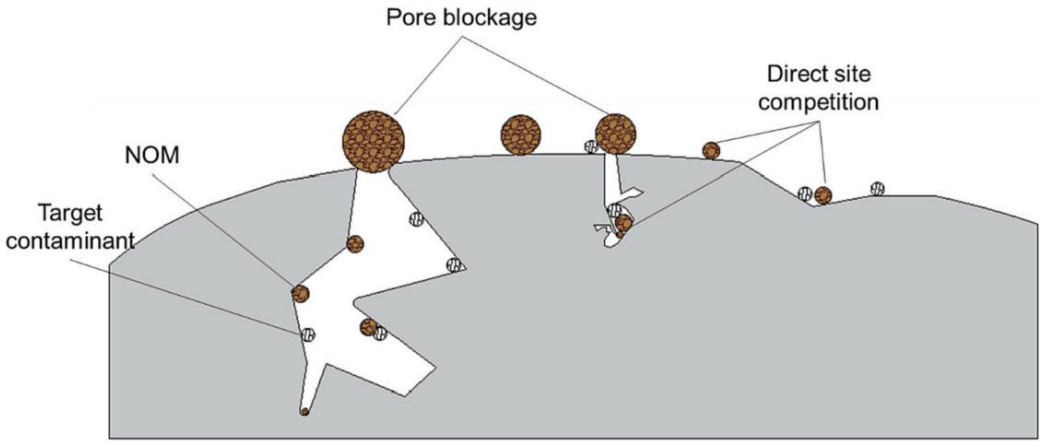

Figure 6 Schematic illustrating the difference between pore blocking and direct competition for adsorption sites (Paulino et al., 2023).

The dosage of adsorbents can be based on 2-MIB concentration, as when GSM and 2-MIB are present at similar levels, 2-MIB is more challenging to remove (Srinivasan & Sorial, 2011).

Even though GSM and 2-MIB have been recognized to be reduced by activated carbon with up to 96% efficiency at low levels in drinking water treatment systems, such effects are not expected in RAS water due to the relatively high organic substance concentration, often exceeding 10 mg/L (Gupta et al., 2024). As suggested by Wang et al. (2020), taste and odour compound removal using any type of activated carbon can be diminished due to strong competition from other natural organic matter in water for

adsorption sites. According to a study by Asghar et al. (2015), the most widely used granular activated carbon achieved 82% and 73% removal of geosmin and 2-MIB in drinking water. However, these efficiencies are not sufficient for reducing geosmin and 2-MIB in RAS water down to human detection threshold levels (e.g. <10 ng/L). Considering the above, activated carbon was not selected as a study topic in this thesis.

2.5.2 AOPs (Advanced Oxidation Processes)

AOPs are technologies that are based on the generation of very reactive hydroxyl radicals (OH) that oxidize organic chemicals in water like GSM and 2-MIB (Antonopoulou et al., 2014).

Many studies are dedicated to studying various AOPs. The most common are ozonation, UV radiation, and hydrogen peroxide, and other hydroxyl radical sources (Lindholm-Lehto & Vielma, 2019). Antonopoulou et al. (2014) and Rosenfeldt et al. (2005) reviews summarize the field in terms of degradation kinetics, operating conditions, water quality, and transformation pathways, while experimental studies show that ozone alone is often less effective than coupled processes such as ozone/UV or UV/H_2O_2. Pilot-scale work also shows that water-matrix effects can strongly reduce performance and increase energy demand, so laboratory results do not always translate directly to real waters (Klausen & Grønborg, 2010). Even so, full-scale O_3/H_2O_2 application has achieved treated-water concentrations below 10 ng/L for both compounds with bromate remaining undetectable, suggesting that carefully optimized AOPs can be practical for utility-scale odor control (Peng et al., 2024).

Although destructive methods such as UV with advanced oxidation and electrochemical treatments have proved efficient in the removal of geosmin and 2-MIB, their industrial applications have large operating costs and energy consumption (Gupta et al., 2024).

Water quality parameters such as pH and natural organic matter (NOM) levels also affect GSM and 2-MIB removal by the AOP. These technologies, especially for large scale applications, could be very costly in terms of capital and energy (Srinivasan & Sorial, 2011).

Another challenge is the risk of the creation of toxic disinfection byproducts (DBP). For example, aldehydes, ketones, carboxylic acids and bromines DBPs could be formed from ozonation in water with bromide (Huang et al., 2003).

Nerenberg (2000) suggested that ozonation followed by biological treatment could stabilize highly degradable ozonation products, reduce biological regrowth, and limit chloride usage in the system. Additionally, potentially increased biofilter biomass resulting from the higher instability of ozonated water may enhance the degradation of odour and taste producing compounds.

2.5.3 Adsorption by Zeolites

Zeolites are microporous, crystalline aluminosilicate minerals consisting of aluminum, silicon, and oxygen, forming three-dimensional tetrahedral frameworks (SiO_4 and AlO_4) with regular pore structures of molecular dimensions (3-10 Å) and a negatively charged surface (Payra & Dutta, 2004). These structural properties give zeolites high surface area and homogeneous pore size, enabling effective adsorption of organic and inorganic pollutants through multiple mechanisms including electrostatic interaction, π-π stacking, hydrogen bonding, and pore filling (Al-Hazmi et al., 2022). Zeolites are classified as natural or synthetic; synthetic zeolites are generally preferred due to their tailorable physicochemical properties, and can be fabricated from waste materials, reducing production costs (Kumari et al., 2024). Zeolite-Y (synthetic) was selected for this study.

Various standard adsorption mechanisms of organic and inorganic contaminants on zeolite are illustrated on Figure below.

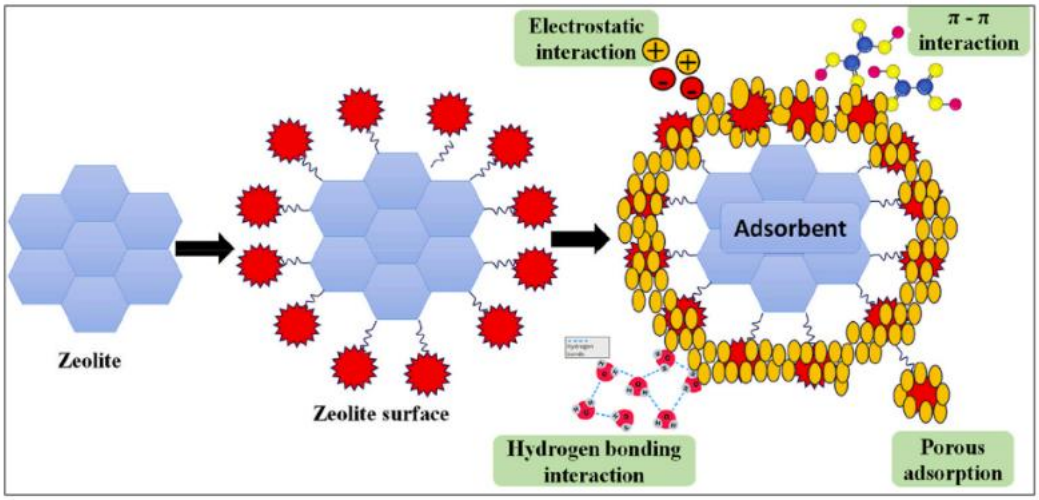

Figure 7 Possible adsorption mechanisms by which zeolite removes organic and inorganic pollutants (Kumari et al., 2024).

2.5.3.1 Zeolite doped with nanoparticles

The incorporation of metal oxide or carbon-based nanoparticles into zeolite frameworks, known as nanoparticle doping, has emerged as a significant development in water treatment, substantially improving adsorption capacity, catalytic activity, selectivity, and mass transfer kinetics. Synthesis methods including hydrothermal synthesis, sol-gel techniques, and chemical vapour deposition allow precise control of particle size and surface characteristics (Ruíz-Baltazar, 2024).

The introduction of metal oxide nanoparticles enhances catalytic degradation of organic contaminants through advanced oxidation, while carbon-based nanoparticles improve adsorption of hydrophobic pollutants. Nanoparticle-doped zeolites thus offer a versatile, tunable toolkit for addressing a broad range of water treatment challenges (Ruíz-Baltazar, 2024).

Table below highlights the mostly commonly used zeolite supported TiO_2 composites with their applications, key properties and benefits (Armaković & Armaković, 2025).

Table 3 Commonly used zeolites in combination with TiO2 and their applications.

Zeolite	Properties	Applications	Benefits with TiO_2
ZSM-5	High silica content, thermal stability, adjustable acidity	Dyes: methylene blue, methyl orange VOCs: toluene, formaldehyde	Enhances adsorption and TiO_2 dispersion
Y Zeolite (Faujasite)	Large pore size, high cation-exchange capacity	Heavy metals: Pb^{2+}, Cd^{2+} Air purification: NOx, VOCs	Provides large surface area for TiO_2 deposition
Beta Zeolite	High hydrophilicity, large surface area	Pharmaceuticals: antibiotics, effluents Dyes: rhodamine B	Improves photocatalytic efficiency
Mordenite	High thermal stability, channel-like structure	Heavy metal removal: Cr^{6+}, Ni^{2+} Organic pollutants: pesticides, hydrocarbons	Synergizes with TiO_2 under UV light
Clinoptilolite	Natural zeolite, high cation-exchange capacity	Heavy metals Pesticides: atrazine	Cost-effective and widely available
Zeolite A	Small pore size, strong ion-exchange capacity	Water softening: hardness removal Selective adsorption: arsenic	Ensures close interaction with TiO_2 active sites

2.5.3.2 Synergistic Mechanisms of TiO2 Photocatalysis and Zeolites

TiO_2-zeolite composites by UV photocatalysis work through three synergistic mechanisms: enhanced adsorption, improved charge separation, and optimal TiO_2 dispersion (Armaković & Armaković, 2025). The zeolite component concentrates organic pollutants at photocatalytic sites through dual hydrophilic-organophilic surface affinity, while the zeolite framework prevents electron-hole recombination through Ti-O-Si chemical bonding - addressing the primary limitation of pure TiO_2 photocatalysis (Foura et al., 2017; Shaw et al., 2020). As a result, TiO_2-zeolite composites demonstrate higher performance with 2-6 fold organic pollutant removal compared to either material alone. They also achieve 90-98% degradation efficiency for various organic compounds under UV irradiation, and outperforming alternative composites such as Zeo-ZnO by a factor of three (Foura et al., 2017; Kabadayi et al., 2024). The anatase phase of TiO_2 exhibits optimal band gap energy (3.1-3.2 eV) for UV absorption, and zeolite support maintains TiO_2 dispersion at the nanoscale, preventing agglomeration while increasing active sites (Nematov, 2024).

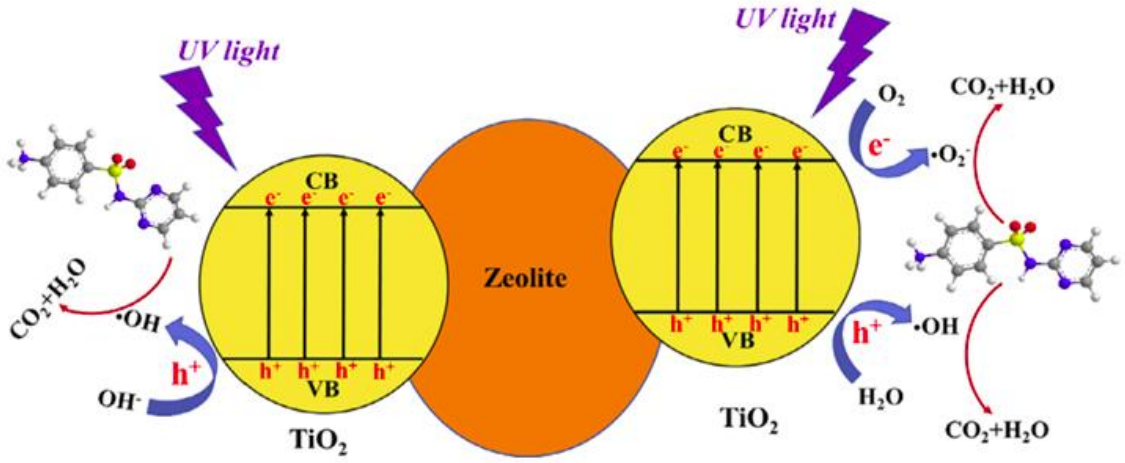

Figure 8 General photocatalytic mechanism operating in the TiO2/Zeolite+UV system (CB: conduction band; VB: valence band; e−: electron; h+: hole) (X. Liu et al., 2018)

The figure above presents a schematic representation of the common UV photocatalytic mechanism of titanium dioxide in a zeolite-supported composite coating.

Table 4 Roles of zeolite in improving the photocatalytic degradation mechanisms of TiO2 (Armaković & Armaković, 2025).

Role	What Happens	Why It Is Important	Example
Adsorption	Zeolite's porous structure traps and concentrates pollutants near TiO_2 active sites.	Increases pollutant concentration close to TiO_2, enhancing reaction efficiency.	Molecules adsorbed into zeolite pores are degraded efficiently by TiO_2.
Dispersion	Zeolite prevents TiO_2 particles from agglomerating by evenly distributing them on its surface.	Better TiO_2 active surface area, allowing more pollutants to interact with catalytic sites.	Without zeolite, TiO_2 particles might cluster, reducing the available surface area for catalysis.
Enhanced mass transfer	Zeolite's porous structure facilitates diffusion of pollutants to TiO_2 and removal of products.	Ensures efficient transport of reactants and intermediates, avoiding reaction block.	Pollutants diffuse through zeolite pores to TiO_2 for degradation by ROS.
pH regulation	Zeolite buffers change in pH during the reaction, maintaining optimal conditions for TiO_2 activity.	Stabilizes TiO_2 photocatalytic performance, especially under varying reaction conditions.	Acidic products are neutralized by zeolite, maintaining an ideal pH for pollutant degradation.
ROS	TiO_2 generates ROS under light, which degrades pollutants adsorbed on zeolite.	Zeolite ensures pollutants are close to TiO_2, improving their interaction with ROS and enhancing degradation.	Molecules are degraded into CO_2 and water by ROS generated on TiO_2.

Among the GSM removal methods tested in RAS environment, photocatalysis is considered the most promising approach by its cost and efficiency (Lindholm-Lehto & Vielma, 2019). TiO_2-based photocatalysis has been identified as a favorable method for GSM and 2-MIB removal in RAS due to its ability to completely mineralize these compounds under UV irradiation without generating secondary chemical residues (Lawton et al., 2003). The method is further preferred for its low material cost, chemical

stability, and absence of chemical inputs, characteristics well-suited to closed-loop RAS environments (A. Müller et al., 2010). When combined with zeolite as an adsorptive carrier, the synergistic effect pre-concentrates trace-level contaminants onto the catalyst surface, substantially accelerating degradation kinetics, with TiO_2-zeolite composite coatings demonstrating up to 99% geosmin removal at concentrations as low as 4 ng/L, directly relevant to aquaculture conditions (Wee et al., 2015). Wee et al. (2015) developed a stable TiO_2-USY zeolite composite via a layer-by-layer dip-coating method, enhancing efficiency of both photocatalytic and adsorptive removal of GSM from water, reducing GSM concentrations to as low as 4 ppt. However, commercial applications are not yet available for photocatalysis in RAS (Lindholm-Lehto & Vielma, 2019) and its application for 2-MIB removal is not studied.

The EU ban on TiO_2 as a food additive (E171) under Commission Regulation does not directly govern its use as a water treatment agent in RAS facilities. However, concerns remain about free TiO_2 nanoparticles potentially leaching into tank water and accumulating in fish tissue (Gupta et al., 2024). The use of immobilized TiO_2, fixed onto a solid substrate, addresses this concern by preventing nanoparticle release into the water column, and has therefore been considered an acceptable approach for photocatalytic water treatment in aquaculture settings (Frederichi et al., 2021; A. Müller et al., 2010). However, significant challenges remain. Transitioning from laboratory to large-volume RAS reactors introduces mass transfer limitations, uneven UV light distribution, and reduced photocatalytic efficiency (Ruíz-Baltazar, 2024). As TiO_2 is predominantly UV-active, artificial UV sources add operational energy costs in indoor facilities (Pelaez et al., 2012). Long-term coating stability under continuous flow conditions, and the risk of nanoparticle release into fish-rearing water, also require further validation before full-scale deployment (Frederichi et al., 2021). As Ruíz-

Baltazar (2024) notes, overcoming these issues demands sustained research into greener synthesis routes, refined material characteristics, and practical integration into existing water treatment infrastructure.

2.5.4 Other methods

2.5.4.1 Ultrasound

Nam-Koong et al. (2016) demonstrated an alternative treatment method using ultrasonically induced degradation at 850 kHz. Its main advantage is the effective removal of GSM and 2-MIB regardless of other organic or inorganic matter in the aquaculture system, which is a major limitation of other treatment strategies. However, the method may involve significant energy costs, and its applicability at scale remains uncertain, as existing studies have been conducted only at the laboratory level.

2.5.4.2 Electrolysis

Ben-Asher et al. (2024) proposed a novel approach for eliminating odour and taste compounds by replacing the nitrification biofilter with electrolysis during the purging period. This method not only oxidizes ammonia but also disinfects the water and removes off-flavour compounds. The concept was tested on rainbow trout at both laboratory and pilot-plant scales, with and without organic load, and evaluated in water and fish flesh. GSM and 2-MIB were fully removed within seven days in water and 11 days in fish. The study confirmed that detachment from the biofilter combined with electrooxidation disinfection prevented the generation of additional off-flavour compounds. The authors estimated that this approach could enable a 10% annual production increase in commercial RAS farms.

2.5.4.3 Alginate and biological treatment

Azaria et al. (2021) found that hydrophobic alginate-oil carriers can remove geosmin (GSM) and 2-MIB from RAS water through adsorption and biodegradation, even at very low levels and in the presence of organic matter. The carriers first trap these compounds, then support microbes that slowly break them down. Over time, bacteria involved in terpene degradation and nitrate reduction grow on the carriers, helping to break down GSM and 2-MIB. This shows that such carriers can support natural biological processes to improve water quality in aquaculture systems.

2.5.4.4 Depuration

Despite numerous studies and considerable efforts to reduce off-flavour compounds in water to human detection thresholds, freshwater purging remains the primary method for removing odorants such as geosmin and 2-MIB. However, this approach requires access to high-quality freshwater and entails financial investment in purging equipment (Lindholm-Lehto & Vielma, 2019).

Research indicates that the ideal GSM purification period can be as brief as six days when pre-purifying the water pool with H_2O_2 (Davidson et al., 2014). Even more effective outcomes are achieved by withholding fish food and raising the water exchange rate (Lindholm-Lehto & Vielma, 2019).

Depuration is the process when harvest ready fish are placed to the biofilm free fresh water and not fed for 6-14 days. This process provides a reduction in off-flavour components, but also causes fish weight loss. The Freshwater Institute in Shepherdstown in the study conducted determined that for 7.38 kg RAS-grown Atlantic salmon, lost on average 2.1% of sellable biomass during the first six days of depuration, and if off-flavour issues remain an additional 1.4% of sellable biomass is lost during the subsequent four days of depuration. It has been found that the revenue and potential

profit of the RAS is directly affected by biomass weight loss from purging. For instance, a minimum six-day purging period of the 10,000 ton land-based RAS Atlantic salmon farm every harvest results in approximately $1.5 million per year less revenue due to fish mass loss equivalent to 2.1 percent of weight lost. If the purging period must be increased to 10 days, an additional $1.019 million per year in sellable biomass will be lost. Values are calculated from the year-to-date average price per kg head-on-gutted for salmon in the 7.3 kg size class (Kropp et al., 2022).

Abd El-Hack et al. (2022) suggest that, in the US, approximately 30% of the profits from the catfish aquaculture industry, are lost due to geosmin and other odorous and undesirable-tasting compounds.

2.5.4.5 Commercial Technologies

A novel Advanced Oxidation Process, the Exciton Advanced Oxidation Process® (eAOP®), has been evaluated for accelerated removal of GSM and 2-MIB from Atlantic salmon recirculating aquaculture systems (RAS) during depuration, employing combined mechanisms of photocatalysis, UV photolysis, electrolysis, and UV/oxidant AOP. In trials with market-sized fish, eAOP® treatment reduced fillet GSM concentrations 60% faster than conventional water flushing, achieving on-flavour status in under six days compared to ten days in controls, while also reducing water consumption and fish biomass loss (Kropp et al., 2022). However, as this technology is proprietary and commercially patented under the eAOP® trademark, full methodological details are not openly available in the literature, limiting its independent replication and broader scientific evaluation.

Similarly, ULTRAAQUA offers a commercial UV-AOP system combining chemical oxidation and photolysis for geosmin and 2-MIB mitigation in RAS facilities, with site-specific configurations tailored to individual farm management conditions (“Geosmin

MIB Mitigation UV Disinfection," n.d.). While this solution is actively deployed in the aquaculture industry, it remains a proprietary commercial product with limited peer-reviewed validation in the open scientific literature.

2.5.5 Chapter Summary

This chapter reviewed the current literature on recirculating aquaculture systems (RAS), the occurrence and sources of geosmin and 2-MIB, and the analytical and treatment methods used to address these compounds. RAS offer a sustainable approach to fish farming, but the accumulation of geosmin and 2-MIB remains a key challenge, as these compounds cause earthy and musty off-flavours in fish at low concentrations. They are mainly produced by cyanobacteria and actinomycetes, which thrive in the warm, nutrient-rich conditions typical of RAS environments.

GC-MS combined with SPME extraction is the most widely used and reliable method for detecting these compounds at trace levels. For treatment, activated carbon adsorption is the most common approach in practice, while powder zeolite and TiO_2-based photocatalysis combined with zeolite has shown promise as an alternative. However, practical treatment solutions at RAS remain an area requiring further research.

The following chapter describes the materials and methods used in this study, including the development and validation of a GC-MS analytical method for geosmin and 2-MIB detection in a seawater matrix, as well as the experimental procedures for zeolite adsorption and TiO_2-zeolite photocatalysis treatment experiments.

Chapter 3

3.1 Materials and methods

The analytical materials and methods used in this research are presented in this chapter. The materials include samples, detection equipment, characterization of products for treatment and gas chromatography. The detection methods include solid phase micro-extraction (SPME) and gas chromatography mass spectrometry (GC-MS). Treatment methods include application of adsorption with zeolite powder and UV photocatalysis. Characterization methods include optical microscopy and SEM.

3.1.1 Reagents and materials

The following reagents were used:

1. Geosmin analytical standard, 1 mL of 2 mg/ml in methanol 98%, (Merck).
2. 2-methyl-isoborneol (2-MIB) analytical standard, 1 mL at 10 mg/ml in methanol 98% (Merck).
3. Artificial sea water was prepared in Type 1 water according to the ASTM standard (Table 5).
4. Aquarium sea water salt mixture (Red Sea) - was replaced by item 3.
5. Type 1 water (Lab supply).
6. Internal standard, 2-isobutyl-3-methoxypyrazine 99% (Sigma Aldrich).
7. Methanol, HPLC grade (Lab supply, Fisher Scientific).
8. Acetone (Lab Supply, Merck).
9. Sodium Chloride, NaCl (Lab supply, Merck).
10. Magnesium Chloride, $MgCl_2$ (Lab supply, UNILAB).
11. Sodium Sulfate, Na_2SO_4 (Lab supply, Merck).

12. Calcium Chloride, $CaCl_2$ (Lab supply, Merck).
13. Potassium Chloride, KCl (Lab supply, Merck).
14. Zeolite Y (Thermofisher Scientific).
15. TiO_2 (Lab supply, Ajax Finechem).
16. Poly (ethylene glycol)-block-poly (propylene glycol)-block-poly (ethylene glycol) (Sigma Aldrich).
17. Hydrochloric acid 36%, HCl, reagent grade (Lab Supply, ajax Finechem).
18. Nirtic acid 65% (Lab supply, Merck).
19. Ethanol, reagent grade (Lab Supply, Merck).
20. Sea water samples from the Tauranga campus of the University of Waikato.

The following equipment was used:

1. Agilent model 7890B GC with PAL auto-sampler and MS triple quad.
2. ZB5-MS column (30m x 0.25mm x 0.25um) (Zebron).
3. SPME were performed with an auto CAR/DVB/PDMS fibre holder.
4. Divinylbenzene/carboxen/polydimethylsiloxane (DVB/CAR/PDMS) fibre.
5. Optical microscope (Leica).
6. SEM microscope (Hitachi).
7. Muffle furnace (DAIHAN Scientific).
8. Oven (Memmer).
9. Desiccator (Lab supply).
10. 10, 100 and 1000 mL, 5 and 10 mL autopipettes (Eppendorf).
11. Centrifuge (Sigma).
12. Incubator Shaker (Bioline).
13. Magnetic stirrer (IKA C-MAG HS4).
14. Analytical scale (4 dp) (METTLER TOLEDO).

15. Quartz photocatalyst reactor and quartz tube (fabricated locally).

16. LED UV lamp, 365 nm wavelength (Vusum).

17. UV spectrophotometer (Shimadzu UV-1900) and quartz cuvettes.

18. Turbidity meter (Hach).

Table 5 Artificial sea water composition (per ASTM).

Compound	Concentration (g/L)
NaCl	24.53
$MgCl_2$	5.20
Na_2SO_4	4.09
$CaCl_2$	1.16
KCl	0.695
Type 1 water	balance

3.1.2 Stock solution preparation

Initially geosmin and MIB standard solutions were diluted in 10% methanol and 90% type 1 water in A grade 100 mL volumetric flasks to 10^6 and 10^8 ng/L intermediate stock solutions respectively and stored in 150 ml amber Shott bottles, sealed by parafilm, in the fridge. These higher concentrations were further diluted in type 1 water to 10^6 (for MIB), 10^4 and 10^3 ng/L working solutions and were stored in 500 ml amber bottles, sealed by parafilm, in the fridge. However later, due to the loss of geosmin and MIB over time from volatilization in the bulk solutions, intermediate stock solutions were prepared at 10^6 ng/L concentration purely in methanol and were distributed in 2 mL vials filled to the top (to minimize headspace) and stored in the freezer at -20°C. Further dilution was carried out with artificial sea water.

3.1.3 Sample preparation

10 mL samples were prepared in artificial sea water solution in transparent 20 mL GC-MS headspace vials at 0, 10, 50, 100, 500 and 1000 ng/L concentrations using the GSM and MIB stock solutions for building calibration curve. 3 g of NaCl were added to each

sample to promote salting-out and improve analyte partitioning into the headspace. 40 µL of 1000 ng/L internal standard was also added to each sample. For the initial method development stage, the internal standard was not added, due to unavailability and late delivery. For all treatment experiments the internal standard was added.

3.1.4 Sample extraction and analysis

GC-MS coupled with SPME by Agilent was used for sample analysis. Samples were incubated with agitation and subsequently extracted prior to GC-MS analysis using a PAL auto-sampler equipped with an SPME fibre injection system (Figure 9 and 10). The PAL auto-sampler (Figure 10) was programmed to incubate samples at 60°C for 30 min using a heated agitator. Following incubation, the syringe needle was inserted through the vial septum and the SPME fibre was exposed to the sample headspace, allowing analytes to adsorb onto the fibre coating for 15 min. The needle-fibre assembly was then transferred to the GC injector, where the analytes were thermally desorbed at 250°C for 5 min (Figure 11). The desorbed analytes were subsequently separated in the capillary column using the GC-MS parameters in the Table below and detected by mass spectrometry (Figure 12).

After each analysis, the SPME fibre was conditioned at 270°C for 5 min to remove residual compounds. Prior to sample extraction, the fibre was also pre-conditioned at 270°C for 1 min to minimize potential contamination and carryover. The GC cycle time was approximately 18 min, resulting in a total analysis time of about one hour per sample.

Table 6 GC-MS parameters.

Analytical Column	ZB5-MS (30m x 0.25mm x 0.25µm), max T 350°C
Injection type	Splitless
Fibre type	Divinylbenzene/carboxen/polydimethylsiloxane (DVB/CAR/PDMS)
Carrier gas type	Helium
Carrier gas flowrate	1 mL/min

3.1.4.1 Fibre Selection

The DVB/CAR/PDMS fibre was selected for this study based on its performance for headspace extraction of volatile and semi-volatile compounds in water. This fibre coating is reported to provide good GC response enhancement compared to other coatings for taste and odour compounds, including geosmin and 2-MIB, and has been specifically applied in HS-SPME methods for analyzing these compounds in water (Tang et al., 2025).

Figure 9 Agilent model 7890B GC with PAL auto-sampler and MS Triple quad.

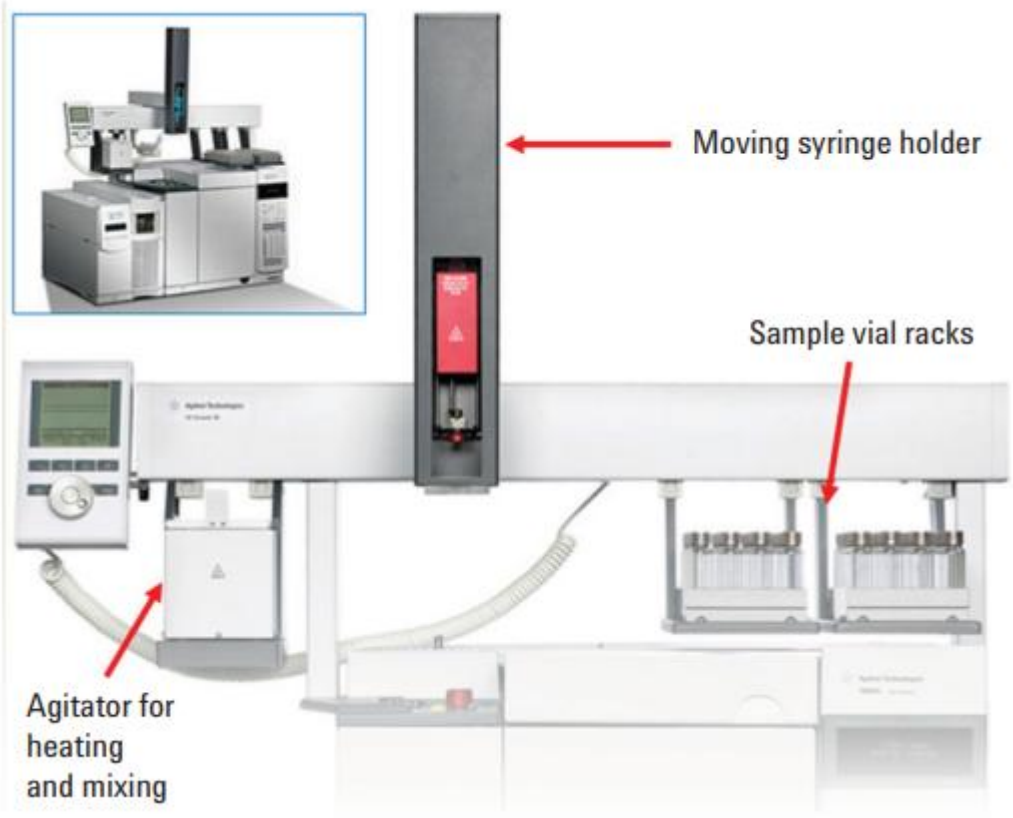

Figure 10 The PAL Automated Sample Injector with SPME accessory mounted on the Agilent 7890A GC (inset) and its labelled components (You, 2012).

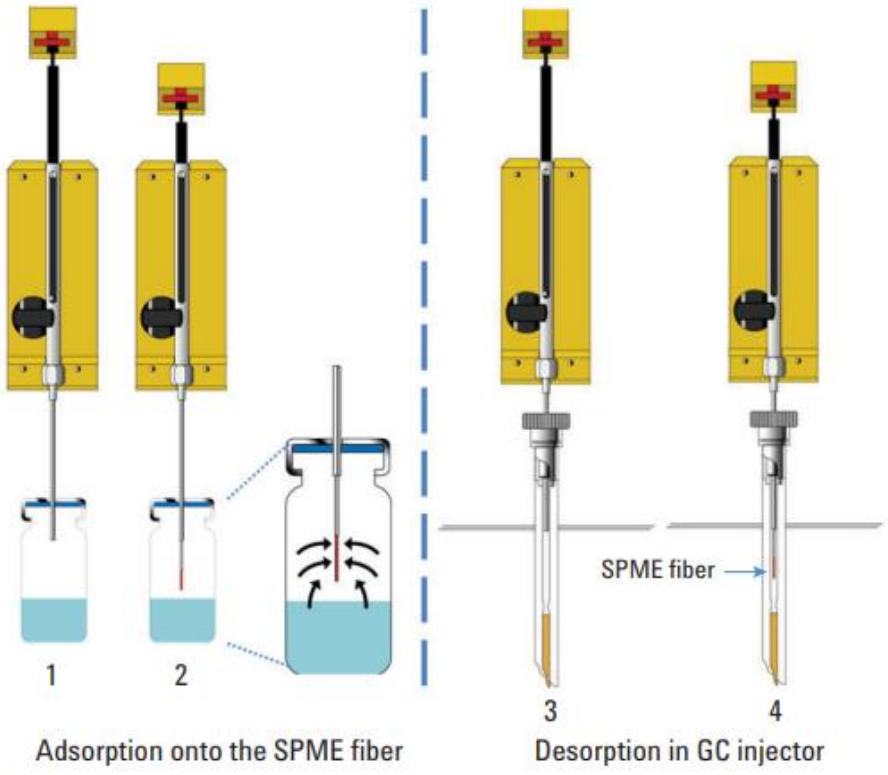

Figure 11 Syringe injection to the vial (1) SPME adsorption (2) and, syringe injection into GC inlet (3) subsequent desorption (4) in the GC injector (You, 2012).

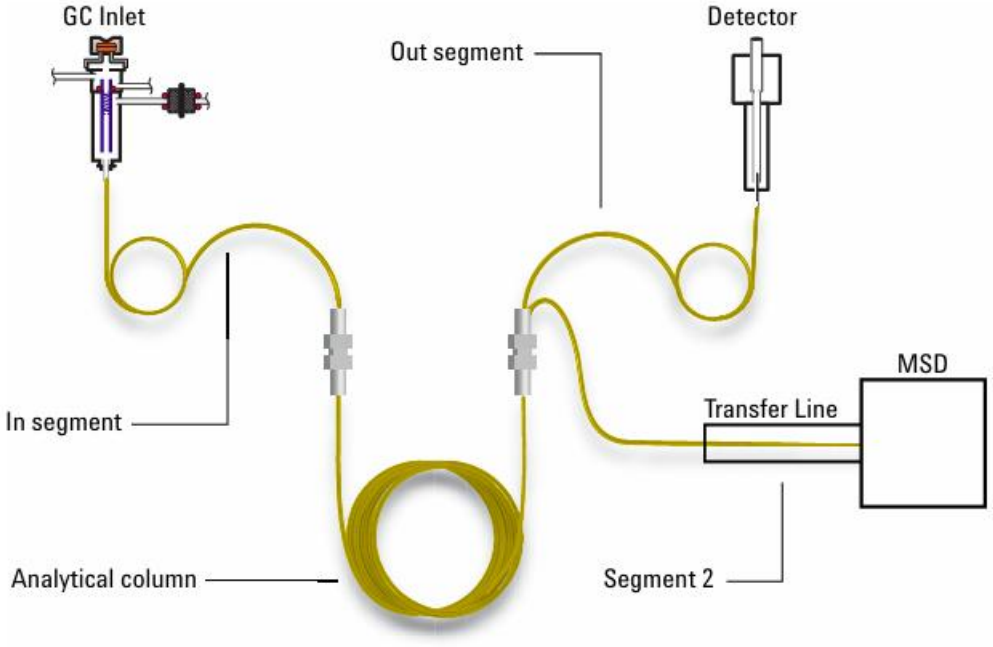

Figure 12 GC-MS column (Agilent 7890B Gas Chromatograph Operation Manual, 2015)

Analytes were separated on a ZB5-MS capillary column (30 m × 0.25 mm × 0.25 µm) as shown on the Figure 12 using the temperature program detailed in Table 8.

Eluting compounds were ionized by electron ionization (EI) and detected by mass spectrometry, producing characteristic fragmentation patterns for compound identification.

3.1.5 Mass Spectrometric Detection (MSD)

Mass spectrometric detection was performed in Selected Ion Monitoring (SIM) mode rather than full-scan (SCAN) mode. In SCAN mode, the instrument acquires data across a wide mass-to-charge (m/z) range, providing an overview of all ionizable compounds in the sample; however, this approach offers limited sensitivity for trace-level analysis. SIM mode, by contrast, monitors only a small number of pre-selected diagnostic ions specific to the target compounds. By dwelling exclusively on these ions, the instrument collects more signal per unit time, reducing chemical background noise.

Target and qualifier ions for geosmin and 2-methylisoborneol (2-MIB) were identified using pure standards analyzed in full-scan (SCAN) mode to determine retention times and the most abundant, structurally characteristic fragment ions (Figures 13 and 14). These ions were then used to develop a selected ion monitoring (SIM) method, which was initially run using the most abundant ions at the widest mass resolution to maximize sensitivity and assess potential interferences. For the strongest ions, nearby m/z values were subsequently evaluated at unit mass resolution to optimize ion selection. The final SIM method employed one target (quantifier) ion and one qualifier ion for each compound. This approach improved both sensitivity and selectivity by excluding co-eluting matrix components that did not produce the monitored ions, resulting in cleaner chromatograms and lower limits of detection and quantification (Thomas, 2022).

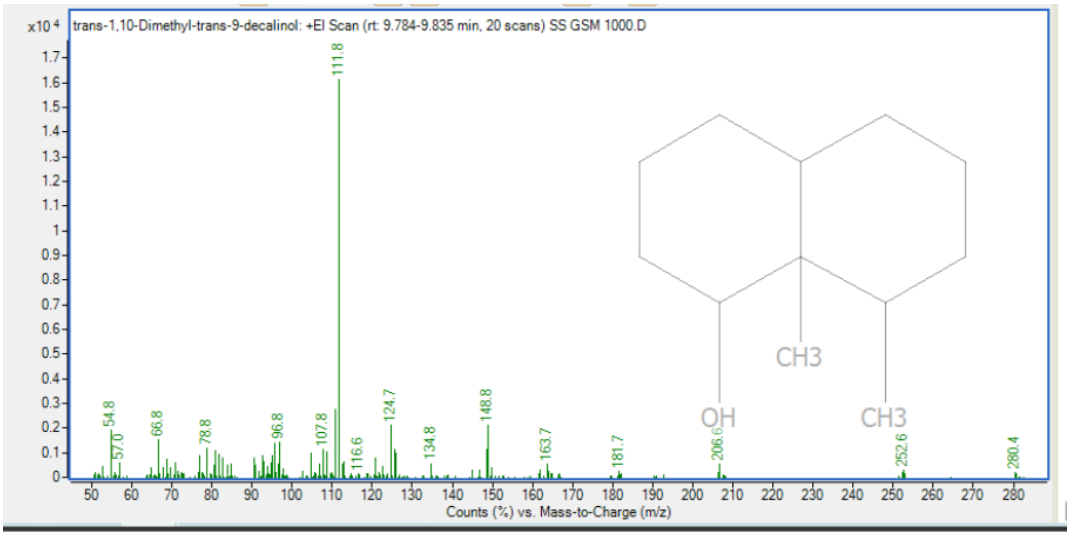

Figure 13 Example of Ions from MS spectrum of the Scan mode for geosmin.

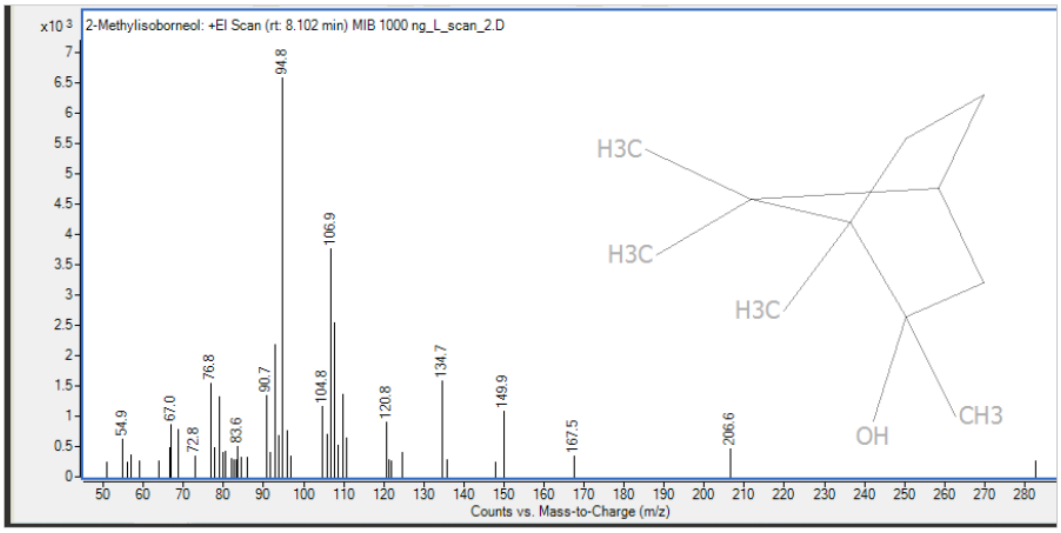

Figure 14 Example of Ions from MS spectrum of the Scan mode for geosmin.

3.1.5 Method parameters adjustments

200 ng/L samples of geosmin and MIB standards were prepared in artificial sea water to adjust method parameters.

Fibre conditioning time, sample incubation time and temperature, sample extraction and desorption time, oven temperatures/times, column inlet temperature, oven temperature profile and ion source temperature were adjusted to optimize the method (tested parameters are presented in the table below). The final parameters of the method

are presented in Chapter 4. Parameters were optimized mainly based on the peak area and for reducing the overall sample analysis time.

Table 7 Method parameters adjustments.

	Adjustments
Sample incubation time Incubation temperature 60 °C	10 min, 20 min 30 min
Extraction to SPME fibre	10 min 15 min
Desorption time	2 min 4 min 5 min
SPME fibre conditioning time and Conditioning Temperature 270° C	0 min 5 min
Column inlet temperature	200 °C 250 °C
Ion source temperature	250 °C 270 °C

GC-MS oven temperature, rate and hold time were adjusted to increase selectivity and sensitivity and to reduce overall time as shown in the Table below.

Table 8 Oven temperatures, rate and holding time adjustments.

		Rate (°C/min)	**Value (°C)**	**Hold Time (min)**
1	Initial	-	50	3
	Ramp-1	20	180	0.5
	Ramp-2	10	270	0.5
2	Initial	-	50	3
	Ramp-1	30	120	0
	Ramp-2	7	170	0
	Ramp-3	40	250	2
3	Initial	-	60	2
	Ramp-1	10	180	0.5
	Ramp-2	20	270	0.5
4	Initial	-	50	1
	Ramp-1	30	140	0
	Ramp-2	5	170	2
	Ramp-3	40	250	3
5	Initial	-	50	1
	Ramp-1	30	140	0
	Ramp-2	5	170	0

	Ramp-3	40	250	2
6	Initial	-	50	2
	Ramp-1	20	180	0.5
	Ramp-2	10	250	0.5

3.1.6 Effect of SPME enrichment

To evaluate the enrichment recovery of the SPME fibre, samples were analyzed by both direct liquid injection (DLI) and SPME, and the results were compared on the basis of analyte mass injected into the GC-MS system. For direct injection method GSM and MIB samples were prepared in 100, 1000, 10 000, 100 000, 250 000, 500 000 and 1000 000 ng/L concentrations in pure methanol in 2 mL sample vials. Acetone and methanol were used as solvents. Method parameters for DLI were same as for SPME. Injected volume was 10 µL. For the SPME method GSM and MIB samples were prepared in artificial sea water at 10, 50, 100, 500, 1000 and 250 000 ng/L concentration.

3.1.7 Effect of NaCl addition

Geosmin and MIB solutions were diluted to 10, 20, 50, 100, 200 ng/L concentrations in type 1 water and to 0, 10 and 50 ng/L in real sea water. The effect of salt on geosmin and MIB extraction was then investigated by adding 2 g of NaCl to 10 ml of the samples prepared in type 1 water. 2 and 3 g of NaCl was added to each of the samples prepared in sea water in the sample vial for each of the dilutions and sealed. NaCl was first baked in the muffle furnace at 550°C for 5 hours and then stored in the desiccator to eliminate moisture ingress. All samples were analyzed using GC-MS.

3.1.8 Effect of internal standard addition

Internal standard solution was prepared by serial dilution of the standard in methanol, to the final concentration of 10^3 ng/L and was stored in 2 mL vials in the freezer.

To evaluate the internal standard correction, series of samples at 0, 10, 50 and 100 ng/L were prepared in the artificial sea water. 40 mL internal standard was added to each sample and 3 g of NaCl was added. Samples were analyzed using GC-MS.

3.1.9 Effect of contamination

The effect of contamination from reusing GC-MS vials was studied by comparing the following washing methods. 1) Vials were washed with acetone, rinsed with type 1 water, and dried at 70°C. 2) Vials were rinsed with methanol and baked at 250°C for 5 hours. Blank samples of water were analyzed by GC-MS.

3.1.10 Matrix effect

The matrix effect of the solution on GC-MS was assessed by preparing MIB and geosmin samples in sea water, type 1 water and artificial sea water at 10, 50, 100 and 200 ng/L concentrations. These were analyzed by GC-MS. Filtered (with 0.45 micron filter) and unfiltered sea water samples were also assessed to see the difference in analyte detection.

The organic and protein content of the sea water, artificial sea water was measured in quartz cuvettes (10 mm path length) using UV spectrometry at 215 and 280 nm, and turbidity was measured in 20 ml turbidity vials using the Hach turbidity meter.

3.1.11 Effect of competitive sorption to the fibre

MIB and GSM were prepared in mixed samples and in separate samples at 10, 50, 100, 500 and 1000 ng/L concentrations in type 1 water, and subsequently analyzed by GC-MS to determine if detection was affected by competitive sorption onto the fibre.

3.1.12 Effect of time on GSM and MIB volatilization

To examine degradation and loss of GSM and MIB from stock solutions during storage due to volatility, stock solutions at 10^8, 10^6, 10^4 and 10^3 ng/L were prepared on the dates shown in the table below. From these stock solutions, 100 ng/L samples were prepared and analyzed with GC-MS.

Table 9 Standard stock solution concentrations and prepared dates.

	Initial Standard Solution concentrations (ng/L)	**Date of preparation**
GSM	1,000	Oct-25
	10,000	Aug-25
	1,000,000	3-Dec-25
MIB	1,000	Oct-25
	10,000	Nov-25
	1,000,000	Oct-25
	100,000,000	Dec-25

To determine the degradation and evaporation of analytes during experiments and GC-MS analysis time, where samples can sit for up to 8 hours in the sample rack of the GC-MS PAL tool while waiting for analysis, 1000 ng/L samples were prepared and analyzed at 0, 2, 4, 6 and 8 hour intervals from the same vial and from different vials. Due to analyte volatilization and degradation over time, and because each sample analysis required approximately one hour, an average of 8-10 samples per day were analyzed, including blanks.

3.2 Treatment methods

3.2.1 Adsorption by Zeolite

15 mL samples were prepared in 20 mL GC-MS glass vials by spiking artificial seawater with geosmin and MIB to a final concentration of 1000 ng/L each. Two milligrams of zeolite powder were added to each vial, and the samples were mixed on a vertical incubation shaker. At 0, 30, 60, 120, and 240 minutes, duplicate aliquots were transferred into 15 mL polypropylene centrifuge (Falcon) tubes. The suspensions were centrifuged at 4000 rpm for 10 minutes, and 10 mL of the supernatant was then transferred by autopipette into clean 20 mL GC-MS vials. Internal standard and 3 g NaCl were added to each vial prior to GC-MS analysis.

3.2.2 Photocatalysis

3.2.2.1 Preparation of coating

The TiO_2-zeolite Y composite coating was prepared using the dip-coating method. A suspension was prepared by mixing 5 g of zeolite Y powder, TiO_2, with the triblock copolymer P123 in 100 mL of ethanol, followed by the addition of 2.5 mL of 0.1 M HCl. The resulting mixture was stirred vigorously with a magnetic stirrer at room temperature overnight to ensure homogeneity. Quartz tubes were cleaned with 65% nitric acid and dried in an oven overnight prior to coating. The dip-coating process was performed by immersing the quartz tube into the prepared suspension for 5 minutes, followed by air drying for another 5 minutes. This procedure was repeated seven times to achieve a uniform zeolite coating on the outer surface of the quartz tube (Figure below). After the completion of seven coating cycles, the coated tubes were dried in an oven at 60°C overnight to remove residual solvents and subsequently calcined in the muffle furnace at 350°C for 5 hours, with a heating rate of 1°C/min.

Figure 15 TiO2 and Zeolite composite Coating

3.2.2.2 Preparation of samples

150 ml solution was prepared in the quartz reactor with 1000 ng/L geosmin and MIB in the artificial sea water. 10 mL samples were taken from that solution at the start and after 4 hours to measure analyte degradation without photocatalysis and adsorption. Then the solution was exposed to the coating and UV photodegradation and immediately another two 10 ml samples were taken at 0 h. After that two 10 ml samples were taken at 30, 60, 120 and 240 min for analysis. 40 µLinternal standard and 3 g NaCl were added to all the samples collected before analyzing with GC-MS. The same sample preparation procedure was used for UV treatment only and adsorption only experiments.

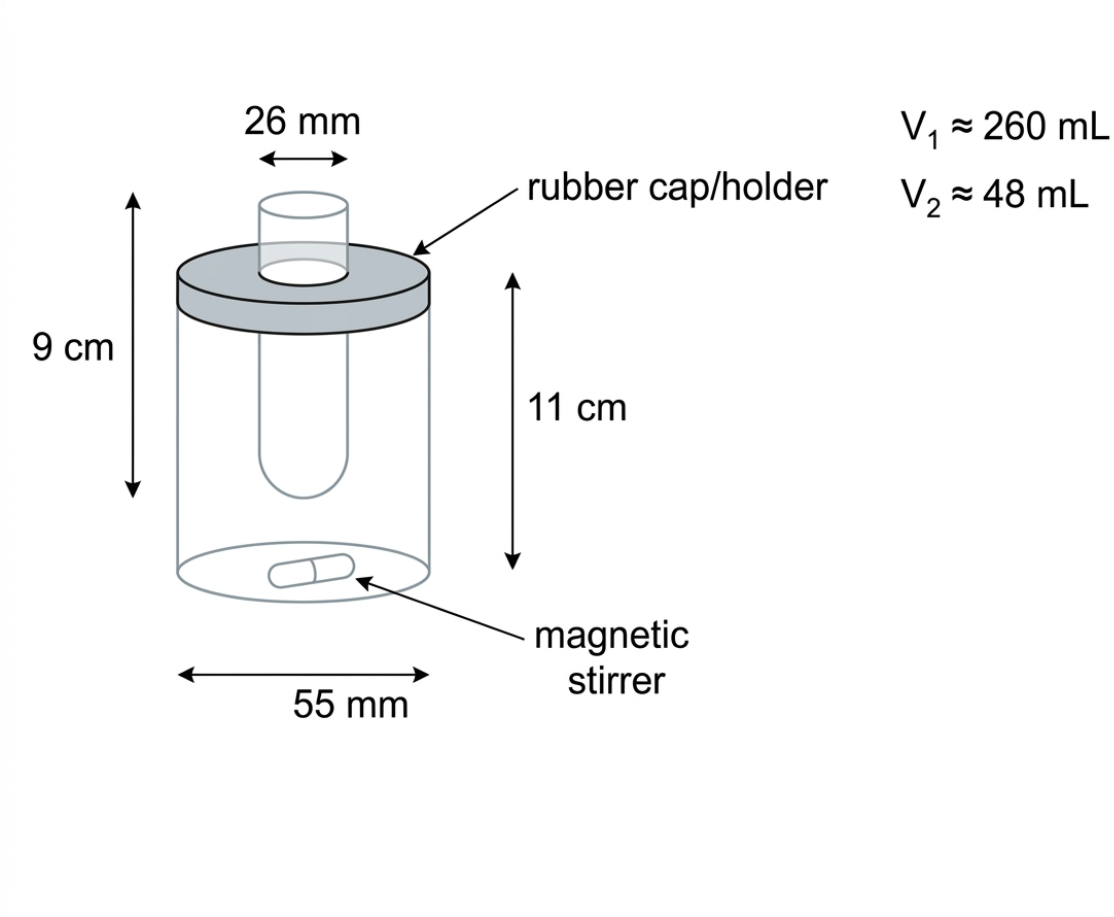

Figure 16 Photocatalytic reactor dimensions.

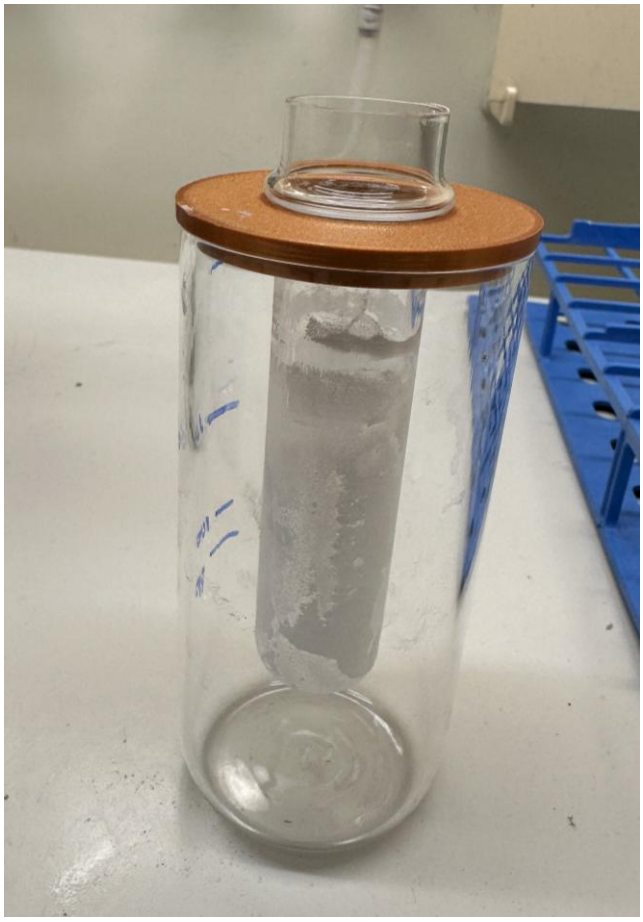

Figure 17 Photocatalysis reactor (quartz)

The mass of the coated tube was measured using a 4 dp electronic balance before and after experiments. The turbidity of the solution was measured with the Hach turbidity meter before and after the experiments.

To prevent an increase in temperature during UV irradiation, the photocatalytic reactor was cooled by continuously circulating distilled water through the inner channel of the coated quartz tube.

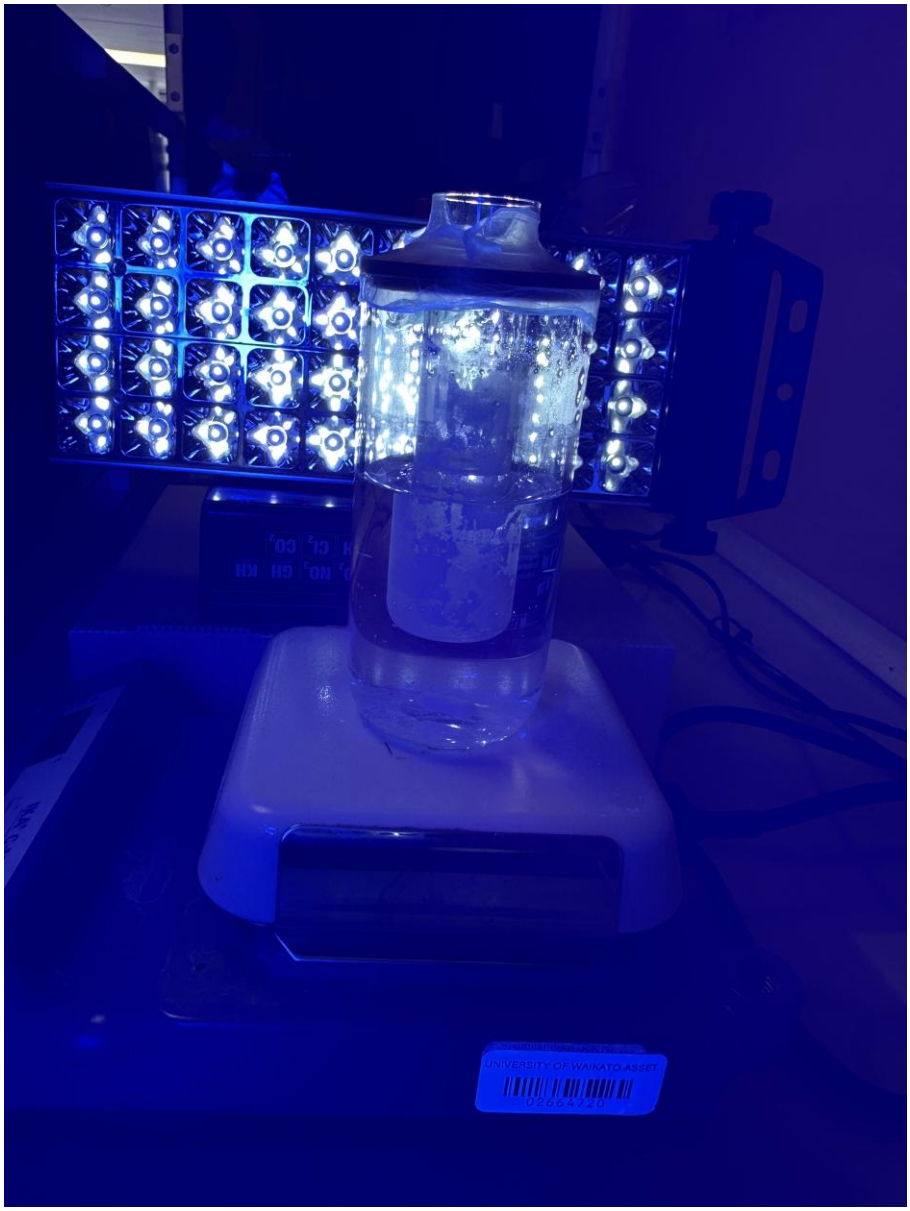

Figure 18 Experiment Setup (Photocatalysis reactor, UV lamp and magnetic stirrer).

3.2.2.3 Characterization of the coating

The composite coating was characterized using optical microscopy and scanning electron microscopy (SEM) image sets at 3.0 kV. Samples were prepared for SEM by mounting small fragments onto the metal stubs using double-sided carbon adhesive tape. After that, graphite paint was applied around the edges to improve electrical contact and minimize charging. The stubs were then gently polished to obtain a smooth, representative surface while avoiding deformation or introduction of artefacts. After

that, the stubs were placed in a sputter coater (Figure 20) and coated once with a 5 nm thick conductive layer of platinum to further reduce surface charging and enhance image quality during SEM analysis.

Figure 19 SEM equipment

Figure 20 Sputter Coating equipment

3.3 Chapter Summary

This chapter described all materials, reagents, instrumentation, and experimental procedures used in this study. Geosmin and 2-MIB analytical standards were prepared by serial dilution in methanol and stored in 2 mL amber vials at -20°C to minimize analyte loss from volatilization. Sample extraction was performed using headspace SPME with a DVB/CAR/PDMS fibre, coupled to an Agilent 7890B GC-MS system operated in SIM mode with internal standard calibration. Key instrumental parameters including fibre conditioning time, incubation temperature, extraction time, desorption time and oven temperature program were systematically optimized to maximize peak area and minimize total analysis time, the results of which are described in Chapter 4.

A series of method validation experiments were conducted to characterize the performance of the analytical method under relevant conditions. These included evaluation of SPME enrichment recovery by comparison with direct liquid injection, assessment of the salting-out effect of NaCl addition, internal standard correction, potential contamination from vial reuse, matrix effects across different water types, competitive sorption between geosmin and 2-MIB on the SPME fibre, and analyte stability over storage and analysis time. These experiments confirmed that analyte volatilization and matrix composition are significant factors requiring careful control throughout sample preparation and analysis.

Treatment experiments were conducted using two approaches: adsorption with zeolite Y powder and UV photocatalysis using a TiO_2-zeolite Y composite coating applied to quartz tubes in a custom-fabricated photocatalytic reactor. Samples were collected at defined time intervals and analyzed by GC-MS. The methods and parameters described in this chapter form the experimental basis for the results presented in the following chapter.

Chapter 4

This chapter presents the results of the GC-MS method development and validation for trace-level detection of geosmin (GSM) and 2-methylisoborneol (2-MIB) in seawater, followed by an evaluation of matrix effects, analyte stability, and practical limitations of the experimental setup. The second part of the chapter applies the validated method to assess four laboratory-scale treatment conditions: powder zeolite, zeolite-TiO_2 composite coating with and without UV irradiation, and UV alone, to identify he most suitable option for marine RAS applications. Results are discussed with reference to the objectives defined in Chapter 1.

4.1 Method Development

About 70% of the experimental work in this study was devoted to developing and optimizing a robust analytical method for trace level detection of 2-MIB and geosmin, with subsequent experiments applying this method to assess photocatalytic and adsorption treatments. The primary objective in the GC-MS method development was to develop and optimize a method able to detect trace level (10 ng/L) geosmin and 2-MIB in seawater.

4.1.1 2-MIB and Geosmin Retention Time Identification

The retention times for geosmin and 2-MIB are given in the figures below. The final retention times for 2-MIB and geosmin are around 7.5 and 9.2 minutes, respectively. Retention time for the internal standard is 7.27 minutes.

Figure 21 confirms that 2-MIB and GSM are well resolved under the final GC-MS method parameters, with retention times of approximately 7.5 and 9.2 minutes, and no

co-eluting interfering peaks at these positions. This separation provided a reliable basis for SIM quantification in subsequent experiments.

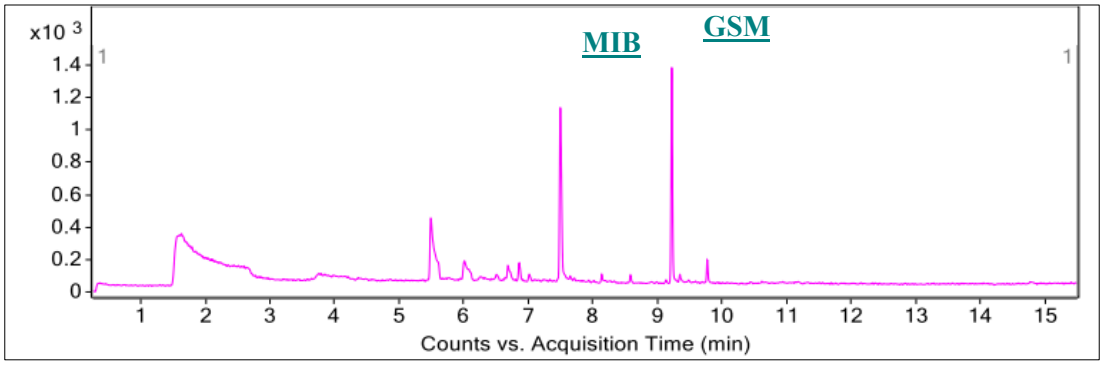

Figure 21 Example of a chromatogram for 2-MIB and GSM standard solutions (100 ng/L) dissolved in artificial seawater measured by GC-MS (SIM mode).

The chromatograms at 500 ng/L (Figures 22 and 23) show symmetrical peak shapes and stable baselines around the target retention times, indicating that the optimized conditions provide adequate sensitivity and chromatographic performance at higher concentrations as well.

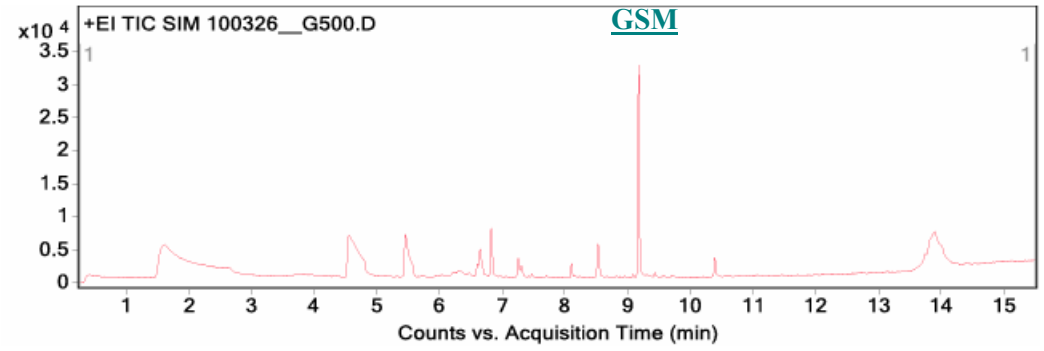

Figure 22 Example of a chromatogram for GSM standard solution dissolved in artificial seawater measured by GC-MS 500 ng/L concentration (retention time 9.125 min)

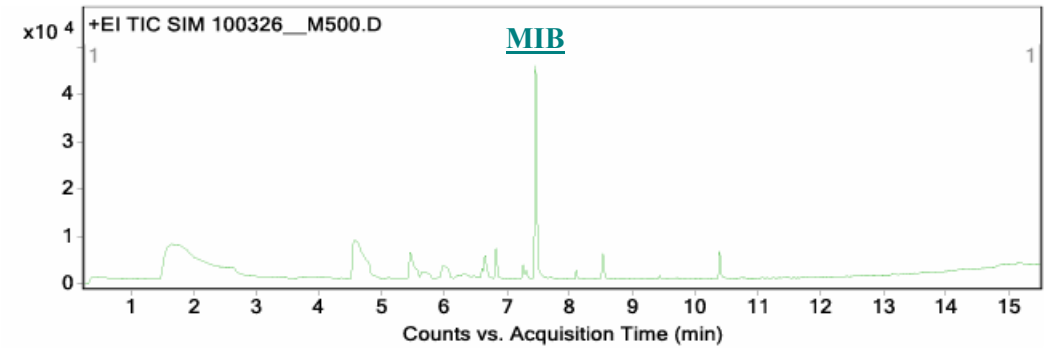

Figure 23 Example of chromatogram for 2-MIB standard solutions dissolved in artificial seawater measured by GC-MS 500 ng/L concentration (retention time 7.7457 min)

Figure 24 presents chromatogram for internal standard (IS) retention time, 7.293 minutes.

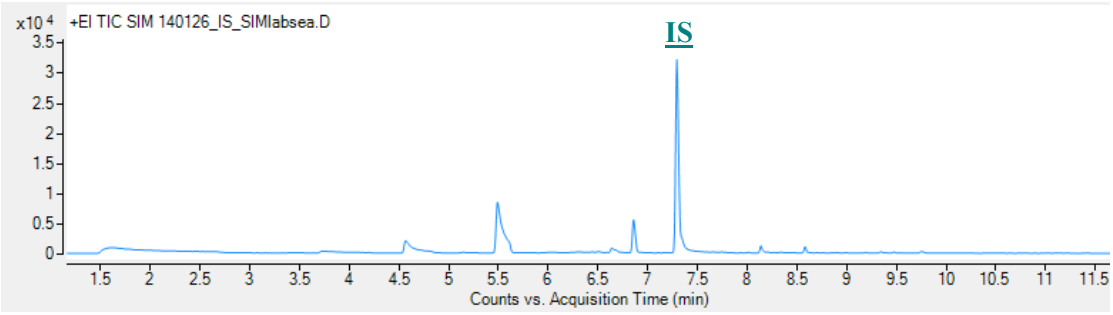

Figure 24 Example of a chromatogram for internal standard solution (100 ng/L) dissolved in artificial seawater measured by GC-MS (retention time 7.293 min)

Possible contamination peaks on chromatogram are trace organic compounds from methanol, sodium chloride, sea salt and type 1 (DI) water; this is discussed in detail in Section 4.3.4.

4.1.2 Detection Mode: Selected Ion Monitoring (SIM) vs Full Scan

GC-MS detection for geosmin and 2-MIB is commonly operated in either full-scan mode (useful for broader confirmation/identification) or selected ion monitoring (SIM) mode (typically higher sensitivity for targeted analysis).

Because total ion chromatogram (TIC) full-scan mode was not sufficiently sensitive for detection at 10 ng/L, a SIM method was implemented. By focusing on only a few ions for a longer time, the instrument collects more ions for those specific signals, reducing background noise. Two ions, one for quantitation and other for confirmation were selected. The SIM ions for Geosmin are 112 and 111; 95 and 107 for 2-MIB and 123.8 and 150.7 for the internal standard (Table below). Full method of selection process is given in Chapter 3.

Table 10 SIM Ions for 2-MIB, GSM and IS.

	Quantifier Ion	Qualifying Ion
2-MIB	95	107
GSM	112	111
IS	123.8	150.7

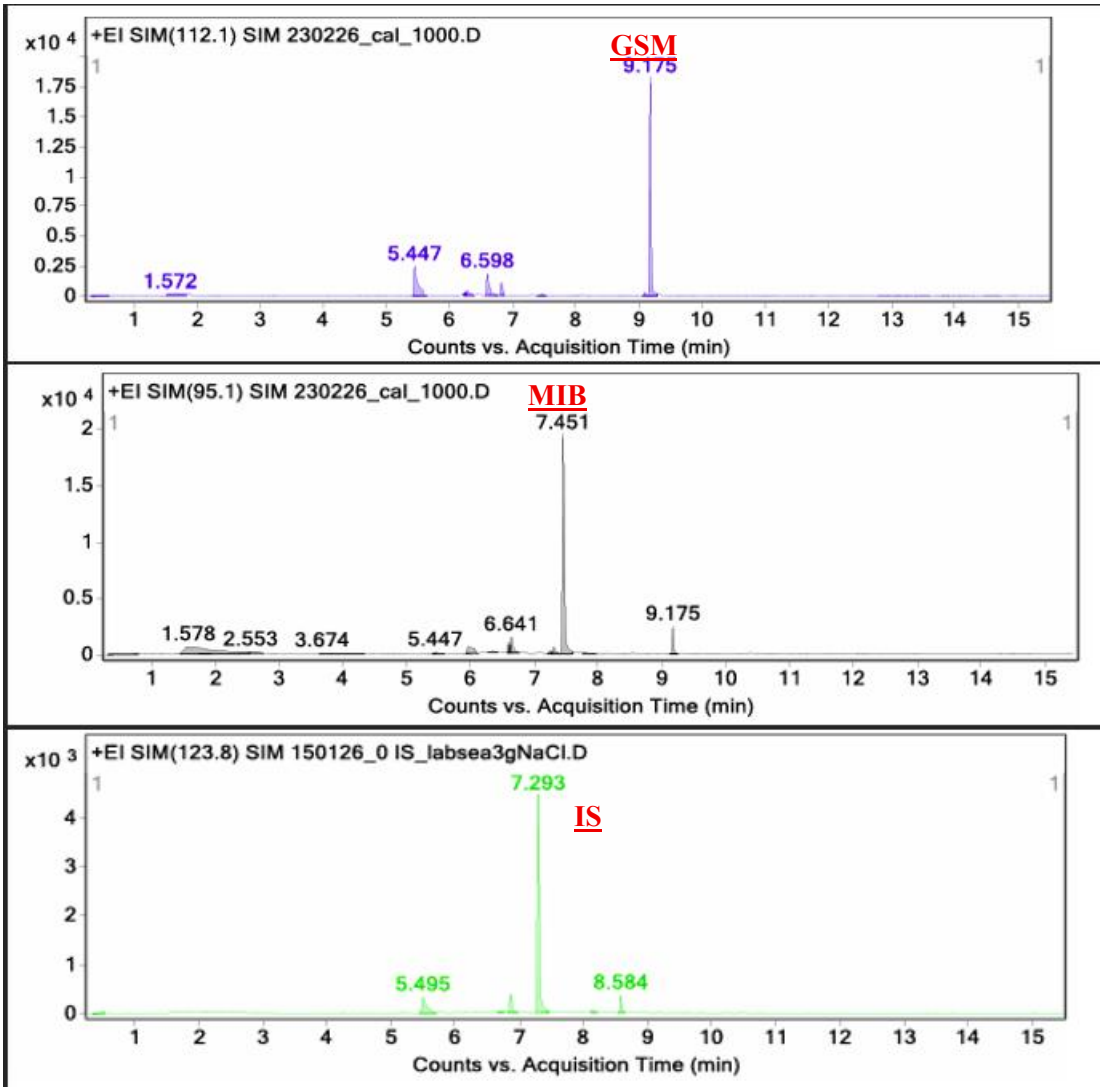

Figure 25 Example of SIM chromatogram for GSM (blue) and 2-MIB (black) (1000 ng/L), and internal standard (green) (40 ng/L) dissolved in artificial seawater.

Figure 25 shows the characteristic mass spectrum of the GSM, 2-MIB and internal standard under the SIM method, with the selected ions providing strong, interference-free signals. This confirms that the chosen quantifier ions are appropriate for selective monitoring and internal standard correction.

4.1.3 SPME Extraction Parameter Optimization

Because these odorants are detectable at ng/L concentrations, analytical methods must routinely reach low ng/L or sub-ng/L detection to be operationally useful for water quality monitoring. Multiple HS-SPME-GC-MS implementations demonstrate that

sub-ng/L LODs are achievable, but they also imply that consistent attainment of these limits depends on tightly controlled extraction and desorption conditions (L. Wang et al., 2025).

The method development involved a careful trade-off, where the timing parameters were optimized to shorten the overall analysis duration without significantly compromising the extraction efficiency and resulting sensitivity.

To reduce the overall analysis time, key timed steps like the extraction and incubation periods were experimentally shortened; however, this acceleration came at the cost of reduced extraction efficiency, leading to lower analyte recovery and diminished sensitivity.

Achieving the highest accuracy and sensitivity in HS-SPME requires optimizing extraction and desorption parameters, including extraction temperature, extraction time, ionic strength (salt), and desorption conditions. After iterative testing of these parameters as summarized in Table below, the following conditions were selected as optimal:

- Incubation temperature 60°C.
- Incubation time 30 minutes.
- Extraction time 15 minutes
- Desorption time 5 minutes.
- DVB/CAR/PDMS Fibre conditioning time 1 minute (before), 5 minutes (after).
- Fibre conditioning temperature 270°C.
- Sample volume 10 mL.
- Column Intel temperature 250°C.
- Ion source temperature 250°C.
- Maximum oven temperature 250°C.

- Helium flowrate 1 mL/min.
- Sodium chloride 3 g.
- Internal standard 40 uL.

Table 11 GC-MS Method Tuning Parameters (sample concentration 200 ng/L, volume in the vial 10 mL).

	Final (selected)	**Adjustments**	**Peak Area, GSM**	**Peak Area, 2-MIB**
Sample incubation time Incubation temperature 60°C	30 min	10 min, 20 min 30 min	8946 15188 21297	N/A
Extraction to SPME fibre	15 min	10 min 15 min	9613 14482	21785 27683
Desorption time	5 min	2 min 4 min 5 min	7233 9004 9613	10529 14338 18056
Column inlet temperature	250°C	200°C 250°C	3294 3566	2893 3766
Helium flowrate	1 mL/min	1.2 mL/min	No change	
Ion source temperature	250 °C	250°C 270°C	9613 10762	21785 19558

Method parameters were optimized based on the peak area responses for both geosmin and 2-MIB, as summarized in the Table above. The results of each parameter adjustment are discussed below.

Incubation time was tested at 10, 20, and 30 minutes. Longer incubation resulted in higher peak areas, indicating improved analyte partitioning into the headspace. Although reducing incubation time would increase sample throughput, it was decided not to compromise extraction efficiency, and 30 minutes was selected as the final parameter.

Extraction time to the SPME fibre was evaluated at 10 and 15 minutes. As with incubation time, longer extraction yielded higher peak areas, and 15 minutes was therefore selected.

Desorption time was tested at 2, 4, and 5 minutes. A desorption time of 5 minutes was selected to ensure complete transfer of analytes from the fibre into the GC inlet.

Column inlet temperature was optimized at 200°C and 250°C. Increasing the inlet temperature from 200°C to 250°C improved 2-MIB peak area by approximately 30%, with a similar improvement observed for geosmin. A temperature of 250°C was therefore selected. This is consistent with the literature, where the majority of published methods (6 out of 9 reviewed) used an inlet temperature of 250°C (Table 12).

Ion source temperature was reduced from 270°C to 250°C. This change resulted in an improvement of over 10% in 2-MIB peak area, while the effect on geosmin was less than 10%. Nevertheless, 250°C was selected as it provided a better overall response. The selected temperature falls within the range of 230-280°C commonly reported in the literature.

Carrier gas flow rate was also evaluated; however, varying the helium flow rate at 1.2 ml/min did not produce a measurable change in peak area for either geosmin or 2-MIB, and the default flow rate of 1 mL/min was retained.

4.1.3.1 Oven temperature profile adjustments

Oven temperature programs reported in the literature vary considerably; however, complete method details are not consistently provided across studies, making direct comparison difficult.

Table 12 Temperature profile in literature.

	Oven Temperature profile						
	Initial, °C	**Ramp up**	**Max T, °C**	**Inlet T, °C**	**Ion source T, °C**	**Transfer line T, °C**	**Reference**
1	50	10°C/min	200	250	230	N/A	(You, 2012)
2	60	10°C/min	270	250	250	280	(Kong & Cao, n.d.)

3	40	5°C/min to 80°C 20°C/min to 140°C 5°C/min to 180°C 50°C/min to 280°C	250	250	230	280	(Tang et al., 2025)
4	35	10°C/min	225	200	280	230	(Lee et al., n.d.)
5	60	10°C/min	300	N/A	N/A	N/A	(Ganegoda et al., 2020)
6	60	30°C/min to 100°C 20°C/min to 300°C	300	250	N/A	N/A	(Schrader et al., 2010)
7	40	10°C/min	250	200	N/A	N/A	(Nam-Koong et al., 2016)
8	60	20°C/min to 150°C 30°C/min to 270°C	270	250	230	280	((Sesha) Pochiraju et al., 2021)
9	60	30°C/min to 100°C 20°C/min to 185°C 40°C/min to 250°C	250	250	N/A	N/A	(Lloyd et al., 1998)

Table 13 oven temperatures tested for 10 ng/L GSM and 2-MIB concentrations.

	Initial temperature and hold time	**Rate and hold time**	**Hold time**	**Run time**	**Retention Time, 2-MIB/GSM**
1	50°C 3 min	20°C/min to 180°C 10°C/min to 270°C	0.5 min 0.5 min	19.5 min	~8.6 / 10.5 min
3	50°C 2 min	20°C/min to 180°C 10°C/min to 240°C	0.5 min 0.5 min	15.5 min	~7.5 / 9.2 min

In this study, the GC oven temperature program was adjusted to reduce total run time while maintaining adequate separation of geosmin and 2-MIB. As shown in Table

above, the overall run time was reduced from 19.5 to 15.5 minutes by optimizing the maximum oven temperature and the initial hold time. The final selected temperature program is presented in Table below.

Table 14 GC-MS Final Oven temperature profile.

	Rate (°C/min)	**Value (°C)**	**Hold Time (min)**	**Run Time (min)**
(Initial)	-	50	2	2
Ramp 1	20	180	0.5	9
Ramp 2	10	240	0.5	15.5

The oven temperature program was adjusted to reduce total run time while maintaining adequate peak separation, though independent optimization of each ramp parameter was not within the scope of this work. Further reduction in cycle time and improvement in peak resolution remain possible through more systematic temperature profile optimization.

4.1.4 Salt Addition

In HS-SPME-GCMS analysis of geosmin and 2-MIB, salt (usually NaCl) is often added to increase ionic strength and create a salting out effect. This helps push the analytes into the headspace and can improve extraction and detection (Tang et al., 2025). However, the benefits of adding salt vary depending on the compound and the sample matrix. Some studies report improved signals, while others show that higher salt levels can reduce extraction due to changes in partitioning, viscosity, or competition at the fibre surface (Manickum and John 2012). Because of this, some validated methods include salt, while others avoid it, especially when low purity salts may introduce extra background peaks.

In this work, salt was not added initially because earlier results suggested that salt reduced 2-MIB and GSM extraction (Yan, 2016). Artificial seawater used in the samples already contained 2.4% NaCl as well.

However, when salt addition was tested, linear trendline analysis confirmed that both slope and R^2 improved with NaCl addition: at 10-200 ng/L, R^2 increased from 0.96 (no salt) to 0.99 (2 g NaCl) and 0.999 (3 g NaCl) for 2-MIB, with similar trends for GSM (Figures 26 and 27). On this basis, 3 g NaCl per 10 mL sample was selected

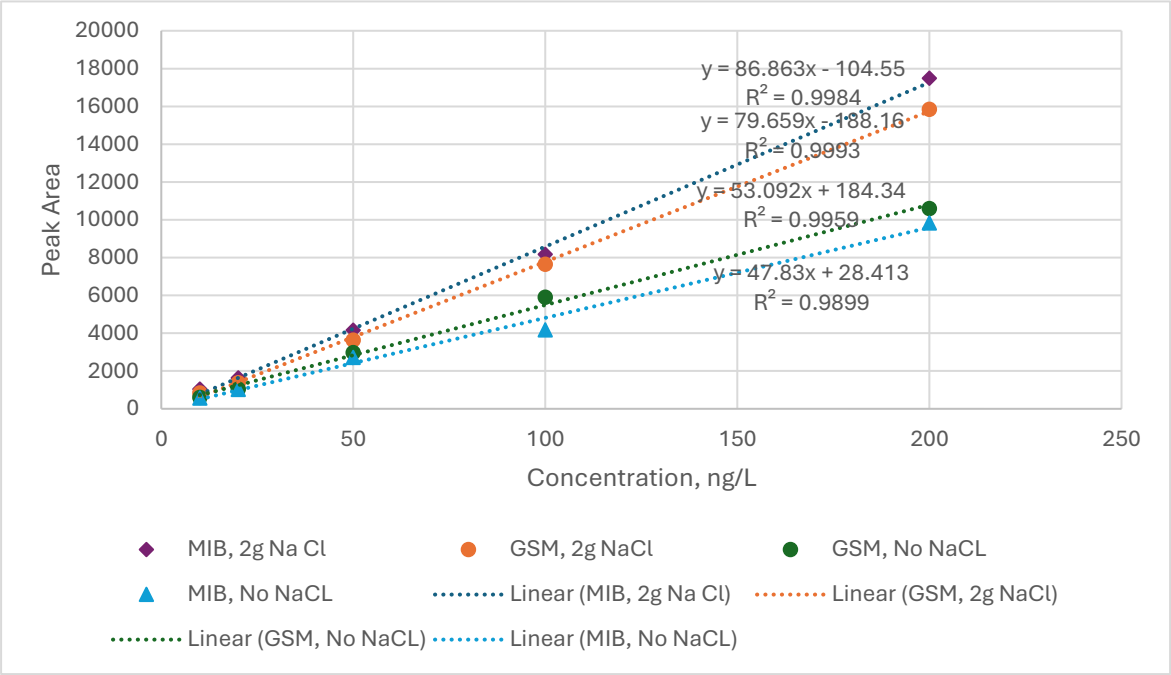

Figure 26 Comparison of calibration curves for samples without addition of NaCl and with addition of 2g NaCl.

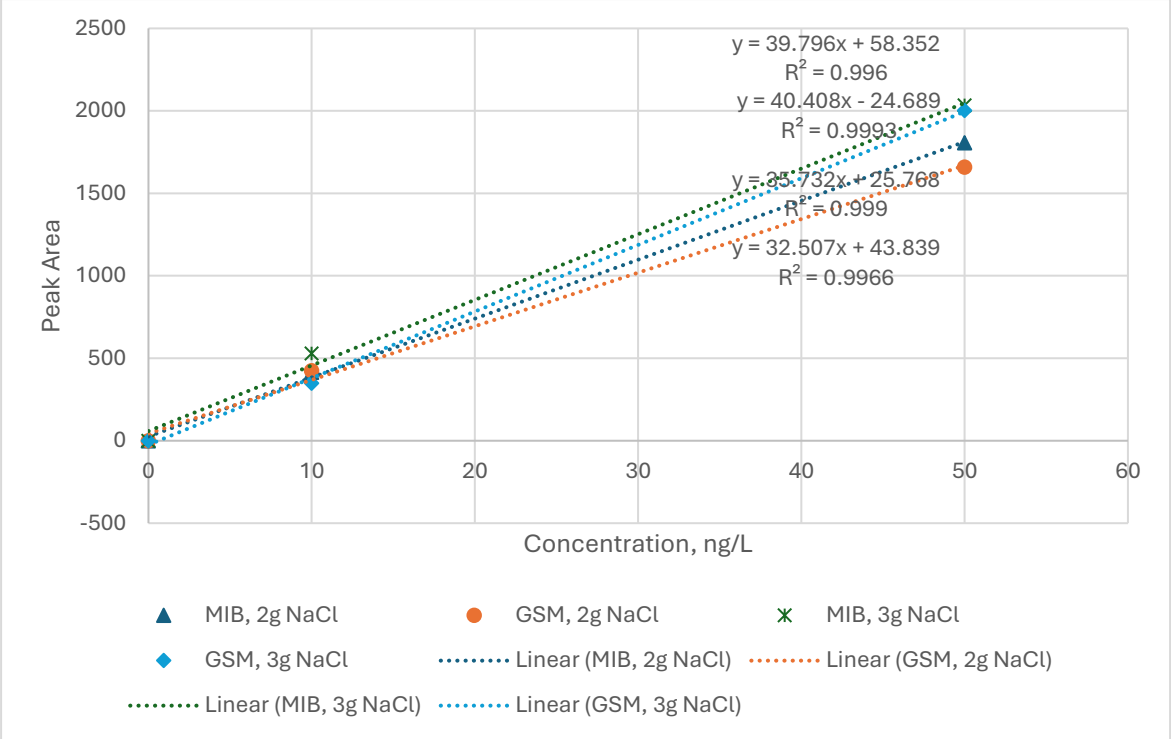

Figure 27 Comparison of calibration curves for samples adding 2g and 3g of NaCl.

As shown on the figure above R^2 of the trend lines and the slopes of the calibration curves with 3 g of NaCl were higher than with 2 g NaCl. Therefore 3 g NaCl was added to further samples.

4.1.5 SPME Fibre Conditioning

Pre-extraction conditioning is mainly used for a new fibre or one that has been stored for a long time. In this step, the fibre is heated to remove manufacturing residues and adsorbed background compounds so that the stationary phase is clean and active for extraction. Post-desorption conditioning is performed right after the sample is injected into the GC to remove any remaining analytes from the coating and avoid carryover in the next run.

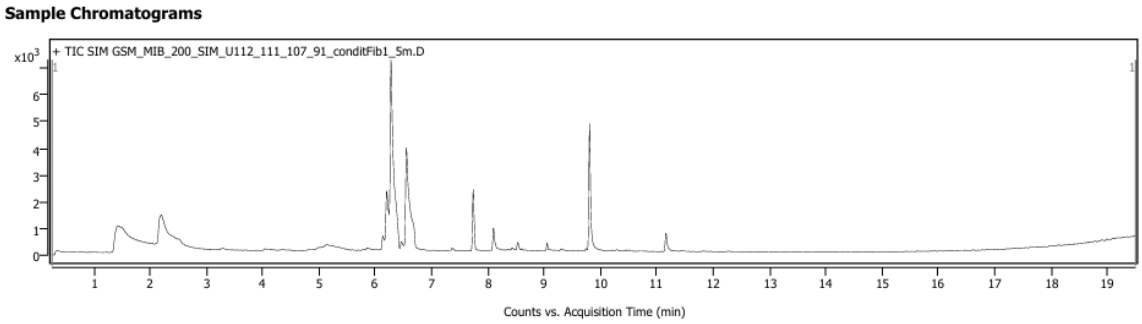

Figure 28 Before post-conditioning fibre for 5 minutes.

In this study, pre-extraction conditioning of 1 minute and post-desorption conditioning of 5 minutes was selected as optimal. The effect of post-desorption conditioning was evaluated by comparing chromatographic noise at the retention time (6.25 min) before and after conditioning. The background signal decreased from 30,379 to 21,800 peak area units - a reduction of over 30% - confirming that 5 minutes of post-desorption conditioning was sufficient to achieve a clean baseline (Figures 28 and 29).

The 30% reduction in background signal following 5-minute post-desorption conditioning confirms that residual analytes from the previous injection were effectively removed from the fibre. This step was therefore applied consistently between all sample runs to prevent carryover and maintain baseline stability.

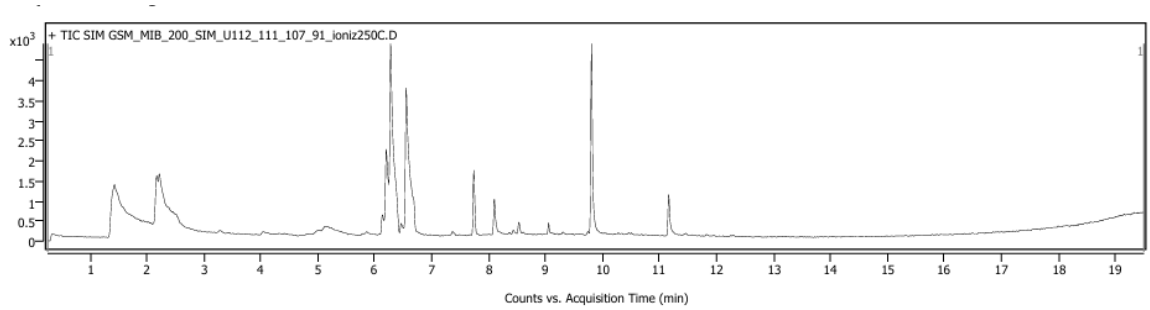

Figure 29 After post conditioning 5 minutes

4.2 Method Validation

4.2.1 Internal Standard and Method Reproducibility

As an internal standard, 2-isobutyl-3-methoxypyrazine was selected, following its use in published drinking water analyses of GSM and 2-MIB (Kong & Cao, n.d.). This compound is not an isotope-labelled standard but a structurally unrelated surrogate with similar chromatographic behavior, chosen for its practical availability and established use in the literature for this application. A volume of 40 µL was added to each sample. Although isotope-labelled standards such as D3-MIB or D5-geosmin (McCallum et al., 1998) would in principle provide better correction for matrix effects and extraction variability, these were not available for this study. The selection of a surrogate internal standard represents a practical compromise; further trials comparing different internal standard candidates could improve method reproducibility and are recommended for future work.

The relative standard deviation (RSD) for geosmin at 10 ng/L was 8%, and for 2-MIB it was 15%, based on three replicate samples. RSD was calculated by dividing the standard deviation of the peak areas by the mean peak area of the three replicates, expressed as a percentage.

$$RSD = (SD/mean) \times 100$$

- RSD (%) - Relative standard deviation, the spread of the data relative to the mean.
- SD - Standard deviation of the dataset.

$$\mathrm{SD} = \sqrt{\frac{\sum(x_i - \bar{x})^2}{n-1}}$$

- mean (or $\bar{x}$) - Arithmetic average of all measurements in the dataset.
- x_i - The i-th individual measurement (each data point in the set).

- n - Total number of measurements (sample size).

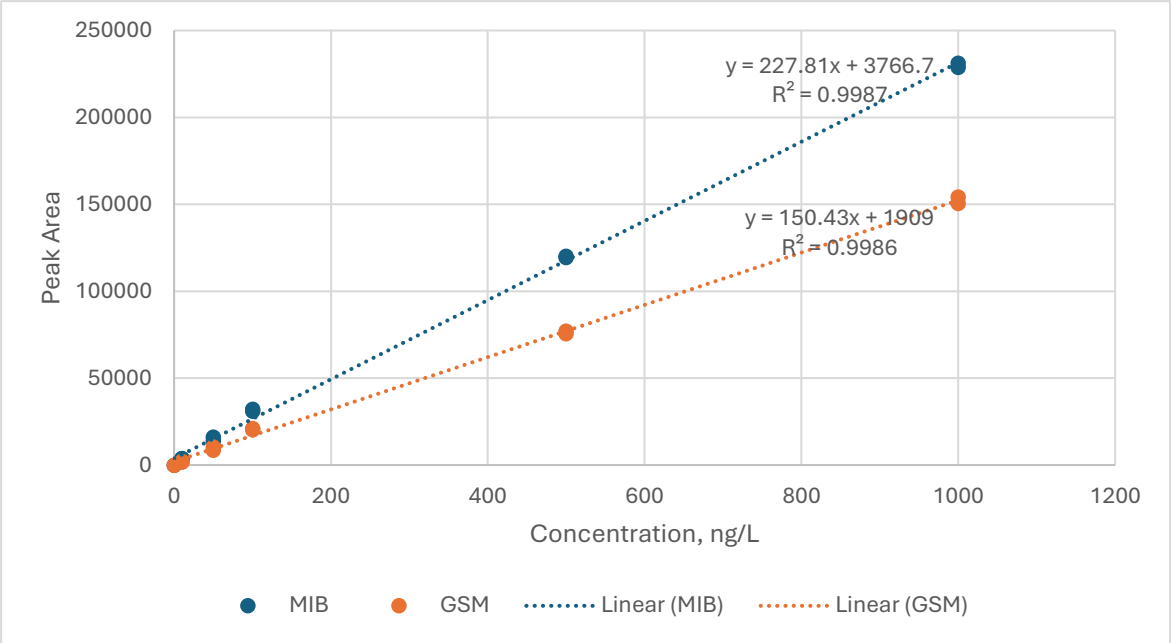

Figure 30 2-MIB and GSM calibration curve with 15% and 8% relative standard deviation at 10 ng/L.

These RSD values at 10 ng/L demonstrate acceptable repeatability for trace-level analysis in seawater, particularly for GSM, and confirm that the internal standard correction stabilizes the response despite the inherent variability of HS-SPME extraction.

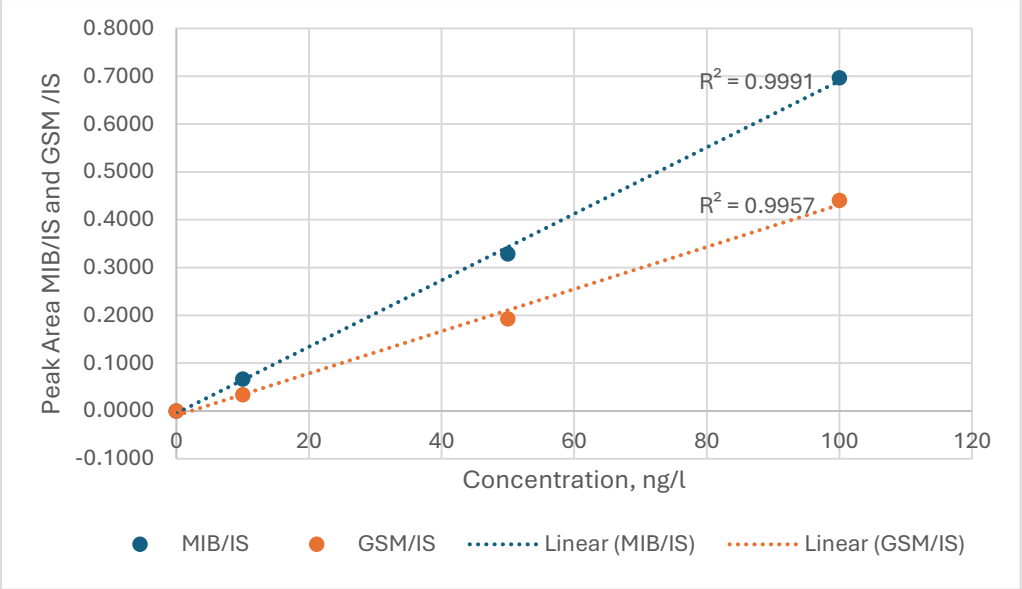

Figure 31 Calibration curve and trend line R^2 with internal standard correction.

As shown in Figure 31, calibration curves constructed with internal standard correction exhibited excellent linearity over the investigated range, with $R^2 = 0.9991$ for 2-MIB and 0.9957 for GSM. This confirms that instrument response is proportional to concentration in the ng/L range relevant for sensory and regulatory thresholds.

In contrast, some calibration curves without internal standard correction (Figure 32) showed markedly poorer linearity ($R^2 = 0.9044$ for 2-MIB and 0.9343 for GSM), illustrating the impact of SPME variability and matrix effects when no internal normalization is applied.

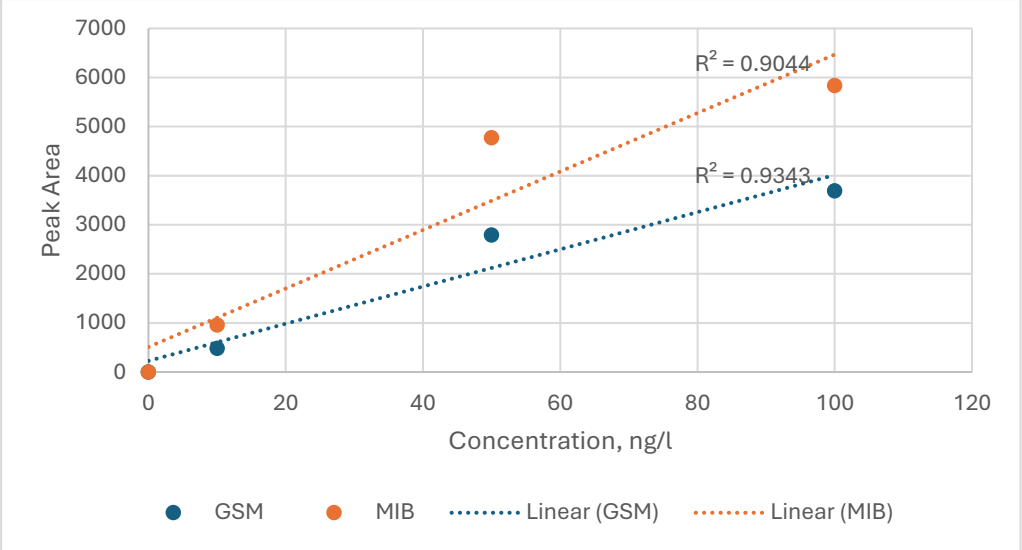

Figure 32 Calibration curve and trend line R2 without internal standard correction.

4.2.2 Calibration curves

For both 2-MIB and GSM in artificial seawater calibration curves showed R^2>0.99 (Figures 33). For real seawater (Figure 34) slopes and R^2 were slightly lower but still within acceptable range, above 0.968 for GSM and 0.997 for 2-MIB. This confirms that the method is valid for these two matrices.

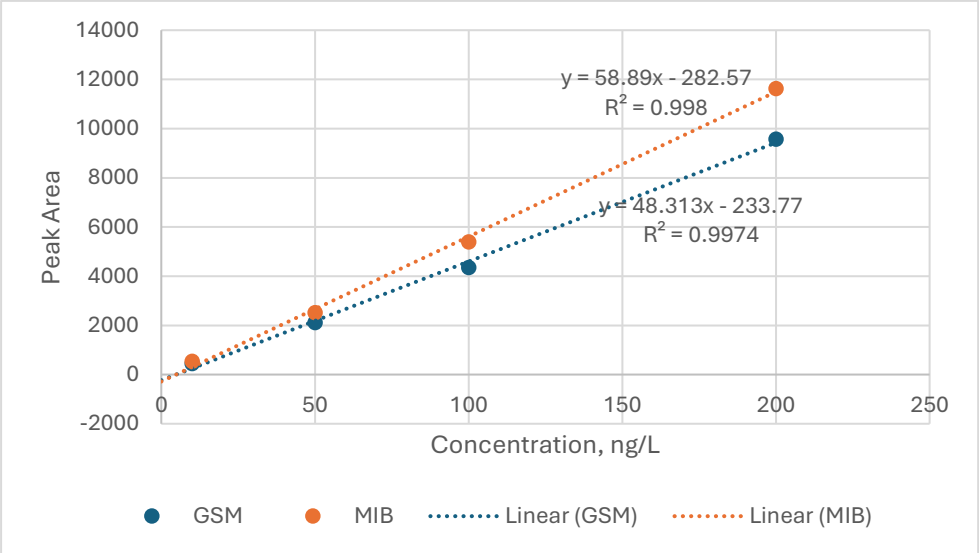

Figure 33 Calibration curves for 2-MIB and GSM in artificial seawater matrix.

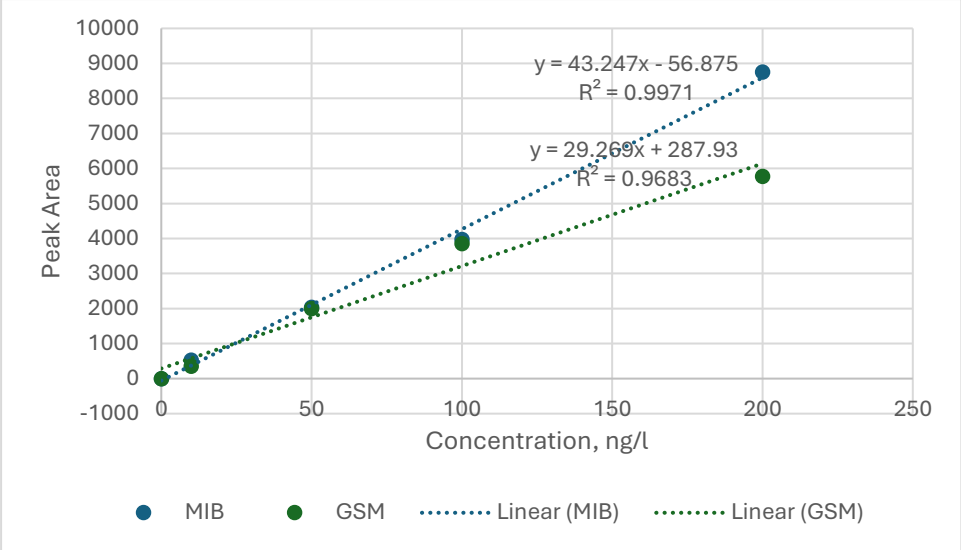

Figure 34 Calibration curves for 2-MIB and GSM in real seawater matrix.

4.2.3 Recoveries

4.2.3.1 Spiked recovery

The method recovery for 2-MIB ranged from **77-87%** when using the internal standard, and **79-93%** for geosmin, which are consistent with RSDs, 15% and 8%, respectively, provided in the Section 4.2.1. Recoveries were calculated by spiking samples with a known concentration of the analyte, determining the measured concentrations from the calibration-curve equation, and then comparing the measured values with the initially spiked concentrations (Equation below).

$$R_{i,\,\mathrm{Total}} = C_{i,\,\mathrm{Meas}} / C_{i,\,\mathrm{Add}} \times 100\%$$

- $R_{i,\,\mathrm{Total}}$ - Total (spike) recovery of compound *i*, (%)
- $C_{i,\,\mathrm{Meas}}$ - Measured concentration of compound *i* in the spiked sample (ng/L)
- $C_{i,\,\mathrm{Add}}$ - Known concentration of compound *i* added to the sample (ng/L)

4.2.3.2 SPME fibre enrichment recovery compared with direct liquid injection method

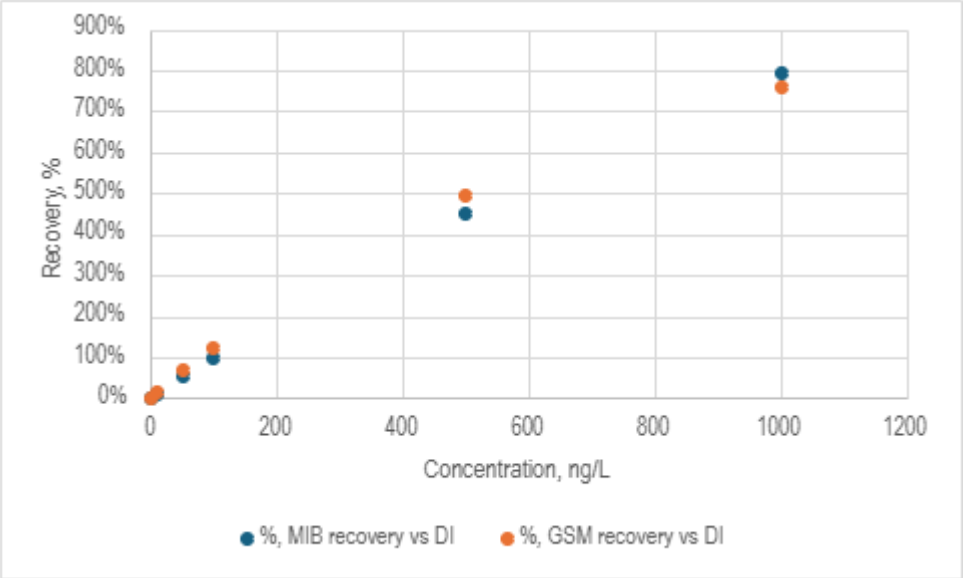

Figure 35 Recovery (fibre enrichment) of SPME extraction vs direct liquid injection by concentration.

Figure above compares analyte recovery between HS-SPME and direct liquid injection across the calibration range. Recovery was calculated by comparing measured peak areas from HS-SPME against those from direct liquid injection, where full equilibrium partitioning, complete headspace transfer, and quantitative fibre adsorption are assumed, giving a theoretical maximum of 100% (sample preparation details are given in the Chapter 3). At concentrations below 100 ng/L, SPME fibre sorption recovery was low, 11% for GSM and 14.6% for 2-MIB at 10 ng/L. Recovery increased at higher concentrations, consistent with the equilibrium-limited nature of HS-SPME extraction and the competitive fibre sorption effects described in Section 4.2.4.

The calibration curves for both methods, based on the mass of the analytes, are shown in the figures below.

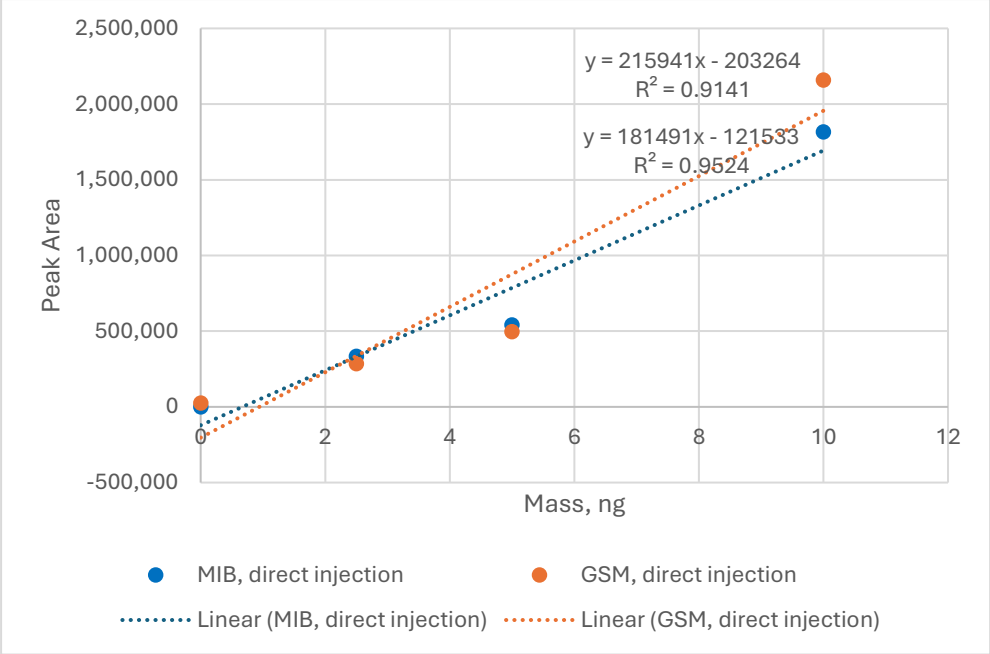

Figure 36 Calibration curves for liquid direct injection method, by mass of the analyte injected (for samples at 250000-1000000 ng/L concentration range).

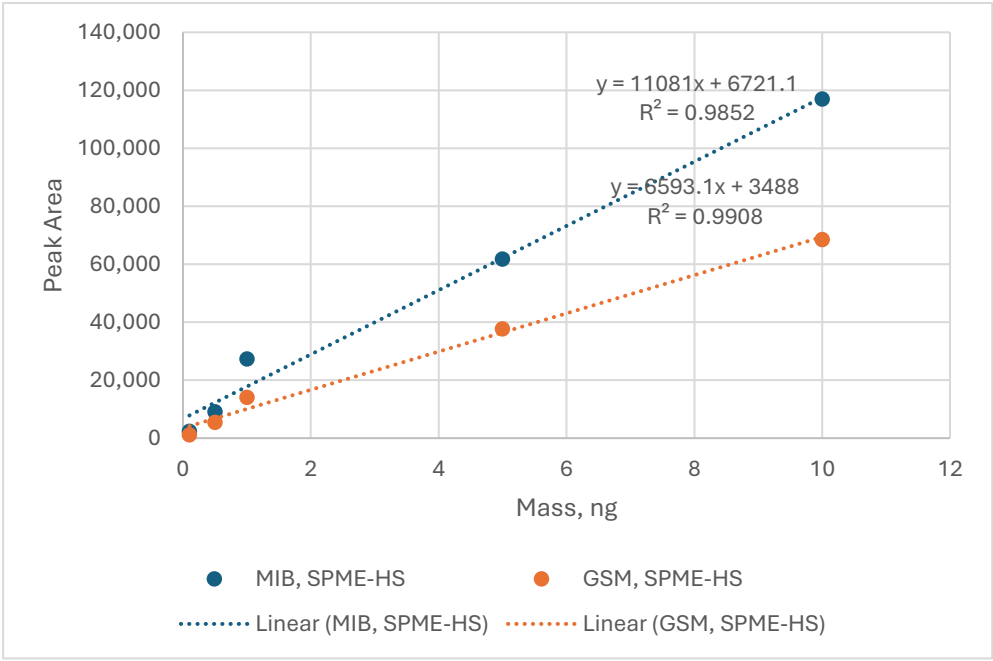

Figure 37 Calibration curves for SPME-HS method, by mass of the analyte in the 10 mL liquid sample (10-1000 ng/L concentration range).

It should be noted that the comparison between HS-SPME and direct liquid injection is not strictly equivalent and should be interpreted carefully. The two methods differ significantly in both sample introduction and matrix composition, with HS-SPME performed from an aqueous sample and direct injection from methanol, and the

comparison based on estimated analyte mass rather than equal concentrations. Because of this, the calculated recoveries represent apparent values under idealized assumptions (such as full equilibrium and complete fibre adsorption), rather than true extraction efficiencies. However, the overall trends remain meaningful, with low apparent recovery at ng/L levels and increasing response at higher concentrations, which is consistent with the equilibrium-limited nature of HS-SPME extraction as outlined in the paper (Lord & Pawliszyn, 2000).

4.2.4 Competitive Sorption Effects

Figures 38 and 39 demonstrate that 2-MIB and GSM peak areas are systematically lower in mixed solutions than in single-analyte solutions, even after internal standard correction. This indicates competitive adsorption on the SPME fibre, meaning that co-occurrence of GSM and 2-MIB in real samples can reduce individual recoveries and must be considered when interpreting quantitative results.

The internal standard correction partially compensates for this, but cannot fully eliminate it, and this limitation should be considered when interpreting absolute recovery values.

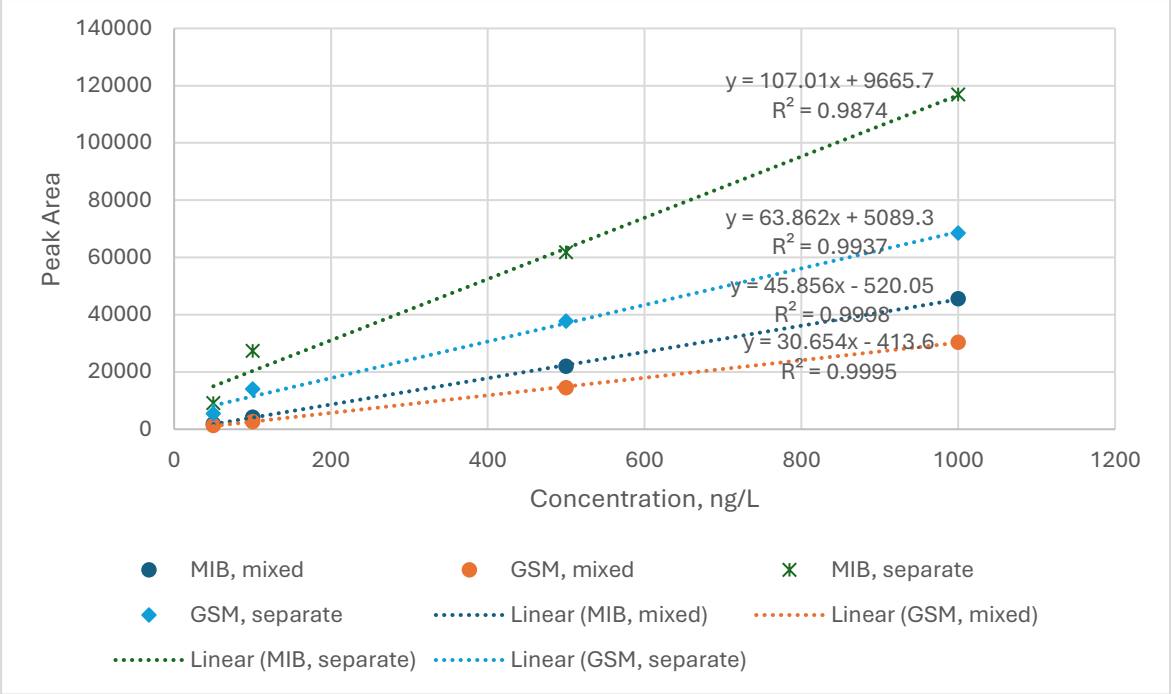

Figure 38 2-MIB and GSM responses in mixed versus single analyte solutions

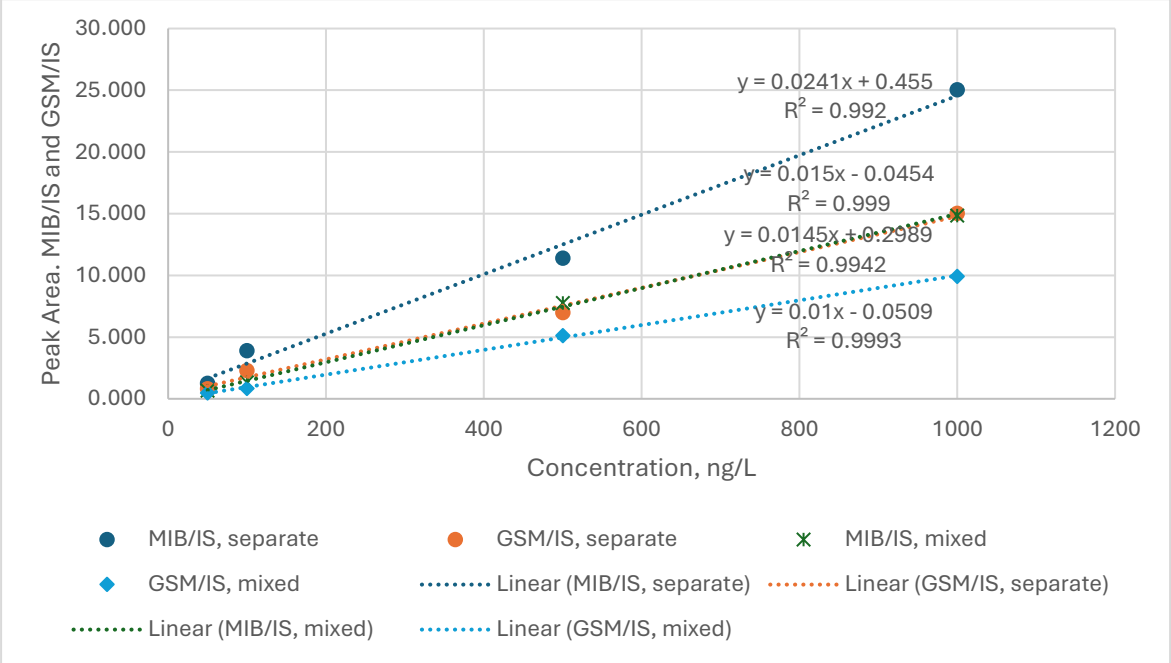

Figure 39 2-MIB/IS and GSM/IS responses in mixed versus single analyte solutions.

In mixed solutions at 50-1000 ng/L, 2-MIB recovery relative to single-analyte samples was 16-39% and GSM recovery was 19-44%, with both declining at higher concentrations (Figure below). This reduction is due to competitive adsorption on the

SPME fibre, when both compounds are present simultaneously, they compete for limited sorption sites, reducing individual extraction efficiency compared to single-analyte conditions.

Since GSM and 2-MIB always co-occur in real RAS water, all measurements in this study are subject to this effect, meaning reported concentrations likely represent a systematic underestimation of true values. Internal standard correction partially compensates for run-to-run variability but cannot eliminate the bias arising from inter-analyte fibre competition. This should be considered when interpreting absolute concentrations and removal percentages reported in the treatment experiments.

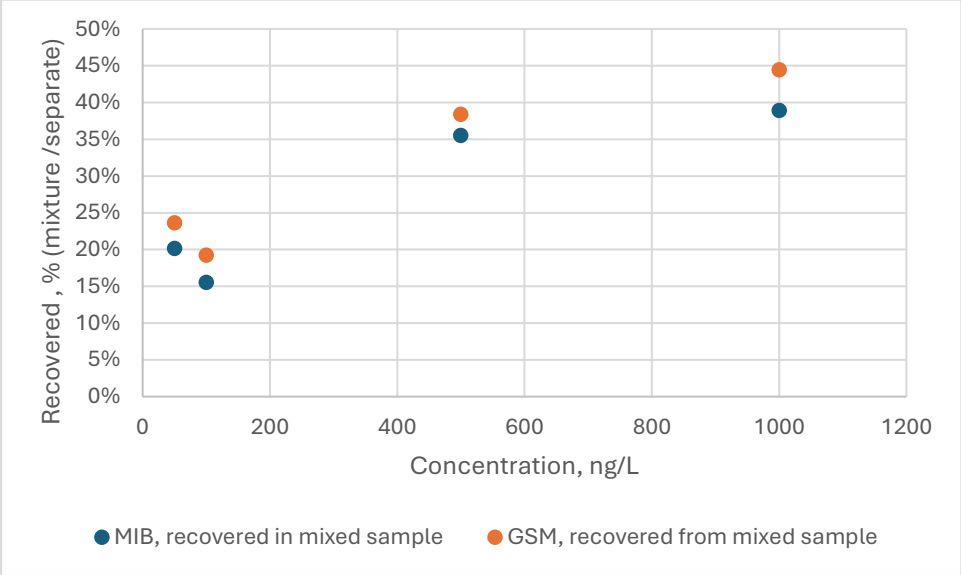

Figure 40 Effect of Competitive Sorption on 2-MIB and GSM Recovery in the mixed Sample.

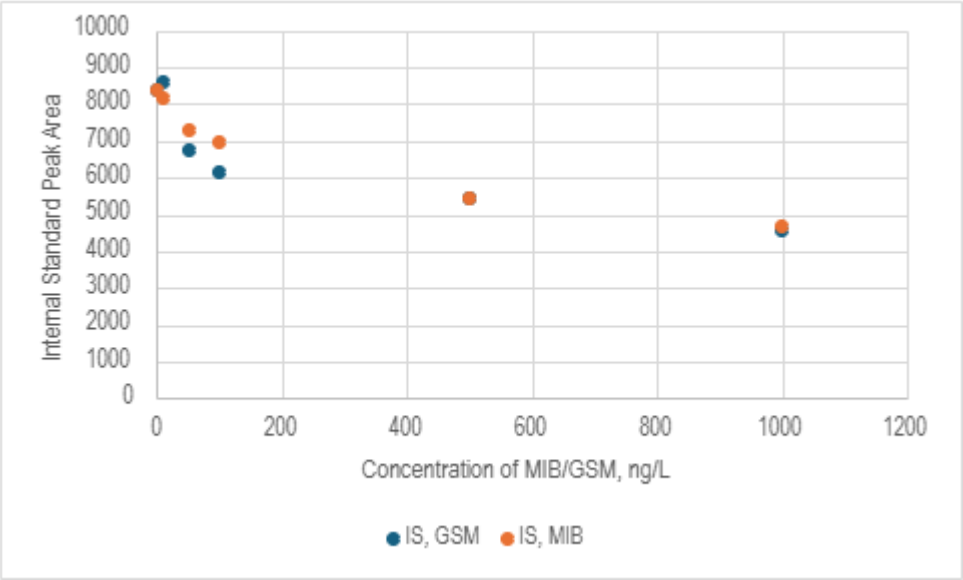

Figure 41 Internal standard Peak Area for 2-MIB and GSM separate samples.

Figure 41 shows that internal standard peak area decreases progressively as 2-MIB and GSM concentrations increase, confirming competitive adsorption on the SPME fibre. This displacement of the internal standard at higher analyte loads directly justifies its use as a correction factor: by tracking fibre saturation effects across all samples, the internal standard normalizes for the variable extraction efficiency inherent to mixed-analyte SPME analysis.

4.2.5 Limit of Detection (LOD) and Limit of Quantitation (LOQ)

Limits of detection and quantification were calculated according to ICH Q2(R1) guidelines as (*Validation of Analytical Procedures: Text and Methodology Q2(R1)*, 2005):

$$LOD = 3.3\sigma/S \text{ and } LOQ = 10\sigma/S,$$

where σ is the standard deviation of the response at the lowest calibration level and S is the calibration curve slope.

The LOD and LOQ for GSM and 2-MIB were determined at 10 ng/L across three water matrices: artificial seawater, real seawater, and Type 1 water.

Table below summarizes signal to noise (S/N) - based LOD and LOQ values for GSM and 2-MIB in artificial seawater, real seawater, and Type 1 water. In all cases, LODs are below 10 ng/L, confirming that the method can detect both compounds at the target trace level, while LOQs reveal that reliable quantification in saline matrices requires concentrations above approximately 25-30 ng/L.

Table 15 S/N, LOD and LOQ values at 10 ng/L concentration of GSM and 2-MIB in different matrices.

		S (signal height)	N (noise height)	S/N	LOD	LOQ
Artificial seawater	GSM, 10 ng/L	800	200	4.00	7.5	25.0
	MIB, 10 ng/L	1105	360	3.07	9.8	32.6
Seawater	MIB, 10 ng/L	245.04	75.7	3.24	9.3	30.9
	GSM, 10 ng/L	216.22	60.0	3.60	8.3	27.7
Type 1 water	MIB, 10 ng/L	435.51	98.0	4.44	6.8	22.5
	GSM, 10 ng/L	535.72	67.0	8.00	3.8	12.5
Artificial seawater*	MIB, 10 ng/L	N/A	N/A	N/A	7.70	23.32
	GSM, 10 ng/L	N/A	N/A	N/A	3.32	10.06

*LOD and LOQ Calculated Based on the Standard Deviation of a Linear Response and a Slope (*Validation of Analytical Procedures: Text and Methodology Q2(R1)*, 2005).

For artificial seawater, LOD and LOQ were additionally calculated using the ICH Q2(R1) standard deviation of a linear response and slope method (*Validation of Analytical Procedures: Text and Methodology Q2(R1)*, 2005), yielding lower values of 3.32-7.70 ng/L (LOD) and 10.06-23.32 ng/L (LOQ), consistent with the S/N-derived estimates.

The additional ICH-based calculations for artificial seawater yield slightly lower LOD and LOQ values, but remain consistent with the S/N estimates, providing independent support for the method's sensitivity at low ng/L levels.

Across all matrices, LOD values were confirmed to be below the target analytical threshold of 10 ng/L, demonstrating that the developed GC-MS method can detect both

GSM and 2-MIB at the regulatory and sensory significance level established in Chapter 1. LOQ values above 10 ng/L indicate that while detection is achievable at this concentration, reliable quantification requires concentrations above approximately 25-33 ng/L in saline matrices. This is consistent with the known challenges of SPME enrichment efficiency and matrix-induced signal suppression in high-salinity water, discussed further in Section 4.3.1.

In summary, consistent quantification at 10 ng/L is technically demanding. Variability arises from three interconnected sources: sample preparation (pipetting errors, incomplete extraction, evaporation, and storage degradation), instrumental factors (detector drift, inlet contamination, and column performance), and data processing errors during peak integration. Additional sources include analyte instability, matrix effects, fibre condition, and analyst technique consistency required at ultra-trace concentrations. Batch sizes were kept to 10-12 samples to minimize oxidation, though samples waiting in the autosampler for over an hour remain susceptible to volatilization losses. The internal standard was applied to compensate for this combined variability, and the improvement in R^2 from 0.90-0.93 to 0.996-0.999 upon applying internal standard correction confirms that it substantially reduces analytical uncertainty at trace level.

Overall, the development and optimization of the GC-MS method for trace-level detection (~10 ng/L) required multiple iterative adjustments of both instrumental and SPME parameters to achieve adequate sensitivity and reproducibility. Only the validated method configuration and its associated results are presented in this study

4.3 Matrix Effects and Seawater-Specific Challenges

4.3.1 Matrix Comparison

Matrix composition has a direct and significant impact on GSM and 2-MIB detection by HS-SPME GC-MS. Complex water matrices can introduce compounds with similar mass fragments or elution times to the target analytes, reducing selectivity and requiring careful optimization to confirm molecular identity. Natural organic matter (NOM) and proteins can also reduce extraction efficiency by competing for SPME fibre sorption sites and binding analytes in the liquid phase, limiting their transfer into the headspace. Four matrices were evaluated in this study: Type 1 (deionized) water, reagent-grade artificial seawater, real seawater and aquarium seawater. As shown in Figures 42 and 43, GSM and 2-MIB signals were consistently lower in real seawater than in Type 1 or artificial seawater, confirming that organic matter and dissolved proteins suppress analyte detection.

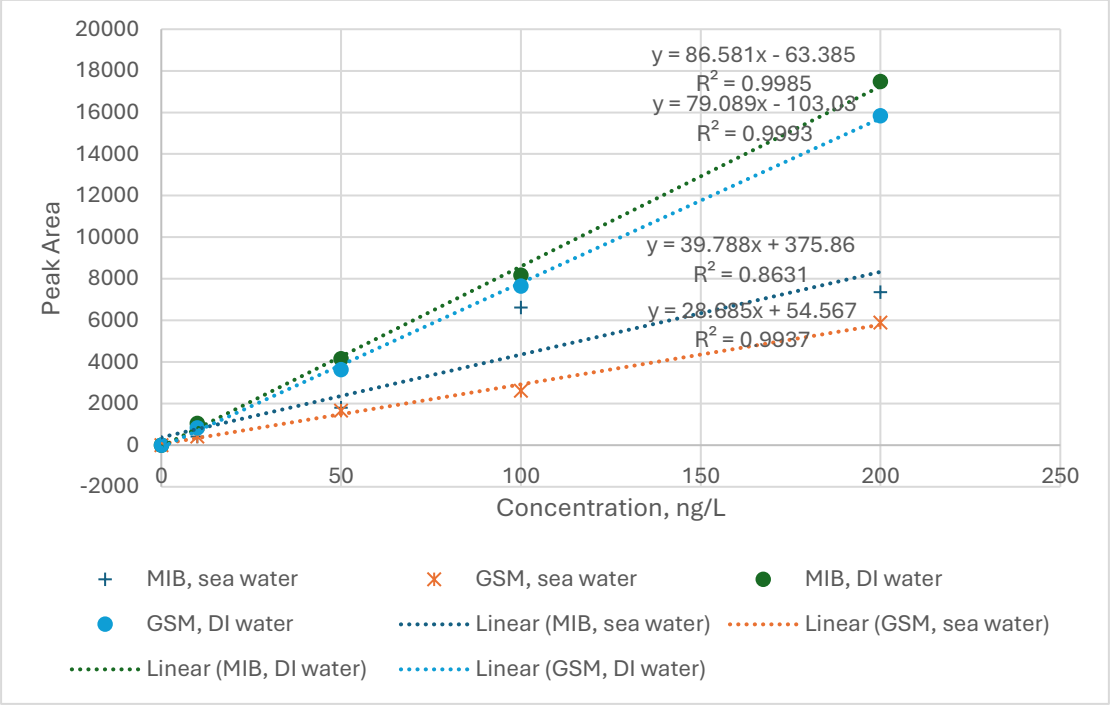

Figure 42 Comparison of 2-MIB and GSM detection in real seawater and deionized water.

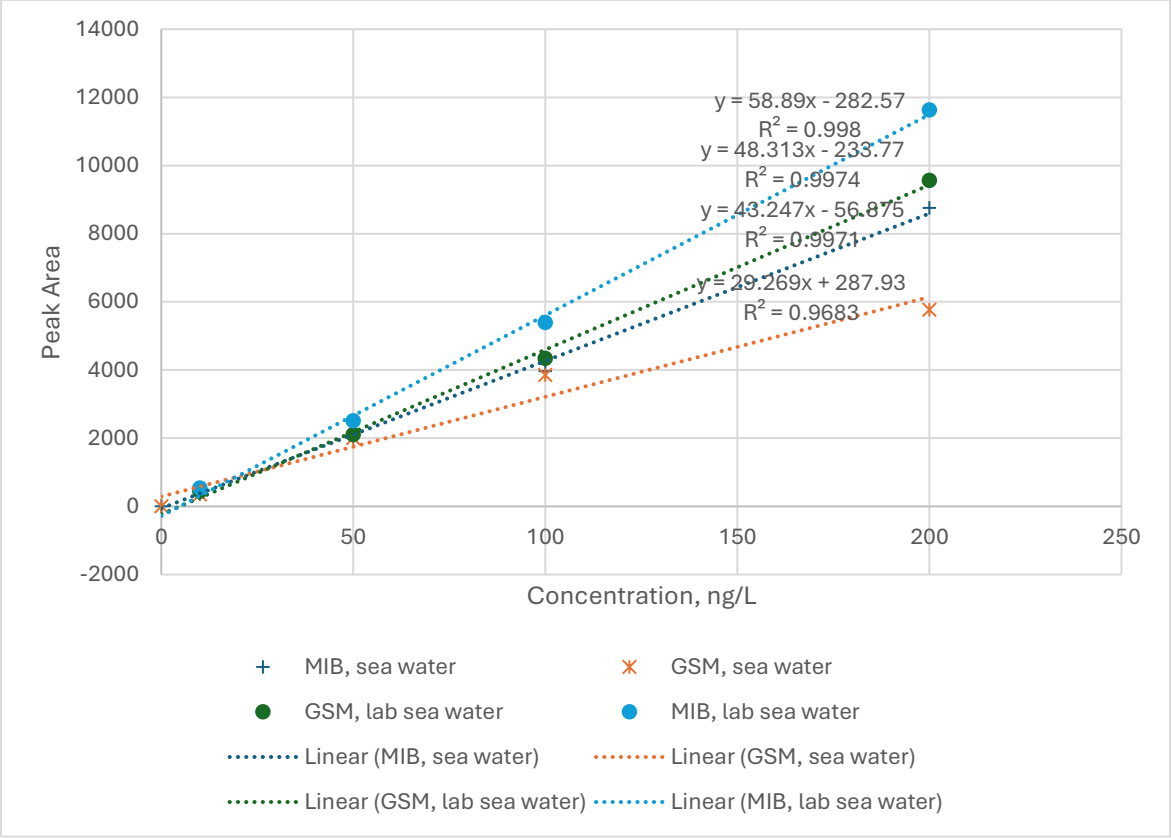

Figure 43 Comparison of 2-MIB and GSM detection in real seawater and artificial seawater.

The most severe case was the aquarium seawater, which had a turbidity of 193 NTU and protein content of UV_{280} = 0.06 - compared to 1.73 NTU and UV_{280} = 0.015 for reagent-grade artificial seawater. These elevated values correspond directly to the numerous interfering peaks observed in the blank chromatogram (Figure below), several of which exceed the 2-MIB signal at 7.5 min, making reliable quantification impossible without extensive pre-treatment.

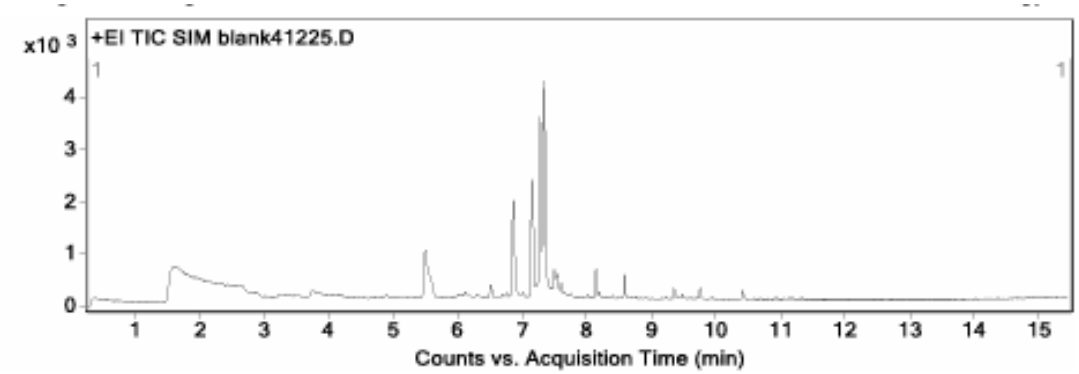

Figure 44 Low purity artificial seawater (for aquarium) matrix effect.

Based on these findings, reagent-grade artificial seawater was selected for calibration. It most closely reflects the ionic strength of real seawater while avoiding the additional interferences present in biological or commercial aquarium mixes. This choice balances matrix-matching requirements with analytical reliability and is supported by the consistently higher and cleaner signals obtained relative to all other matrices tested.

4.3.2 Effect of Filtration on Real Seawater

Analysis showed that filtered real seawater resulted in better extraction of both 2-MIB and geosmin compared with unfiltered seawater, as shown in the figure below. For GSM, the peak area increased from 2976 to 4501 after filtration, while for 2-MIB it increased from 2232 to 3404. This improvement is likely due to the high organic content in unfiltered seawater, which can bind 2-MIB and GSM and reduce their availability for transfer from the liquid phase into the headspace and subsequent adsorption onto

the SPME fibre. In addition, organic compounds may accumulate on the fibre surface, reducing its effective sorption capacity for 2-MIB and GSM.

Comparison of unfiltered and filtered seawater (Figures 45 and 46) reveals that filtration increases GSM and 2-MIB peak areas by roughly 50%, while simultaneously reducing background peaks in the blanks. This suggests that particulate and colloidal organic matter in unfiltered seawater binds GSM and 2-MIB and competes for SPME fibre sites, reducing apparent recovery.

These results are based on a limited number of measurements and should be interpreted as indicative rather than statistically validated findings. Nevertheless, the consistent direction and magnitude of the improvement across both analytes supports the conclusion that filtration is a beneficial pre-treatment step for real seawater samples.

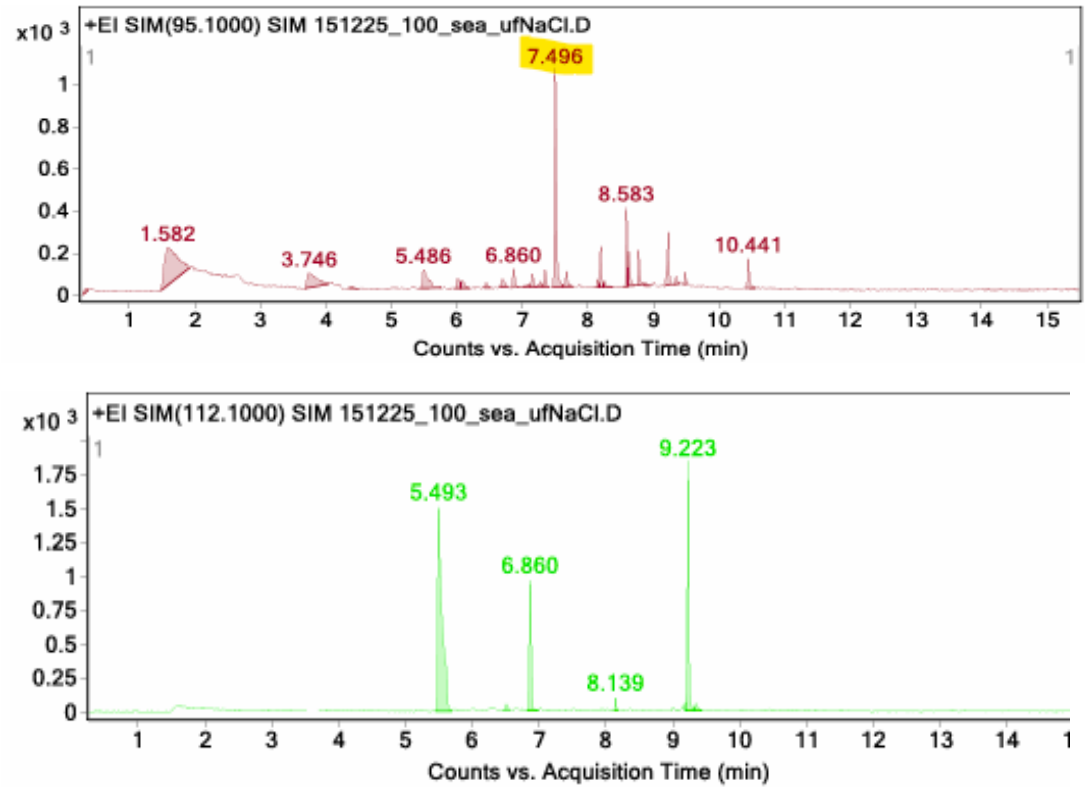

Figure 45 100 ng/L GSM and 2-MIB concentration in unfiltered seawater.

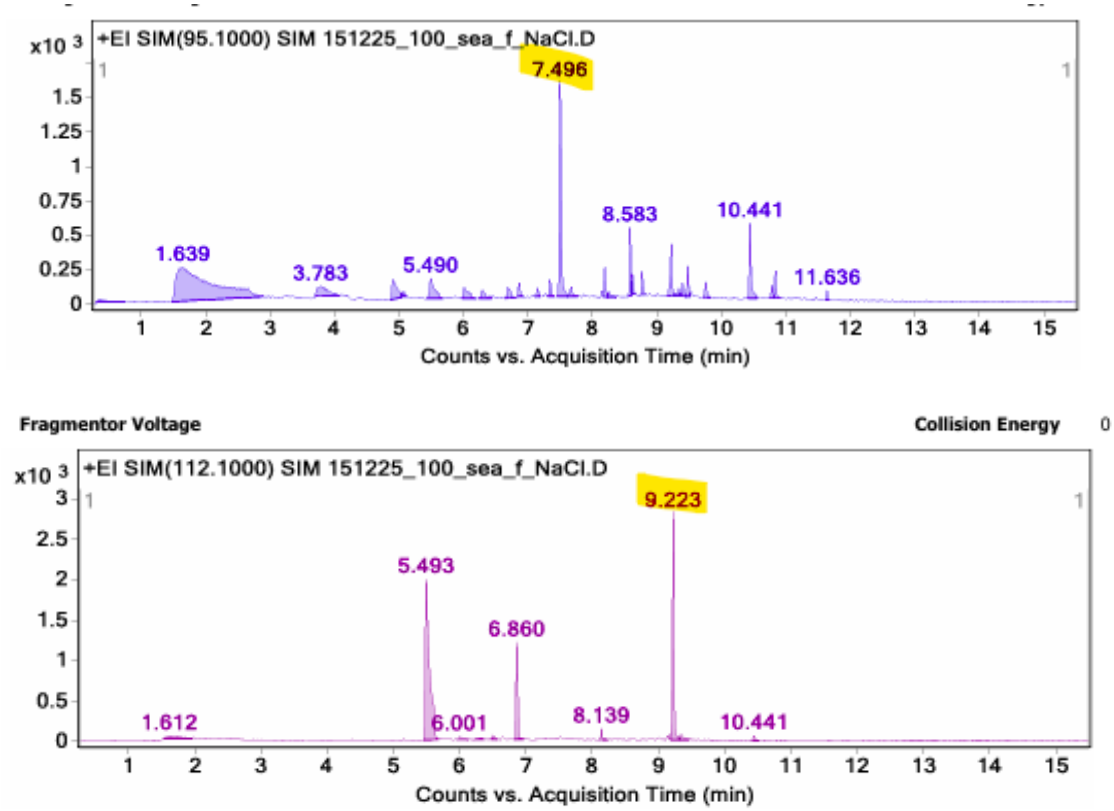

Figure 46 100 ng/L GSM and 2-MIB concentration in filtered seawater.

This effect is supported by the blank sample chromatograms, where unfiltered seawater shows peak intensities more than twice those of filtered samples, indicating a higher level of background interference. In comparison, Type 1 water blanks show a much cleaner matrix with significantly lower interfering peaks, as shown in the figure below. Blank comparisons between unfiltered seawater, filtered seawater, and Type 1 water (Figures 47 and 48) further highlight the impact of matrix composition: unfiltered seawater exhibits more than twice the background signal of filtered seawater, while Type 1 water shows a relatively clean baseline, emphasizing the importance of matrix selection and pretreatment.

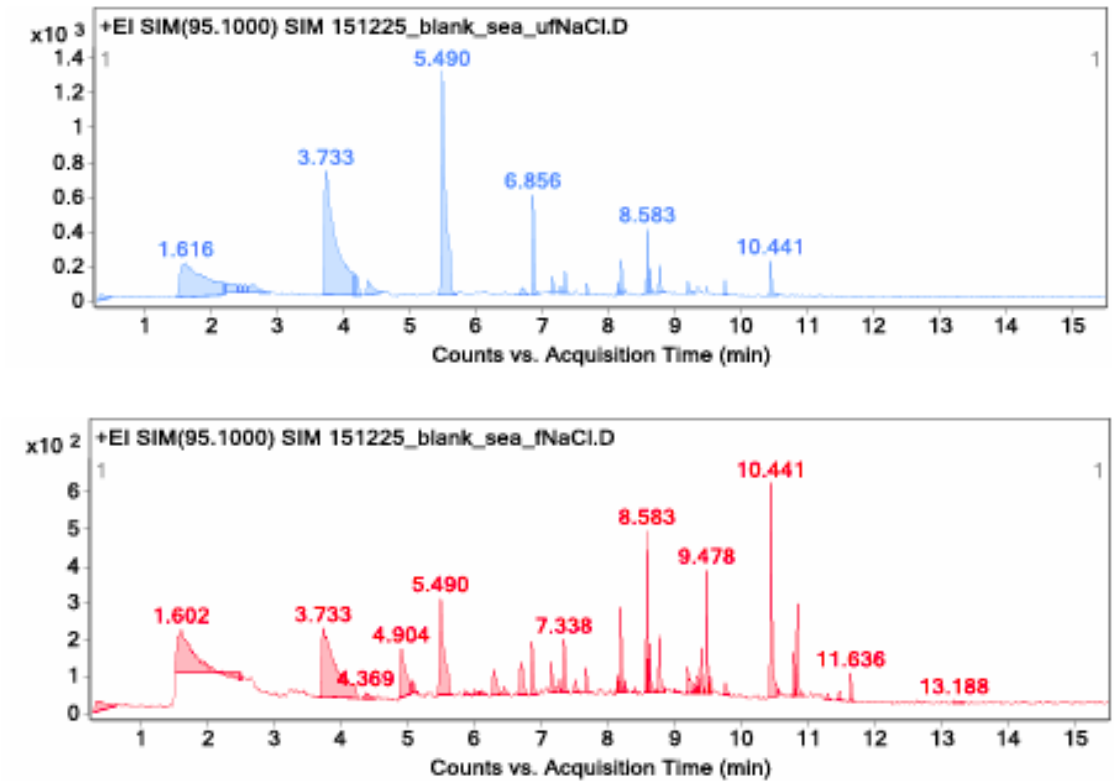

Figure 47 Blank samples of unfiltered and filtered seawater (contaminants peaks).

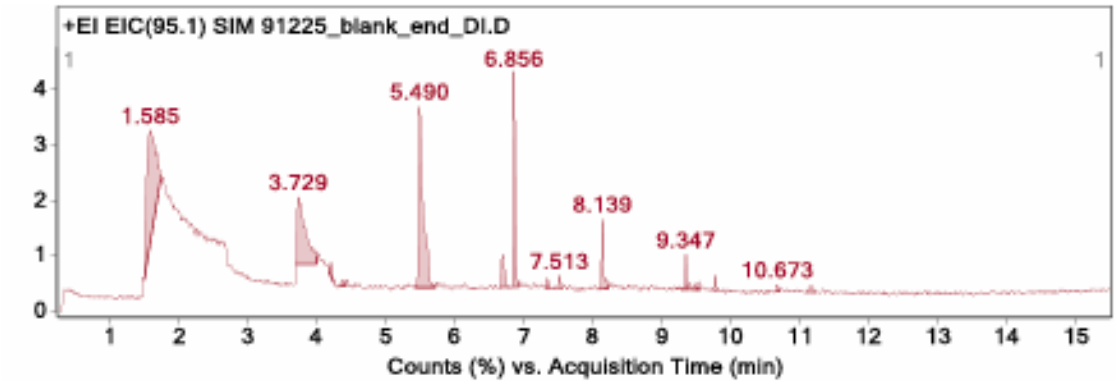

Figure 48 Type 1 water blank sample (contaminants peaks).

Based on these findings, for trace-level detection of 2-MIB and GSM using HS-SPME GC-MS, it is essential to consider both fibre sorption capacity and sample matrix composition, as competitive adsorption of other volatile organic compounds can negatively affect method accuracy and reliability.

4.3.3 Analyte Stability (storage, vaporization over time)

Standard stock solutions were initially prepared in 10% methanol and the rest in deionized water and stored in amber bottles at 10^8, 10^6 and 10^4 ng/L concentrations, prepared at different times (Table 16) at 4°C. These were then used to make samples at 100 ng/L which were then analyzed using GC-MS. Over approximately two months, these solutions degraded by 27-40% for 2-MIB and 13-20% for GSM (Figures below). Due to the GSM and MIB being volatile and also possible degradation over time, the standard solutions were prepared in methanol at 1 mg/L concentration and stored in 2 mL aliquots, filled to the top and in the freezer.

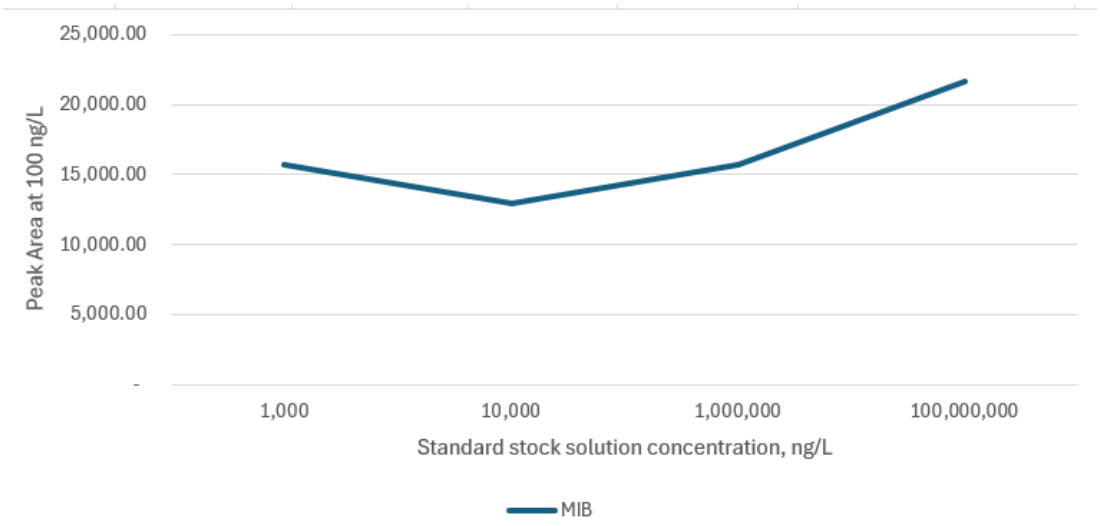

Figure 49 2-MIB Standard stock solution degradation during storage.

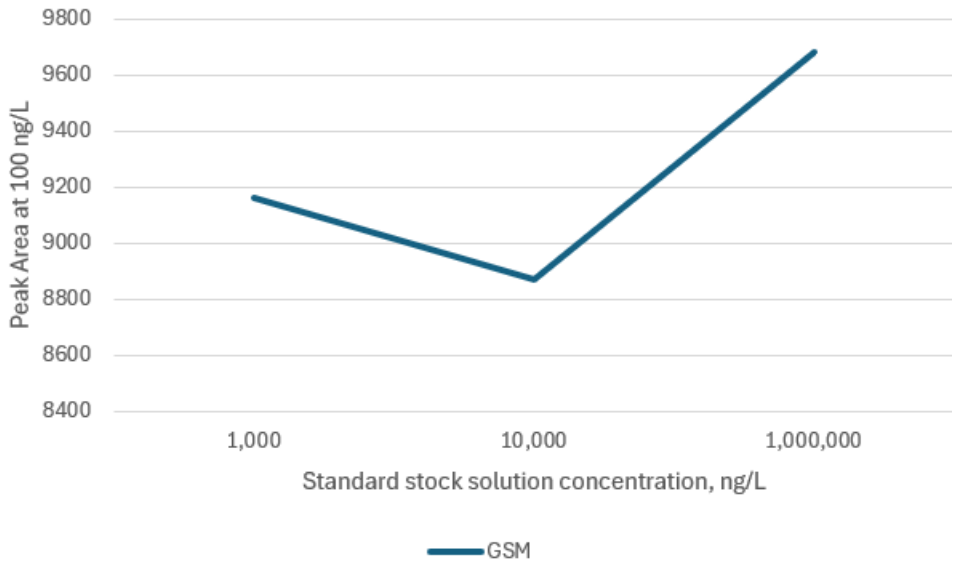

Figure 50 GSM Standard solution stock degradation during storage.

Table 16 shows the date of preparation of the GSM and 2-MIB stock solutions with different concentrations presented in Figures above.

Table 16 Stock standard solution preparation dates and concentrations.

	Initial SS concentration	Date of preparation SS
GSM	1,000	Oct-25
	10,000	Aug-25
	1,000,000	Dec-25
MIB	1,000	Oct-25
	10,000	Nov-25
	1,000,000	Oct-25
	100,000,000	Dec-25

In addition, Figures 51 and 52 demonstrate that peak areas of the same concentrations of 2-MIB and GSM are significantly higher for the samples prepared from the fresh standard stock solution in methanol than in stock solutions prepared months earlier and stored at diluted concentration (1000 ng/L). This confirms volatilization of GSM and MIB from the stock solution during storage.

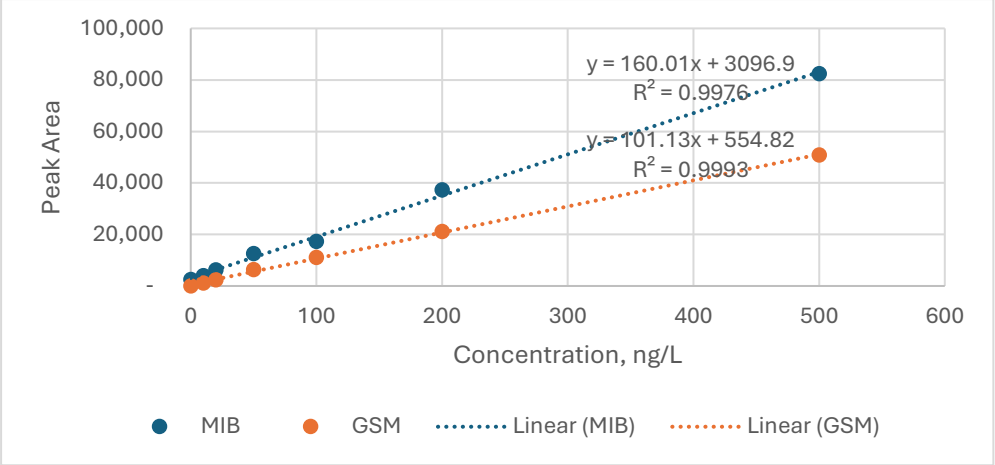

Figure 51 Calibration curves of the 2-MIB and GSM from fresh standard stock solutions in 99.8% methanol.

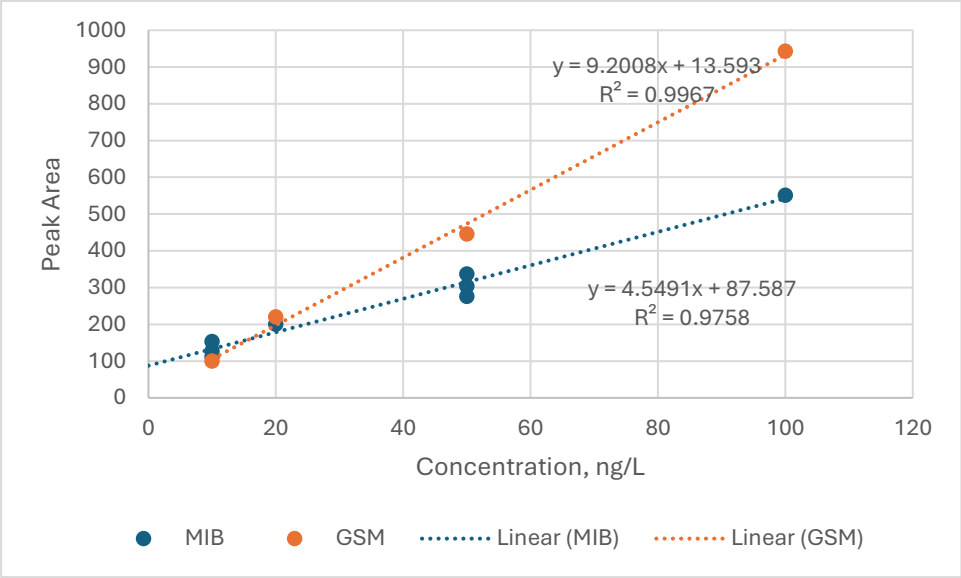

Figure 52 Calibration curves of the 2-MIB and GSM from not fresh standard stock solutions (10% methanol 90% matrix solution and serial dilution).

The following graphs show the variation of the GSM and 2-MIB concentrations over time periods. Figure 53 illustrates the 2-MIB and GSM degradation over a week period in the standard solution. Therefore, the stock solutions in methanol were opened and reused for a week only. Figure 54 shows a slight (6-8%) variation of 1000 ng/L 2-MIB and GSM samples over 8 hours, mostly indicating the instrument drift, which is within RSD range.

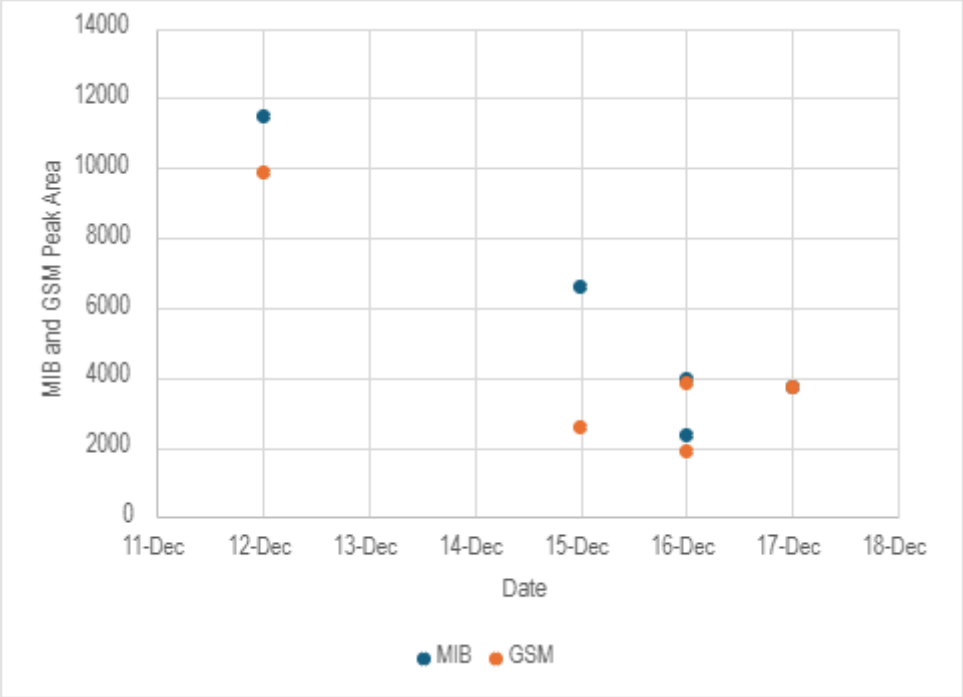

Figure 53 Standard stock solution in 2 mL vials in methanol degradation over a week.

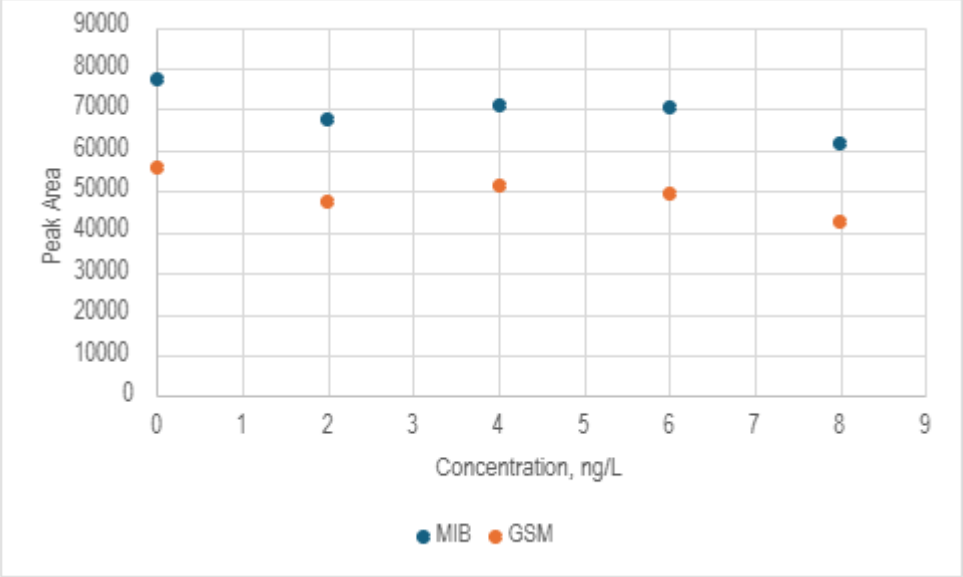

Figure 54 Change in 2-MIB and GSM concentration over 8 hours, different samples, 1000 ng/L concentration.

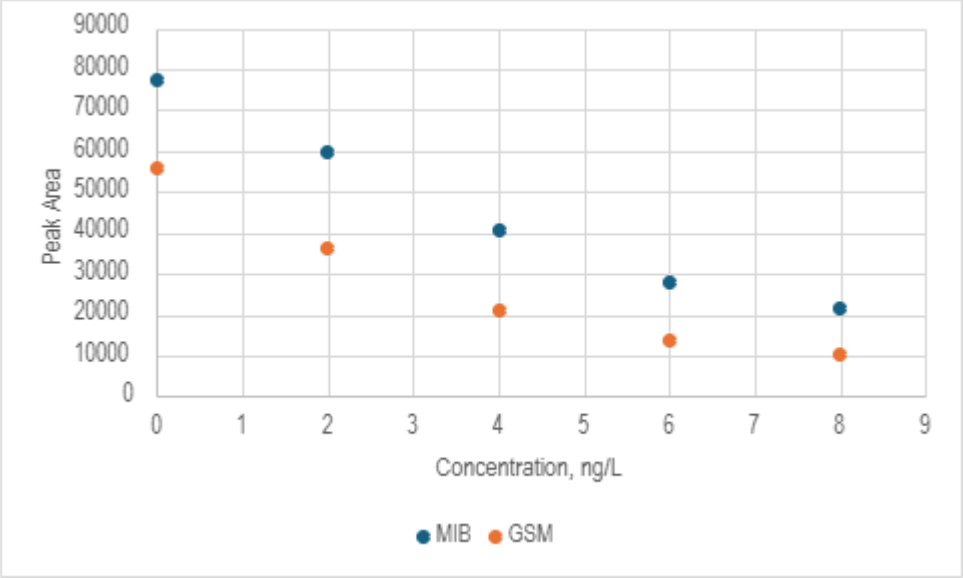

Figure 55 Change in 2-MIB and GSM concentration over 8 hours (same sample, 1000 ng/L).

The figure above shows how GSM and 2-MIB peak areas decrease when the same 1000 ng/L standard is analyzed repeatedly over 8 hours by HS-SPME GC-MS. The gradual signal loss indicates that each SPME exposure extracts only part of the analyte and that equilibrium between liquid, headspace, and fibre is not fully reached in a single run. This supports the recovery results and competitive sorption experiments, and confirms that HS-SPME recoveries represent an equilibrium-limited fraction governed by fibre capacity and competition between GSM and 2-MIB.

4.3.4 Contamination and Vial Cleaning

As part of the troubleshooting of the interfering peaks, contamination from washing vials was assessed. Before new vials were obtained, used vials were washed and various washing and drying methods are tested (including acid washing) to reduce contamination to interfere with SPME fibre headspace analysis. It was found that washing with methanol and subsequent drying at 250°C for 5h substantially improved the results, eliminating interference peaks in chromatograms (Figure 57).

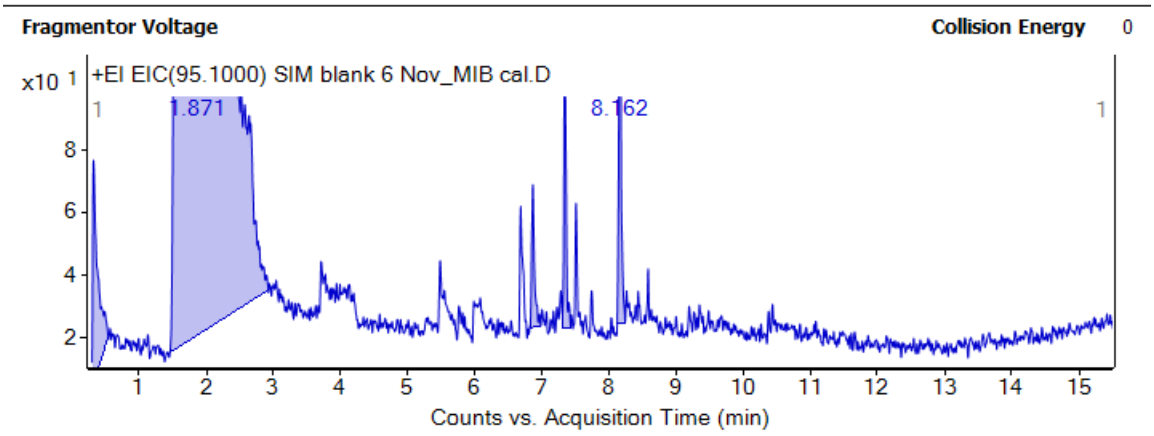

Figure 56 Blank sample analysis before washing, contamination peaks at 6.9, 7.3 and 8.2 min retention times..

The blank chromatograms before vial washing show multiple interfering peaks around the 2-MIB and GSM retention times, whereas these peaks are largely removed after methanol washing and high-temperature baking. This confirms that vial cleaning was a significant source of contamination and that the revised procedure was necessary for reliable trace-level analysis. Interfering peaks at retention times of 6.9, 7.3, and 8.2 min in unwashed vials overlap with the retention time windows of both target analytes, making reliable quantification impossible without prior vial decontamination (Figure above). The peak at 7.3 min is particularly concerning given its proximity to the 2-MIB retention time of 7.5 min. Possible 2-MIB carryover at 7.3 min time was due to possible sticking to the vial walls.

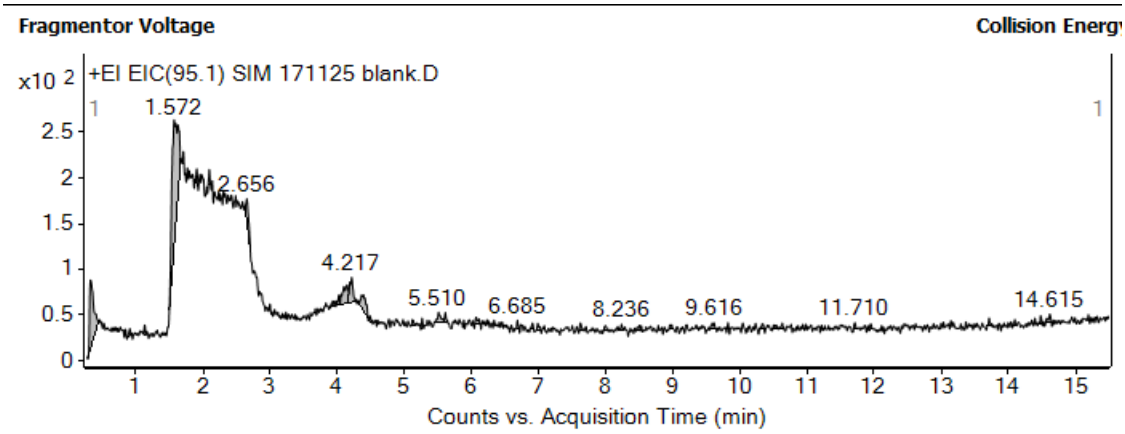

Figure 57 Blank sample chromatogram after vials washing with MeOH and baking at 250°C.

The potential sources of contamination include organic compounds from seawater, cross-contamination from the oven used by other students to dry organic and biological samples, and glassware that may not have been washed properly. The work was carried out in a teaching laboratory rather than a research laboratory, which was not maintained under sterile conditions, so contamination is likely, especially for nanoscale analyte detection.

4.4 2-MIB and GSM Treatment Experiments

The established and validated method was used to quantify the effect of geosmin and 2-MIB removal by powder zeolite adsorption and TiO_2-zeolite photocatalytic coatings with UV in the seawater matrixes.

4.4.1 Powder Zeolite Adsorption

Experiment by adding zeolite powder to samples showed a high percentage, 97-99% of GSM and 2-MIB removal, and 95% 2-MIB and 99% GSM was adsorbed immediately after adding zeolite to the solution.

The graph below (Figure 58) shows the initial concentrations of 2-MIB and geosmin in blank sample, blank samples in 4 hours without adding zeolite (in open circles) and

other samples by adding 2 mg of zeolite that are tested in 0, 30, 60, 120 and 240 minutes. The results around 800-900 ng/L concentration are the blank samples without adding zeolite powder, and all that are below are samples with added zeolites.

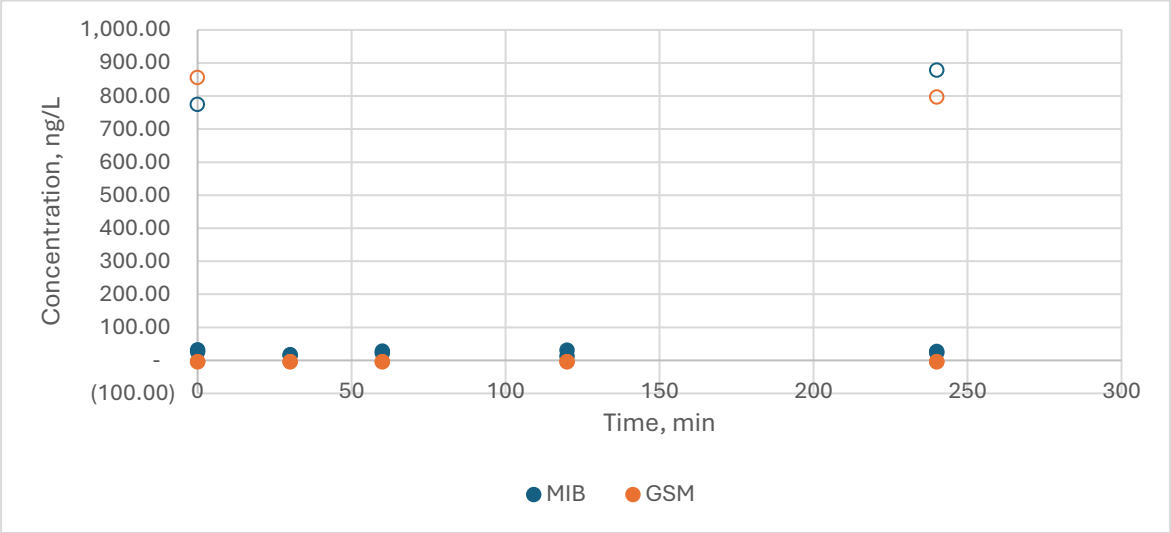

Figure 58 2-MIB and GSM adsorption with 2 mg zeolite powder.

Figure above demonstrates that the addition of powder zeolite resulted in rapid and near-complete removal of GSM and 2-MIB, with 95-99% reduction observed across all sampling times. Blank controls without zeolite showed negligible natural loss, confirming that removal was driven by adsorption onto the zeolite rather than volatilization or degradation.

Powdered zeolite-Y exhibited an adsorption capacity 7.5 ng/mg under the test conditions. In addition, the USY zeolite powder did not remain fully suspended in water, which made it difficult to handle as a stable suspension.

4.4.2 UV Irradiation Only (control)

Exposure of uncoated samples to UV light alone for 4 hours, using the same setup as in the photocatalytic experiments, reduced GSM and 2-MIB concentrations by only 23-27% (Figure below). This modest change indicates that direct photolysis under the

applied UV conditions is weak, and that the main removal mechanism in the composite experiments is adsorption onto the zeolite-TiO_2 coating rather than UV irradiation by itself.

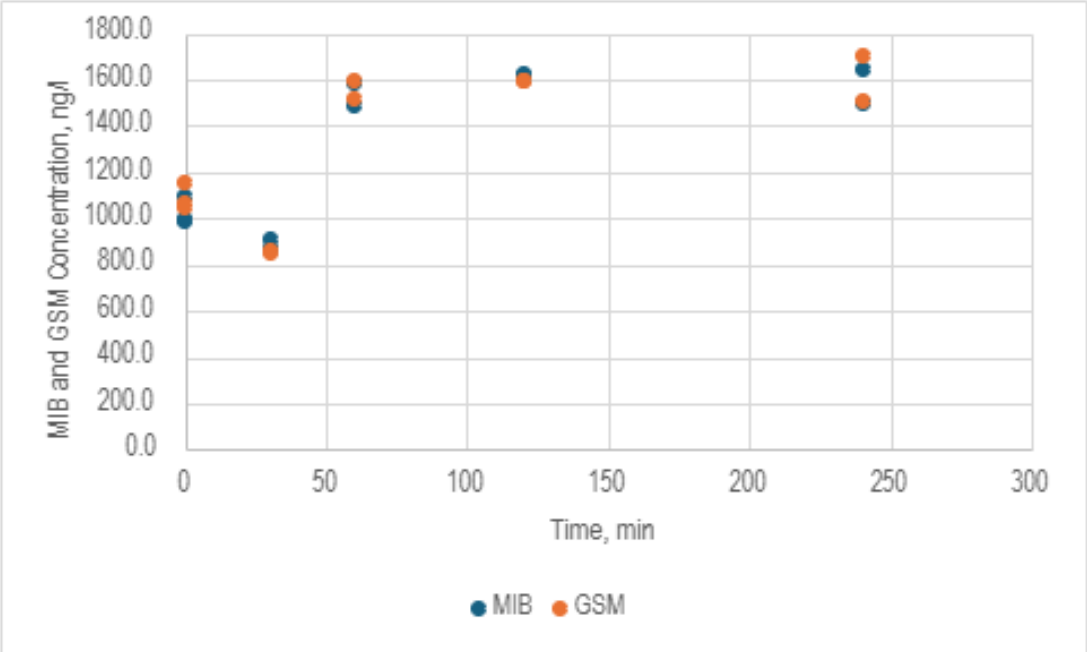

Figure 59 GSM and 2-MIB removal by UV only

Exposure of samples to UV light alone (Figure 59) reduce GSM or 2-MIB concentrations only by 23-27%, confirming that UV irradiation without a photocatalyst is ineffective for removing these compounds under the conditions tested.

4.4.3 Characterization of the TiO2-Zeolite coating

The composite coating was created as described in Section 3.2.2.1 of Chapter 3, and characterized using optical microscopy and scanning electron microscopy (SEM).

Figures 60 and 61 illustrate 50 um and 20 um optical microscopy pictures of the coating particle distribution of the composite. They show that there is not complete particle coverage of the surface.

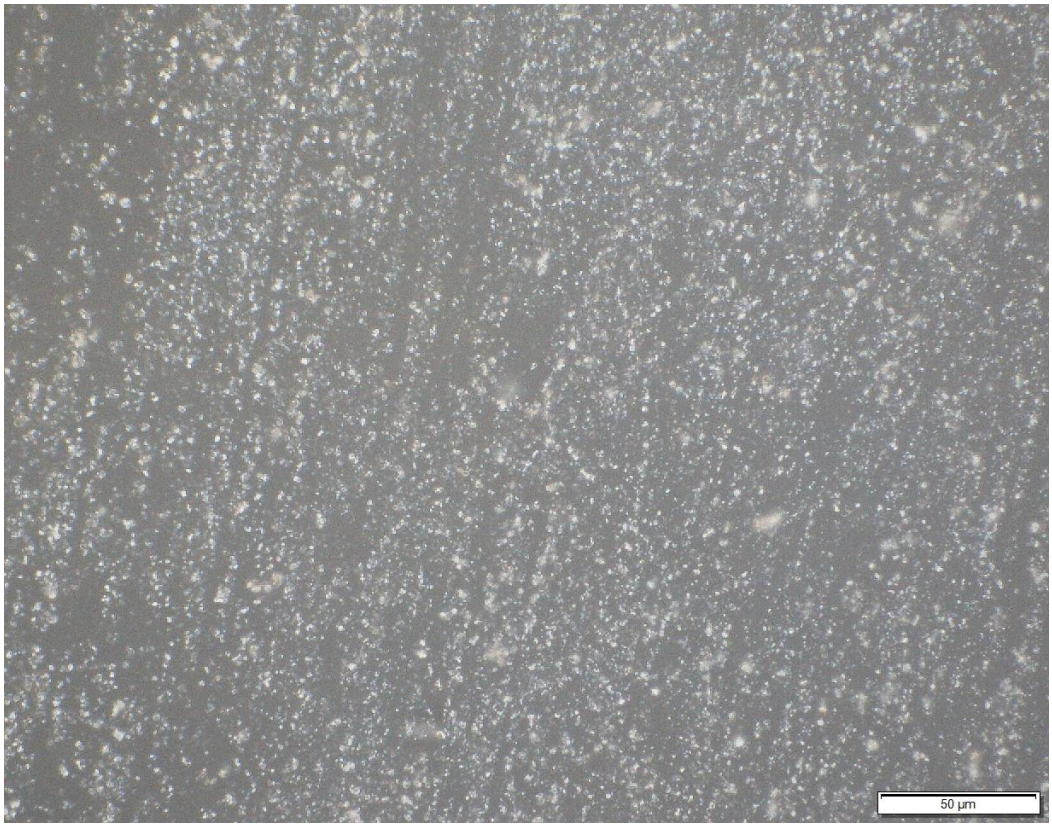

Figure 60 Optical Microscopy image of TiO2 and zeolite coating at 50 um scale.

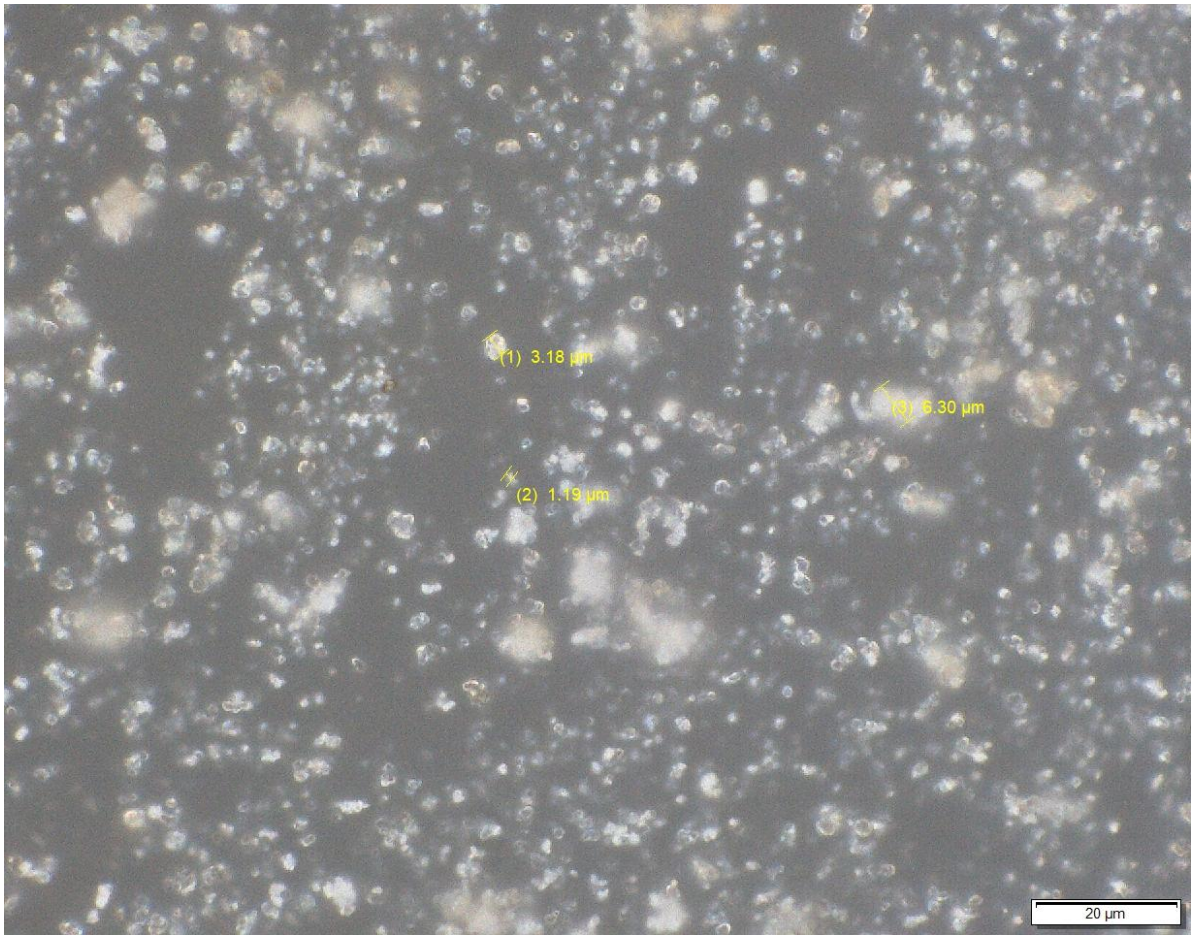

Figure 61 Optical microscope image of TiO2 and zeolite composite coating at 20 um scale.

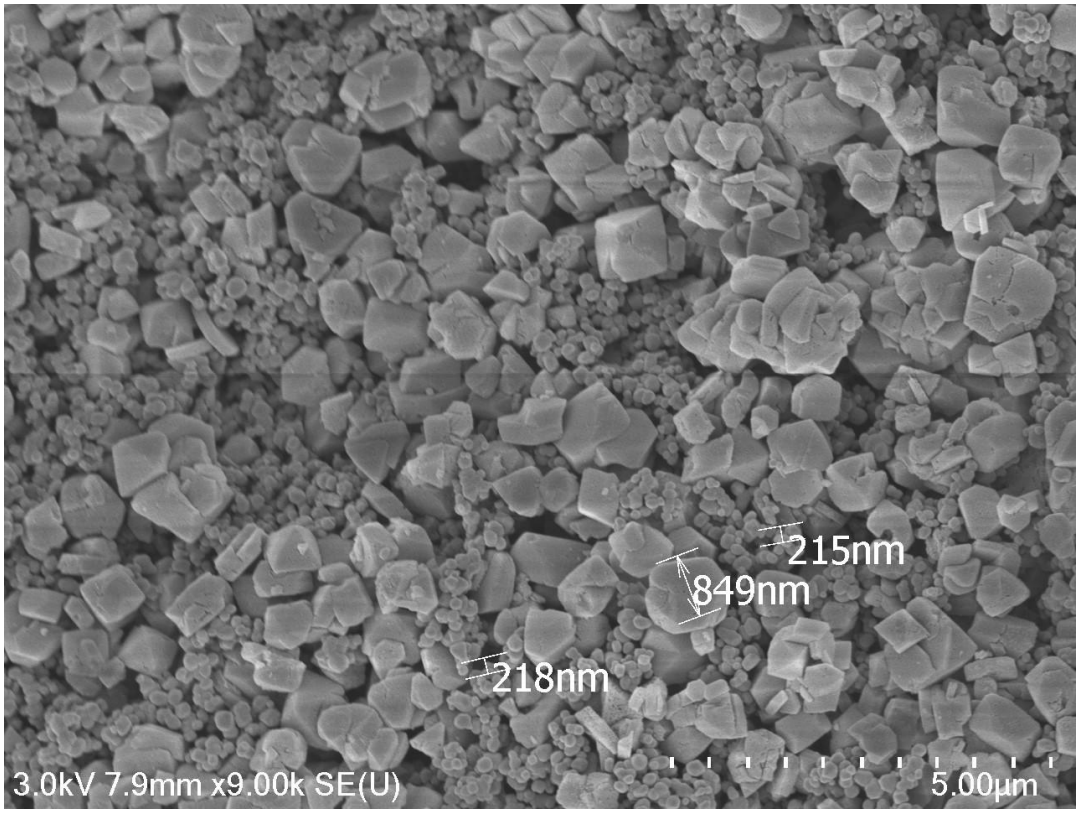

Figure 62 SEM image of TiO2 and zeolite composite coating.

5 um (3.0 kV) SEM image of the coating illustrated in Figure above. Large particles, 215-849 nm size, are Y-zeolite and smaller particles are TiO2.

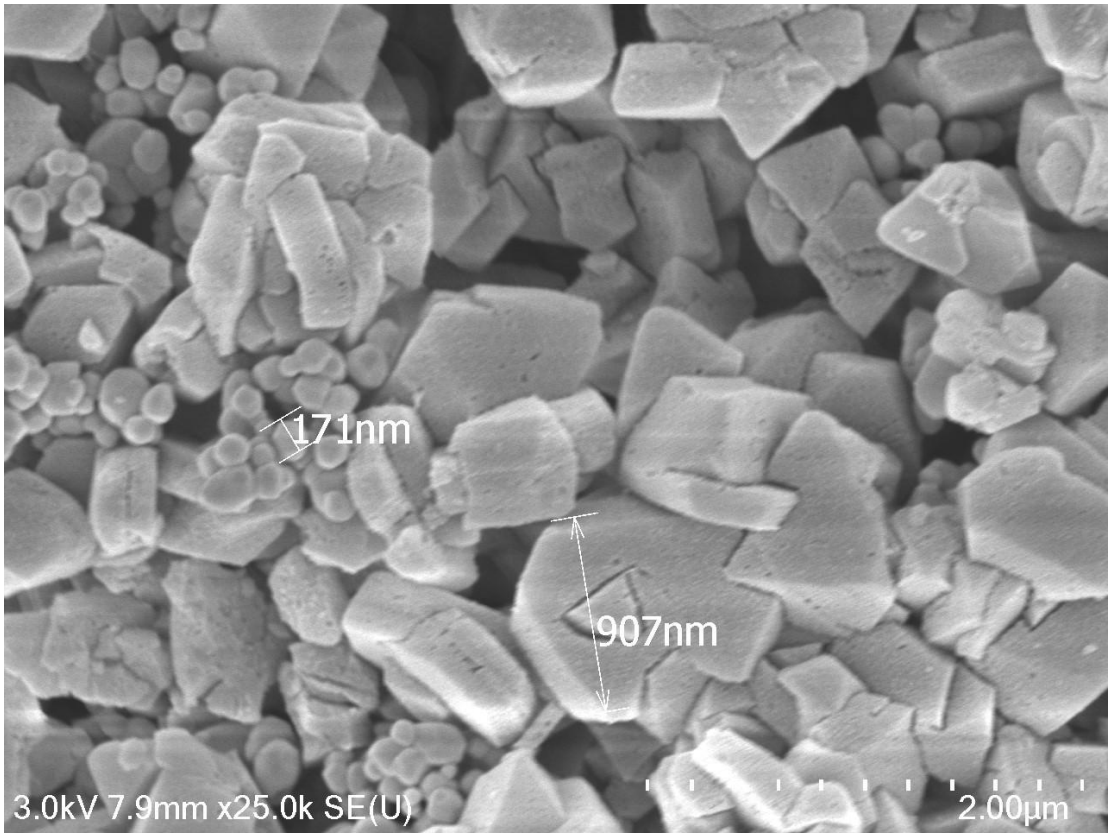

Figure 63 SEM image of TiO2 and zeolite composite coating.

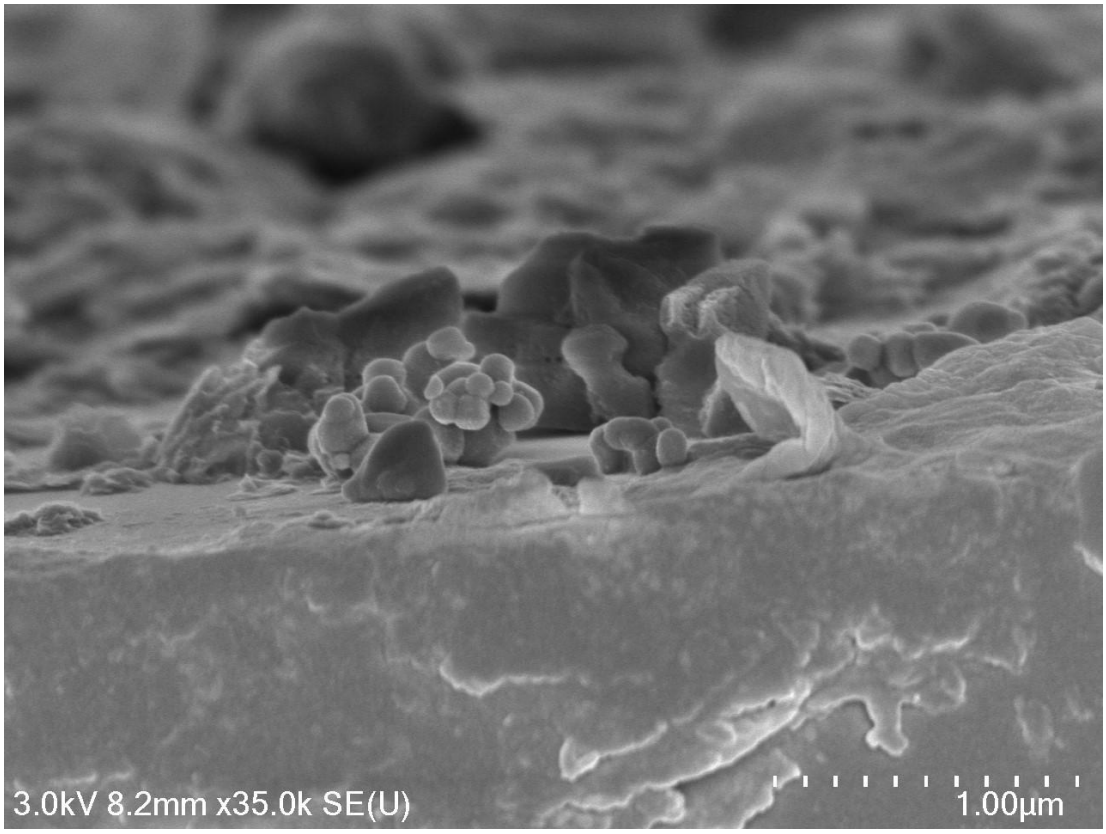

Figure 64 Cross-section of coating.

The cross-section of the coating in 1 um scale shows that the particle distribution is not perfectly even.

Optical microscopy and SEM images (Figures 60-64) reveal incomplete and heterogeneous coverage of the substrate by the zeolite-TiO_2 composite, with discrete zeolite and TiO_2 particles and variable coating thickness. This non-uniform morphology helps explain why adsorption dominates over photocatalysis, and why coating degradation leads to reduced performance on reuse. The coating mechanism and particle distribution could be studied and optimized further to improve treatment performance.

4.4.4 Zeolite-TiO_2 Composite Coating with UV

In the first use of the coating, 96-98% removal of 2-MIB and geosmin was obtained within four hours. While 89% geosmin and 50% of 2-MIB was removed in first 30

minutes (Figure below). The sample without photocatalysis showed 14% and 20% 2-MIB and GSM reduction.

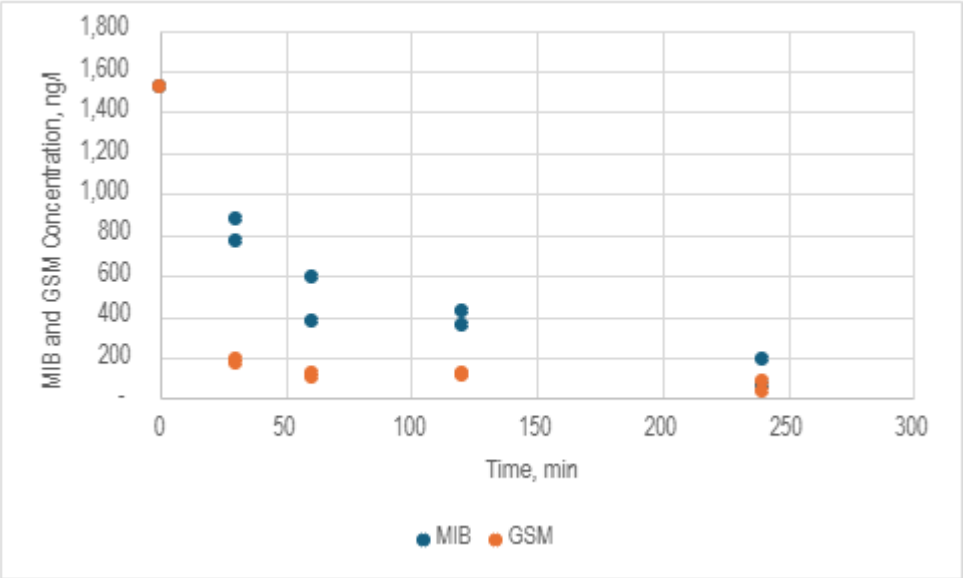

Figure 65 GSM and 2-MIB removal by photocatalysis after the first use of the coating.

As shown in Figure 65, the zeolite-TiO_2 composite coating with UV achieved 96-98% removal of both compounds within four hours, with most GSM and a substantial fraction of 2-MIB removed in the first 30 minutes. The control ran without UV, in darkness, showed only minor loss, indicating that the observed effect is due to adsorption and photocatalysis rather than natural degradation. The composite coating adsorption capacity in the first use was >3 ng/mg.

The coating was used for the photocatalysis experiment three times. 87.6% and 97% efficiency were observed in 4 hours for 2-MIB and GSM, respectively, when reusing the coating.

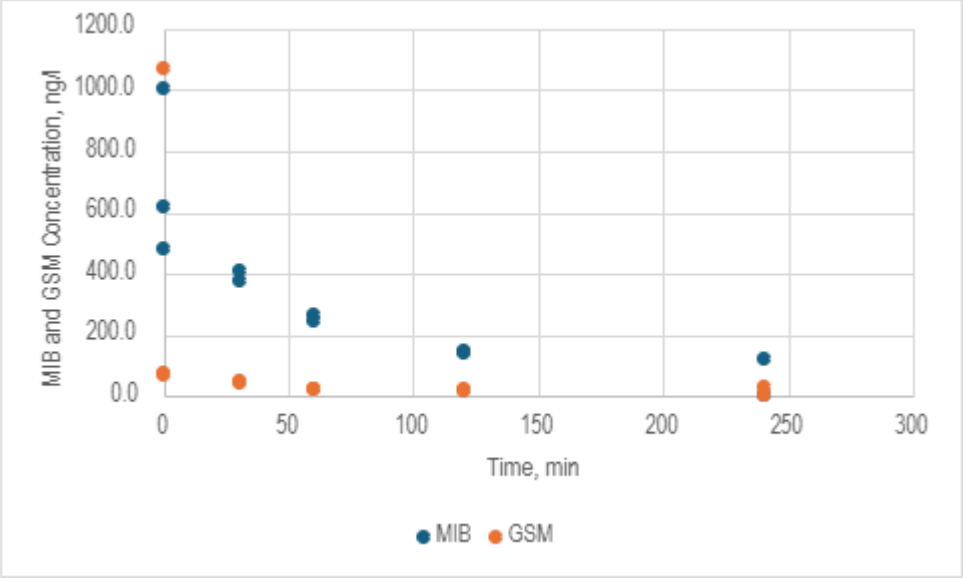

Figure 66 GSM and 2-MIB removal by photocatalysis after 2nd use of coating.

Using it 3rd time showed that geosmin adsorption efficiency dropped to 78-82%, while for 2-MIB maintained 87-89%. This demonstrates that one coating could be effective when reused three times, with gradually reduced efficiencies. However, the capacity of GSM and 2-MIB adsorption is reduced with each reuse, due to reduced active surface area and coating material, as shown in the Table 17. When reusing coting adsorption capacity is dropped to 2 ng/mg

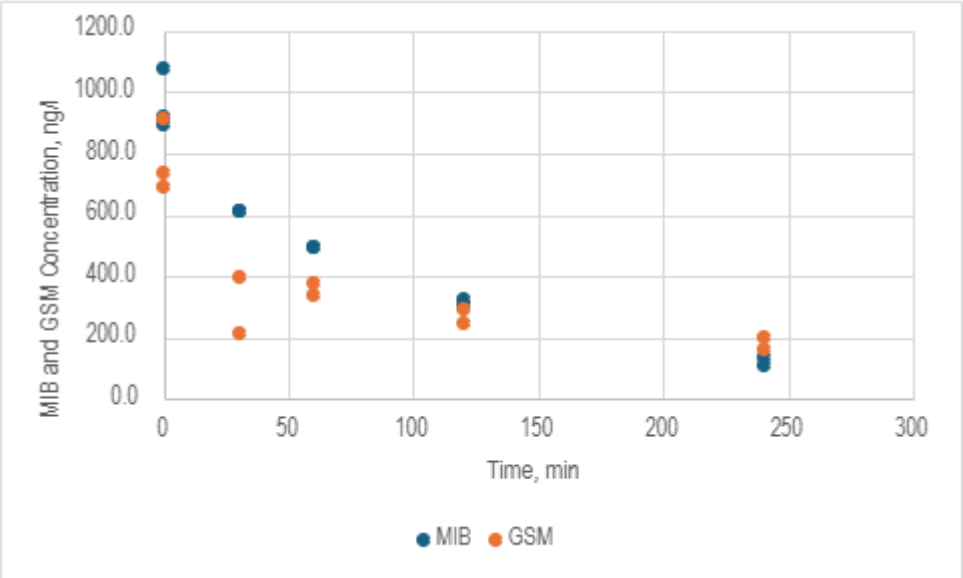

Figure 67 GSM and 2-MIB removal by photocatalysis after 3rd use of the coating.

Figures 66 and 67 show that coating performance declines over successive uses, particularly for GSM, whose removal decreases from ~97% to 78-82% by the third cycle. Upon reuse, the adsorption capacity decreased from 3 ng/mg to 2 ng/mg, which can be attributed to coating mass loss (reducing the effective surface area) and partial deactivation or blockage of active adsorption sites. Combined with the observed coating mass loss and increased turbidity, this indicates that mechanical degradation of the coating reduces the available active surface area over time.

The turbidity of the solution and mass of the coating loss were measured. Turbidity of the solution at the beginning of the experiment was 1.73 NTU, and at the end of the experiment was 277 NTU. This shows that up to 30% of the zeolite and TiO2 came off after the third experiment (Table below).

A final turbidity of 277 NTU represents a substantial increase from the initial value of 1.73 NTU and would be operationally unacceptable in a live RAS environment, where turbidity above approximately 10-20 NTU can increase stress and impair fish gill function according to aquaculture water quality guidelines and manufacturer data (Cumming & Herbert, 2016).This suggests that improving the mechanical bonding of the coating to the substrate could prevent particle shedding, making it more suitable for in-situ RAS deployment.

Table 17 Initial coating mass and mass loss.

	1st use	2nd use	3rd use
Coating mass loss, mg	3.5	0.5	14.1
Initial mass, mg	47.5	44	30.4

Because 20 mL solution was withdrawn from the same reactor at 0, 0.5, 1, 2 and 4 h, both the sample volume and the exposed coating surface area decreased over time (Table below). Consequently, the observed concentration–time profiles reflect not only

adsorption kinetics but also a progressively lower surface-to-volume ratio. This experimental design complicates direct extraction of intrinsic kinetic rate constants or equilibrium isotherm parameters, since each time point represents a different combination of solution volume and exposed coating area.

Table 18 The surface area of the coated tube.

Exposure Time, min	**Sample Volume, ml**	**Exposed Coating Surface Area, mm^2**
0	130	6371
30	110	5146
60	90	3921
120	70	2695.5
240	50	1470.3

4.4.5 Composite Coating without UV

Experiment without UV, but with coating showed that 2-MIB and GSM adsorption in 4h was about 11-26% less than with UV, 74% for 2-MIB and 89.8% for GSM. In first 30 minutes 36% 2-MIB and 86% of GSM was adsorbed to the coating (Figure below). This indicated that around 74-89% of efficiency is contributed by zeolite coating and only rest by TiO_2-UV photocatalysis. In addition, the coating that was used for this experiment was freshly prepared, and about 3.5-4 mg of coating mass was lost after 1st use.

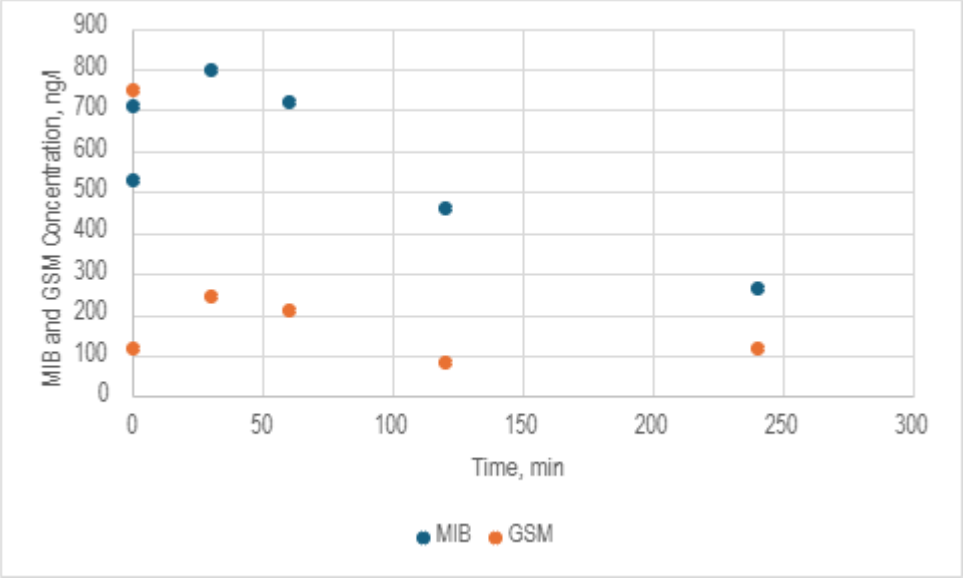

Figure 68 GSM and 2-MIB removal by zeolite and TiO2 composite coating (no UV) after 1st use of the coating.

4.4.6 Comparative Summary of Treatment Conditions

Four conditions were tested for GSM and 2-MIB removal from seawater. Results are summarized in Table below.

Table 19 Summary of removal efficiencies.

Treatment Condition	GSM Removal (4h)	MIB Removal (4h)
Powder zeolite	~99%	95-97%
UV only	23%	23-27%
Composite coating, no UV (1st use)	~89%	~74%
Composite coating + UV (1st use)	98.4%	97.4-97.8%
Composite coating + UV (2nd use)	~97%	~88%
Composite coating + UV (3rd use)	78-82%	87-89%

Powder zeolite achieved the highest and most immediate removal, reaching 95-99% for both compounds within the first measurement interval. UV irradiation alone produced only 23-27% removal, confirming that direct photolysis is negligible under the conditions tested. The composite coating without UV achieved 74-89% removal, demonstrating that adsorption accounts for approximately ~81% of the total removal mechanism, with TiO_2 photocatalysis contributing the remaining ~19% when UV is applied. Coating performance declined with repeated use due to progressive mass loss

and reduction in available surface area, as confirmed by turbidity measurements increasing from 1.73 to 277 NTU.

Practical trade-offs exist for both approaches. Powdered zeolites create a recovery problem after treatment because the fine particles are difficult to separate cleanly from treated water, with one study noting that separating fine-sized zeolite particles from treated water is often a challenge (Bahmanzadegan & Ghaemi, 2025; Buzukashvili et al., 2024). A common workaround is modification of the powder to enable easier recovery, for example by rendering it magnetic so it can be rapidly removed from water after treatment (Buzukashvili et al., 2024). In contrast, the TiO_2-zeolite immobilized coating addresses this recovery challenge directly, as the solid support simplifies post-treatment separation and is one of the main practical advantages over slurry photocatalysis. However, the composite introduces its own limitations: reported reductions in specific surface area following TiO_2 incorporation, and open challenges around material stability, scalability, and cost-effectiveness of TiO_2-zeolite systems (Armaković & Armaković, 2025)

Under the conditions of this study, powder zeolite is identified as the most effective treatment option for GSM and 2-MIB in marine RAS seawater - provided that practical powder-recovery solutions, such as magnetic modification, are integrated into any scaled application.

4.5 Chapter Summary

This chapter described the development and validation of a HS-SPME GC-MS method for trace-level GSM and 2-MIB detection in seawater, and its application to four laboratory-scale treatment experiments.

The optimized method - using SIM detection, internal standard correction, 60°C incubation, 15-minute SPME extraction, and 3 g NaCl addition - achieved $R^2 > 0.99$

calibration linearity and LOD values below 10 ng/L across all matrices. Key challenges included matrix-induced signal suppression in real seawater, analyte degradation in dilute storage solutions, and competitive sorption between GSM and 2-MIB on the SPME fibre.

Treatment experiments showed powder zeolite achieved near-complete removal (95-99%) immediately upon addition. UV alone was ineffective (23-27%). The composite zeolite-TiO_2 coating reached 97-98% removal with UV but declined to 78-89% by the third use due to physical coating degradation. Adsorption was the dominant mechanism (~81%), with photocatalysis contributing to a modest but consistent improvement. Each approach has practical trade-offs: powder zeolite offers superior and immediate removal but presents a particle-recovery challenge in treated water, addressable through modifications such as magnetic functionalization; the immobilized composite simplifies recovery but faces reduced surface area after TiO_2 incorporation and unresolved questions around long-term stability, scalability, and cost. Under the conditions tested, powder zeolite is concluded to be the most effective treatment approach for GSM and 2-MIB in a marine RAS context, subject to appropriate recovery engineering at scale.

Chapter 5

5.1 Conclusions

This chapter presents the main conclusions of the research and outlines recommendations for future work based on the analytical method development and treatment experiments carried out in this thesis.

This study developed and applied an integrated analytical and treatment framework for managing geosmin (GSM) and 2-methylisoborneol (2-MIB) in marine recirculating aquaculture systems (RAS), focusing on seawater matrices relevant to New Zealand's emerging land-based aquaculture sector. The work addressed two knowledge gaps: the absence of a validated GC-MS method for trace-level GSM and 2-MIB in seawater, and the lack of comparative data on affordable, practically applicable treatment options under marine conditions. Powder zeolite adsorption and TiO_2-zeolite photocatalytic coatings with UV (365 nm) were selected from the literature review as the most promising options balancing cost, treatment efficiency and practical implementation potential in aquaculture systems. The target threshold of 10 ng/L for geosmin and 2-MIB was also chosen from published sensory and regulatory literature.

Firstly, the HS-SPME–GC-MS method was developed, optimized and validated for the detection of GSM and 2-MIB at target concentrations around 10 ng/L in seawater. The final method combined SIM detection, the internal standard, 60°C and 30-minute incubation, 15-minute extraction, and 3g NaCl addition in 10 mL samples. Linear calibration (R^2>0.99) and limits of detection below 10 ng/L in artificial and real seawater was achieved. Systematic experiments showed that matrix composition, competitive sorption on the fibre, analyte loss during storage, and vial contamination all had clear and sometimes large effects on analytical performance, therefore careful

control of sample handling, fibre conditioning, filtration and stock-solution preparation is essential. These results indicate that routine trace-level monitoring of GSM and 2-MIB in marine media is very sensitive to small changes in the analytical procedure. Overall, these results show that the final method has acceptable sensitivity and reproducibility for routine trace-level GSM and 2-MIB monitoring in seawater.

Secondly, the validated method was used for removal of GSM and 2-MIB from artificial seawater at 1000 ng/L to compare four laboratory-scale treatment conditions, such as powder zeolite, TiO_2-zeolite composite coating with and without UV, and UV alone. Powder zeolite gave the quickest and most substantial removal, with about 95-99% reduction of both compounds occurring almost immediately after addition and remaining stable over four hours, while blank controls showed negligible natural loss, confirming that adsorption is the main mechanism. UV irradiation without a catalyst removed only about ~23-27% over four hours, which shows that direct photolysis under the applied conditions is ineffective and not enough on its own to meet sensory targets. The immobilized TiO_2-zeolite coating with UV initially achieved ~97-98% removal within four hours, but performance decreased to about ~78-89% after the third reuse, especially for GSM, because some of the coating detached and turbidity increased from 1.73 to 277 NTU. Tests with the same coating in the dark showed ~74-90% removal, which means that most of the effect comes from zeolite adsorption and the UV-driven TiO_2 photocatalysis provides only a smaller extra benefit in this setup.

Overall, the results show that adsorption processes are currently more effective and more practical than UV alone for GSM and 2-MIB control in marine RAS under the conditions tested in this study. Powder zeolite, especially, provided very fast and almost complete removal, but it creates a new engineering challenge of separating and recovering the solid adsorbent without disturbing RAS operation. Immobilized TiO_2-

zeolite coatings are attractive in theory because the composite material is fixed on a surface, but in this study the coating lost some active surface area after TiO_2 loading and was not mechanically strong enough, which caused particle release into the water and lower performance after several uses. Within these limitations, powder zeolite is identified as the most promising of the tested options for reducing GSM and 2-MIB in marine RAS seawater, if suitable recovery and handling strategies are integrated into the system design.

Generally, the thesis shows that reliable evaluation of off-flavor treatment technologies for marine RAS depends on analytical methods that are adapted specifically to seawater and on experiments that clearly separate adsorption and photocatalytic effects. By providing both a GC-MS method for trace-level GSM and 2-MIB in seawater and a comparative assessment of zeolite-based treatment options, this work offers a practical methodological basis for future research on scalable, energy-efficient off-flavor control in marine RAS and supports the development of higher-value, sensory-acceptable aquaculture products in New Zealand and internationally.

5.2 Future work

Several directions for future work arise from the limitations and findings of this study.

- Analytical method development:

  The GC-MS method can be further improved (e.g. trying different HS-SPME fibres to find one with a greater adsorption capacity and specificity for GSM and MIB compared to the current one used, increasing detector voltage to increase MS sensitivity, reducing headspace volume so more of the GSM and MIB is forced to stick to the SPME fibre) to increase sensitivity, robustness, and suitability for routine trace-level monitoring in seawater.

- Application in real RAS conditions:

  Future studies should evaluate both analytical performance and treatment efficiency using real RAS process water under various water qualities (e.g. different organic content and turbidity).

- Optimization of zeolite-based treatments:

  Further work is needed to improve the practical use of zeolite materials, including separation from water (magnetic), recovery for reuse and stability of immobilized coatings (such as sol-gel binding or other polymeric binders could be explored in future work to improve coating durability).

- Pilot-scale validation:

  Testing under pilot or full-scale RAS conditions is recommended to assess performance, operational feasibility, and practical implementation.

- Integration with existing systems:

  Future research should explore how zeolite-based treatments can be integrated into existing RAS processes and whether combined approaches provide additional benefits.

  To summarize, the study successfully achieved its objectives by developing and validating a trace-level GC-MS method for GSM and MIB in seawater, evaluating its performance under marine matrix conditions, and comparatively assessing practical treatment options for RAS applications.

References

Abd El-Hack, M. E., El-Saadony, M. T., Elbestawy, A. R., Ellakany, H. F., Abaza, S. S., Geneedy, A. M., Salem, H. M., Taha, A. E., Swelum, A. A., Omer, F. A., AbuQamar, S. F., & El-Tarabily, K. A. (2022). Undesirable odour substances (geosmin and 2-methylisoborneol) in water environment: Sources, impacts and removal strategies. *Marine Pollution Bulletin*, *178*, 113579. https://doi.org/10.1016/j.marpolbul.2022.113579

Agilent 7890B Gas Chromatograph Operation Manual. (2015). Agilent Technologies, Inc. https://www.agilent.com/cs/library/usermanuals/Public/7890B_Operation.pdf

Ahmed, N., Thompson, S., & Glaser, M. (2019). Global Aquaculture Productivity, Environmental Sustainability, and Climate Change Adaptability. *Environmental Management*, *63*(2), 159–172. https://doi.org/10.1007/s00267-018-1117-3

Ahmed, N., & Turchini, G. M. (2021). Recirculating aquaculture systems (RAS): Environmental solution and climate change adaptation. *Journal of Cleaner Production*, *297*, 126604. https://doi.org/10.1016/j.jclepro.2021.126604

Aich, N., Nama, S., Biswal, A., & Paul, T. (2020). *A REVIEW ON RECIRCULATING AQUACULTURE SYSTEMS: CHALLENGES AND OPPORTUNITIES FOR SUSTAINABLE AQUACULTURE*.

Al-Hazmi, G. A. A., El-Bindary, M. A., El-Desouky, M. G., & El-Bindary, A. A. (2022). Efficient adsorptive removal of industrial dye from aqueous solution by synthesized zeolitic imidazolate framework-8 loaded date seed activated carbon and statistical physics modeling. *Desalination and Water Treatment*, *258*, 85–103. https://doi.org/10.5004/dwt.2022.28397

References

Antonopoulou, M., Evgenidou, E., Lambropoulou, D., & Konstantinou, I. (2014). A review on advanced oxidation processes for the removal of taste and odor compounds from aqueous media. *Water Research*, *53*, 215–234. https://doi.org/10.1016/j.watres.2014.01.028

Aquaculture Plan key to economic growth | Beehive.govt.nz. (n.d.). Retrieved April 23, 2026, from https://www.beehive.govt.nz/release/aquaculture-plan-key-economic-growth

Armaković, S., & Armaković, S. (2025). Zeolite-Supported TiO2 for Enhanced Photocatalytic Performance in Environmental Applications: A Review. *Catalysts*, *15*(2), 174. https://doi.org/10.3390/catal15020174

Asghar, A., Khan, Z., Maqbool, N., Qazi, I. A., & Awan, M. A. (2015). Comparison of Adsorption Capability of Activated Carbon and Metal Doped TiO2 for Geosmin and 2-MIB Removal from Water. *Journal of Nanomaterials*, *2015*(1), 479103. https://doi.org/10.1155/2015/479103

Australian Drinking Water Guidelines | NHMRC. (n.d.). Retrieved April 23, 2026, from https://www.nhmrc.gov.au/about-us/publications/australian-drinking-water-guidelines

Azaria, S., Nussinovitch, A., Nir, S., Mordechai, S., & Van Rijn, J. (2021). Removal of geosmin and 2-methylisoborneol from aquaculture water by novel, alginate-based carriers: Performance and metagenomic analysis. *Journal of Water Process Engineering*, *42*, 102125. https://doi.org/10.1016/j.jwpe.2021.102125

Azaria, S., & Van Rijn, J. (2018). Off-flavor compounds in recirculating aquaculture systems (RAS): Production and removal processes. *Aquacultural Engineering*, *83*, 57–64. https://doi.org/10.1016/j.aquaeng.2018.09.004

References

Badiola, M., Basurko, O. C., Gabiña, G., & Mendiola, D. (2017). Integration of energy audits in the Life Cycle Assessment methodology to improve the environmental performance assessment of Recirculating Aquaculture Systems. *Journal of Cleaner Production*, *157*, 155–166. https://doi.org/10.1016/j.jclepro.2017.04.139

Badiola, M., Basurko, O. C., Piedrahita, R., Hundley, P., & Mendiola, D. (2018). Energy use in Recirculating Aquaculture Systems (RAS): A review. *Aquacultural Engineering*, *81*, 57–70. https://doi.org/10.1016/j.aquaeng.2018.03.003

Bahmanzadegan, F., & Ghaemi, A. (2025). A comprehensive review on novel zeolite-based adsorbents for environmental pollutant. *Journal of Hazardous Materials Advances*, *17*, 100617. https://doi.org/10.1016/j.hazadv.2025.100617

Balami, S. (2021). RECIRCULATION AQUACULTURE SYSTEMS: COMPONENTS, ADVANTAGES, AND DRAWBACKS. *Tropical Agroecosystems*, *2*(2), 104–109. https://doi.org/10.26480/taec.02.2021.104.109

Ben-Asher, R., Zohar, Y., Stromberg, M., & Lahav, O. (2024). A new approach for eliminating off-flavors from RAS fish, as part of the normal grow-out period. *Water Research*, *249*, 121015. https://doi.org/10.1016/j.watres.2023.121015

Bristow, R. L., Young, I. S., Pemberton, A., Williams, J., & Maher, S. (2019). An extensive review of the extraction techniques and detection methods for the taste and odour compound geosmin (*trans*-1, 10-dimethyl-*trans*-9-decalol) in water. *TrAC Trends in Analytical Chemistry*, *110*, 233–248. https://doi.org/10.1016/j.trac.2018.10.032

Brown, M. A., Miller, S., & Emmert, G. L. (2007). On-line purge and trap gas chromatography for monitoring of trihalomethanes in drinking water

distribution systems. *Analytica Chimica Acta*, *592*(2), 154–161. https://doi.org/10.1016/j.aca.2007.04.020

Burr, G. S., Wolters, W. R., Schrader, K. K., & Summerfelt, S. T. (2012). Impact of depuration of earthy-musty off-flavors on fillet quality of Atlantic salmon, *Salmo salar*, cultured in a recirculating aquaculture system. *Aquacultural Engineering*, *50*, 28–36. https://doi.org/10.1016/j.aquaeng.2012.03.002

Buzukashvili, S., Sommerville, R., Rowson, N. A., & Waters, K. E. (2024). An overview of zeolites synthesised from coal fly ash and their potential for extracting heavy metals from industrial wastewater. *Canadian Metallurgical Quarterly*, *63*(1), 130–152. https://doi.org/10.1080/00084433.2022.2160576

Clercin, N. A., & Druschel, G. K. (2019). Influence of Environmental Factors on the Production of MIB and Geosmin Metabolites by Bacteria in a Eutrophic Reservoir. *Water Resources Research*, *55*(7), 5413–5430. https://doi.org/10.1029/2018WR023651

Cook, D., & Newcombe, G. (2004). Can we predict the removal of MIB and geosmin with PAC by using water quality parameters? *Water Supply*, *4*(4), 221–226. https://doi.org/10.2166/ws.2004.0081

Cumming, H., & Herbert, N. A. (2016). Gill structural change in response to turbidity has no effect on the oxygen uptake of a juvenile sparid fish. *Conservation Physiology*, *4*(1), cow033. https://doi.org/10.1093/conphys/cow033

Dalsgaard, J., Lund, I., Thorarinsdottir, R., Drengstig, A., Arvonen, K., & Pedersen, P. B. (2013). Farming different species in RAS in Nordic countries: Current status and future perspectives. *Aquacultural Engineering*, *53*, 2–13. https://doi.org/10.1016/j.aquaeng.2012.11.008

References

Davidson, J., Schrader, K., Ruan, E., Swift, B., Aalhus, J., Juarez, M., Wolters, W., Burr, G., Good, C., & Summerfelt, S. T. (2014). Evaluation of depuration procedures to mitigate the off-flavor compounds geosmin and 2-methylisoborneol from Atlantic salmon *Salmo salar* raised to market-size in recirculating aquaculture systems. *Aquacultural Engineering*, *61*, 27–34. https://doi.org/10.1016/j.aquaeng.2014.05.006

Davidson, J., Van Rijn, J., & Azaria, S. (2024, March 14). Evaluating the feasibility of feeding RAS-produced fish during the depuration process. *Hatchery International*. https://www.hatcheryinternational.com/evaluating-the-feasibility-of-feeding-ras-produced-fish-during-the-depuration-process/

Dickschat, J. S., Bode, H. B., Mahmud, T., Müller, R., & Schulz, S. (2005). A Novel Type of Geosmin Biosynthesis in Myxobacteria. *The Journal of Organic Chemistry*, *70*(13), 5174–5182. https://doi.org/10.1021/jo050449g

Ellis, J., & Korth, W. (1993). Removal of geosmin and methylisoborneol from drinking water by adsorption on ultrastable zeolite-Y. *Water Research*, *27*(4), 535–539. https://doi.org/10.1016/0043-1354(93)90162-B

Foura, G., Chouchou, N., Soualah, A., Kouachi, K., Guidotti, M., & Robert, D. (2017). Fe-Doped TiO2 Supported on HY Zeolite for Solar Photocatalytic Treatment of Dye Pollutants. *Catalysts*, *7*(11), 344. https://doi.org/10.3390/catal7110344

Frederichi, D., Scaliante, M. H. N. O., & Bergamasco, R. (2021). Structured photocatalytic systems: Photocatalytic coatings on low-cost structures for treatment of water contaminated with micropollutants—a short review. *Environmental Science and Pollution Research*, *28*(19), 23610–23633. https://doi.org/10.1007/s11356-020-10022-9

References

Ganegoda, s. s, Chinthaka, M., & Manage, P. (2020). Determination of Geosmin and 2-Methylisoborneol in water using Solid Phase Micro Extraction (SPME) and Gas Chromatography Mass Spectrometry (GC/MS). *Ecology*, *26*, 420–432.

Geosmin MIB Mitigation UV Disinfection. (n.d.). *ULTRAAQUA*. Retrieved April 23, 2026, from https://ultraaqua.com/application/uv-geosmin-mib-mitigation-aop/

Gerber, N. N., & Lechevalier, H. A. (1965). Geosmin, an Earthy-Smelling Substance Isolated from Actinomycetes. *Applied Microbiology*, *13*(6), 935–938. https://doi.org/10.1128/am.13.6.935-938.1965

Górecki, T., Yu, X., & Pawliszyn, J. (1999). Theory of analyte extraction by selected porous polymer SPME fibres†. *The Analyst*, *124*(5), 643–649. https://doi.org/10.1039/a808487d

Gupta, S., Makridis, P., Henry, I., Velle-George, M., Ribicic, D., Bhatnagar, A., Skalska-Tuomi, K., Daneshvar, E., Ciani, E., Persson, D., & Netzer, R. (2024). Recent Developments in Recirculating Aquaculture Systems: A Review. *Aquaculture Research*, *2024*(1), 6096671. https://doi.org/10.1155/are/6096671

Guttman, L., & van Rijn, J. (2008). Identification of conditions underlying production of geosmin and 2-methylisoborneol in a recirculating system. *Aquaculture*, *279*(1–4), 85–91. https://doi.org/10.1016/j.aquaculture.2008.03.047

Hayes, S. J., Hayes, K. P., & Robinson, B. S. (1991). Geosmin As an Odorous Metabolite In Cultures of A Free-Living Amoeba, Vannella Species (Gymnamoebia, Vannellidae). *The Journal of Protozoology*, *38*(1), 44–47. https://doi.org/10.1111/j.1550-7408.1991.tb04798.x

Helfrich, L. A., & Libey, G. (n.d.). *RECIRCULATING AQUACULTURE SYSTEMS*.

Ho, L., Hoefel, D., Bock, F., Saint, C. P., & Newcombe, G. (2007). Biodegradation rates of 2-methylisoborneol (MIB) and geosmin through sand filters and in

bioreactors. *Chemosphere*, *66*(11), 2210–2218. https://doi.org/10.1016/j.chemosphere.2006.08.016

Home | Plant Production and Protection | Food and Agriculture Organization of the United Nations. (n.d.). Plant-Production-and-Protection. Retrieved April 23, 2026, from https://www.fao.org/plant-production-protection/en

Houle, S., Schrader, K. K., Le François, N. R., Comeau, Y., Kharoune, M., Summerfelt, S. T., Savoie, A., & Vandenberg, G. W. (2011). Geosmin causes off-flavour in arctic charr in recirculating aquaculture systems. *Aquaculture Research*, *42*(3), 360–365. https://doi.org/10.1111/j.1365-2109.2010.02630.x

Howgate, P. (2004). Tainting of farmed fish by geosmin and 2-methyl-iso-borneol: A review of sensory aspects and of uptake/depuration. *Aquaculture*, *234*(1–4), 155–181. https://doi.org/10.1016/j.aquaculture.2003.09.032

Huang, W.-J., Tsai, Y.-Y., & Chu, C. (2003). Evaluation of disinfection by-products formation during ozonation of bromide-containing groundwater. *Journal of Environmental Science and Health. Part A, Toxic/Hazardous Substances & Environmental Engineering*, *38*(12), 2919–2931. https://doi.org/10.1081/ese-120025841

Jiadong, H., Xihui, Z., Zhengmao, W., & Zhijun, W. (2009). Investigation on characteristics of odor compounds and bacterial community in a typical urban polluted river. *Research of Environmental Sciences*. https://www.semanticscholar.org/paper/Investigation-on-characteristics-of-odor-compounds-Jiadong-Xihui/c80981a38e0b5eb369eeba18cfa5f0914e4f5b1a

Juck, M., & Technologies, A. (n.d.). *General Information for Agilent Smart SPME Fibers*.

References

Jüttner, F. (1988). Biochemistry of Biogenic Off-Flavour Compounds in Surface Waters. *Water Science and Technology*, *20*(8–9), 107–116. https://doi.org/10.2166/wst.1988.0231

Jüttner, F., & Watson, S. B. (2007). Biochemical and Ecological Control of Geosmin and 2-Methylisoborneol in Source Waters. *Applied and Environmental Microbiology*, *73*(14), 4395–4406. https://doi.org/10.1128/AEM.02250-06

Kabadayi, O., Altintig, E., & Ballai, G. (2024). Zeolite supported zinc oxide nanoparticles composite: Synthesis, characterization, and photocatalytic activity for methylene blue dye degradation. *Desalination and Water Treatment*, *319*, 100433. https://doi.org/10.1016/j.dwt.2024.100433

Kim, K.-Y., Khan, J.-B., Choi, I.-C., Hong, S.-H., Lee, J.-B., Lee, S.-H., & Lee, J.-J. (2015). Temporal and Spatial Distribution of Geosmin and 2-MIB in the Daecheong Reservoir. *Korean Journal of Environmental Agriculture*, *34*(1), 14–20. https://doi.org/10.5338/KJEA.2015.34.1.04

Klausen, M. M., & Grønborg, O. (2010). Pilot scale testing of advanced oxidation processes for degradation of geosmin and MIB in recirculated aquaculture. *Water Supply*, *10*(2), 217–225. https://doi.org/10.2166/ws.2010.246

Kong, Y., & Cao, Z. (n.d.). *Determination of Off-Odor Compounds in Drinking Water Using an SPME Device with Gas Chromatography and Mass Spectrometry* [Application note]. Agilent. Retrieved https://www.agilent.com/cs/library/applications/application-spme-arrow-gc-ms-ms-water-analysis-5994-0626en-agilent.pdf

Krasner, S. W., Hwang, C. J., & McGuire, M. J. (1983). A Standard Method for Quantification of Earthy-Musty Odorants in Water, Sediments, and Algal

Cultures. *Water Science and Technology*, *15*(6–7), 127–138. https://doi.org/10.2166/wst.1983.0137

Kremser, A., Jochmann, M. A., & Schmidt, T. C. (2016). PAL SPME Arrow—Evaluation of a novel solid-phase microextraction device for freely dissolved PAHs in water. *Analytical and Bioanalytical Chemistry*, *408*(3), 943–952. https://doi.org/10.1007/s00216-015-9187-z

Kropp, R., Summerfelt, S. T., Woolever, K., Johnson, S. A., Kapsos, D. W., Haughey, C., & Barry, T. P. (2022). A novel advanced oxidation process (AOP) that rapidly removes geosmin and 2-methylisoborneol (MIB) from water and significantly reduces depuration times in Atlantic salmon *Salmo salar* RAS aquaculture. *Aquacultural Engineering*, *97*, 102240. https://doi.org/10.1016/j.aquaeng.2022.102240

Kumari, S., Chowdhry, J., Kumar, M., & Chandra Garg, M. (2024). Zeolites in wastewater treatment: A comprehensive review on scientometric analysis, adsorption mechanisms, and future prospects. *Environmental Research*, *260*, 119782. https://doi.org/10.1016/j.envres.2024.119782

Kutschera, K., Börnick, H., & Worch, E. (2009). Photoinitiated oxidation of geosmin and 2-methylisoborneol by irradiation with 254 nm and 185 nm UV light. *Water Research*, *43*(8), 2224–2232. https://doi.org/10.1016/j.watres.2009.02.015

Lawton, L. A., Robertson, P. K. J., Robertson, R. F., & Bruce, F. G. (2003). The destruction of 2-methylisoborneol and geosmin using titanium dioxide photocatalysis. *Applied Catalysis B: Environmental*, *44*(1). https://doi.org/10.1016/S0926-3373(03)00005-5

References

Lee, D., Ladak, A., Jeffers, T., & Nutter, A. (n.d.). *Robust analysis of taste and odor compounds in drinking water using purge and trap and single quadrupole GC-MS*.

Lindholm-Lehto, P. C., & Vielma, J. (2019). Controlling of geosmin and 2-methylisoborneol induced off-flavours in recirculating aquaculture system farmed fish—A review. *Aquaculture Research*, *50*(1), 9–28. https://doi.org/10.1111/are.13881

Little, D. C., & MacKenzie, S. (2023). Grand challenges for global aquaculture. *Frontiers in Aquaculture*, *2*. https://doi.org/10.3389/faquc.2023.1232936

Liu, X., Liu, Y., Lu, S., Guo, W., & Xi, B. (2018). Performance and mechanism into TiO2/Zeolite composites for sulfadiazine adsorption and photodegradation. *Chemical Engineering Journal*, *350*, 131–147. https://doi.org/10.1016/j.cej.2018.05.141

Liu, Y., Rosten, T. W., Henriksen, K., Hognes, E. S., Summerfelt, S., & Vinci, B. (2016). Comparative economic performance and carbon footprint of two farming models for producing Atlantic salmon (*Salmo salar*): Land-based closed containment system in freshwater and open net pen in seawater. *Aquacultural Engineering*, *71*, 1–12. https://doi.org/10.1016/j.aquaeng.2016.01.001

Lloyd, S. W., Lea, J. M., Zimba, P. V., & Grimm, C. C. (1998). Rapid analysis of geosmin and 2-methylisoborneol in water using solid phase micro extraction procedures. *Water Research*, *32*(7), 2140–2146. https://doi.org/10.1016/S0043-1354(97)00444-2

Lord, H., & Pawliszyn, J. (2000). Evolution of solid-phase microextraction technology. *Journal of Chromatography A*, *885*(1), 153–193. https://doi.org/10.1016/S0021-9673(00)00535-5

References

Manickum, T., & John, W. (2012). Method Validation for the Trace Analysis of Geosmin and 2-Methylisoborneol in Water by ?Salt-Free? Purge-and-Trap Sampling/GC-MS, Using the Eclipse 4660 Sample Concentrator. *Journal of Waste Water Treatment & Analysis*, *3*(3). https://doi.org/10.4172/2157-7587.1000134

Martins, C. I. M., Eding, E. H., Verdegem, M. C. J., Heinsbroek, L. T. N., Schneider, O., Blancheton, J. P., d'Orbcastel, E. R., & Verreth, J. A. J. (2010). New developments in recirculating aquaculture systems in Europe: A perspective on environmental sustainability. *Aquacultural Engineering*, *43*(3), 83–93. https://doi.org/10.1016/j.aquaeng.2010.09.002

McCallum, R., Pendleton, P., Schumann, R., & Trinh, M.-U. (1998). Determination of geosmin and 2-methylisoborneol in water using solid-phase microextraction and gas chromatography-chemical ionisation/electron impact ionisation-ion-trap mass spectrometry. *The Analyst*, *123*(10), 2155–2160. https://doi.org/10.1039/a803621g

Molleda, M. I. (2007). *WATER QUALITY IN RECIRCULATING AQUACULTURE SYSTEMS FOR ARCTIC CHARR (Salvelinus alpinus L.) CULTURE*.

Müller, A., Nowack, B., Oy, S., & Saari, J. (2010). *Photocatalysis for water treatment*.

Müller, L., Górecki, T., & Pawliszyn, J. (2006). Solid-Phase Microextraction in Analysis of Pollutants in the Field. In *Encyclopedia of Analytical Chemistry*. John Wiley & Sons, Ltd. https://doi.org/10.1002/9780470027318.a0922

Murray, D. R. (2014). Ecological Threat and Psychological Variation. *Psychologia*, *57*(2), 82–101. https://doi.org/10.2117/psysoc.2014.82

References

Murray, R. A. (2001). Limitations to the Use of Solid-Phase Microextraction for Quantitation of Mixtures of Volatile Organic Sulfur Compounds. *Analytical Chemistry*, *73*(7), 1646–1649. https://doi.org/10.1021/ac001176m

Nam-Koong, H., Schroeder, J. P., Petrick, G., & Schulz, C. (2016). Removal of the off-flavor compounds geosmin and 2-methylisoborneol from recirculating aquaculture system water by ultrasonically induced cavitation. *Aquacultural Engineering*, *70*, 73–80. https://doi.org/10.1016/j.aquaeng.2015.10.005

National Health and Nutrition Examination Survey—An overview | ScienceDirect Topics. (n.d.). Retrieved April 23, 2026, from https://www.sciencedirect.com/topics/agricultural-and-biological-sciences/national-health-and-nutrition-examination-survey

Nematov, D. (2024). Titanium Dioxide and Photocatalysis: A Detailed Overview of the Synthesis, Applications, Challenges, Advances and Prospects for Sustainable Development. *Journal of Modern Green Energy*, *3*, 6. https://doi.org/10.53964/jmge.2024006

Nerenberg, R., Rittmann, B. E., & Soucie, W. J. (2000). Ozone/biofiltration for removing MIB AND GEOSMIN. *Journal AWWA*, *92*(12), 85–95. https://doi.org/10.1002/j.1551-8833.2000.tb09073.x

Oh, H.-S., Lee, C. S., Srivastava, A., Oh, H.-M., & Ahn, C.-Y. (2017). Effects of Environmental Factors on Cyanobacterial Production of Odorous Compounds: Geosmin and 2-Methylisoborneol. *Journal of Microbiology and Biotechnology*, *27*(7), 1316–1323. https://doi.org/10.4014/jmb.1702.02069

Our mission | Earth Sciences New Zealand | NIWA. (n.d.). Retrieved April 24, 2026, from https://niwa.co.nz/our-mission

References

Ouyang, G., & Pawliszyn, J. (2008). A critical review in calibration methods for solid-phase microextraction. *Analytica Chimica Acta*, *627*(2), 184–197. https://doi.org/10.1016/j.aca.2008.08.015

Paulino, R., Tamburic, B., Stuetz, R. M., Zamyadi, A., Crosbie, N., & Henderson, R. K. (2023). Critical review of adsorption and biodegradation mechanisms for removal of biogenic taste and odour compounds in granular and biological activated carbon contactors. *Journal of Water Process Engineering*, *52*, 103518. https://doi.org/10.1016/j.jwpe.2023.103518

Payra, P., & Dutta, P. K. (2004). Zeolites: A Primer. *ChemInform*, *35*(38). https://doi.org/10.1002/chin.200438229

Pelaez, M., Nolan, N. T., Pillai, S. C., Seery, M. K., Falaras, P., Kontos, A. G., Dunlop, P. S. M., Hamilton, J. W. J., Byrne, J. A., O'Shea, K., Entezari, M. H., & Dionysiou, D. D. (2012). A review on the visible light active titanium dioxide photocatalysts for environmental applications. *Applied Catalysis B: Environmental*, *125*, 331–349. https://doi.org/10.1016/j.apcatb.2012.05.036

Peng, J., Wang, Q., Li, Z., Wang, X., Liu, S., Li, Y., Xie, Y., & Li, Y. (2024). Pilot testing and engineering application of O3/H2O2 process for 2-methylisoborneol and geosmin removal in drinking water treatment. *Journal of Water Process Engineering*, *60*, 105140. https://doi.org/10.1016/j.jwpe.2024.105140

Percival, S., Drabsch, P., & Glencross, B. (2008). Determining factors affecting muddy-flavour taint in farmed barramundi, *Lates calcarifer*. *Aquaculture*, *284*(1), 136–143. https://doi.org/10.1016/j.aquaculture.2008.07.056

Persson, F., Heinicke, G., Hedberg, T., Hermansson, M., & Uhl, W. (2007). Removal of Geosmin and MIB by Biofiltration—An Investigation Discriminating Between

Adsorption and Biodegradation. *Environmental Technology*, *28*(1), 95–104. https://doi.org/10.1080/09593332808618770

Petersen, M. A., Hyldig, G., Strobel, B. W., Henriksen, N. H., & Jørgensen, N. O. G. (2011). Chemical and sensory quantification of geosmin and 2-methylisoborneol in rainbow trout (Oncorhynchus mykiss) from recirculated aquacultures in relation to concentrations in basin water. *Journal of Agricultural and Food Chemistry*, *59*(23), 12561–12568. https://doi.org/10.1021/jf2033494

Polak, E. H., & Provasi, J. (1992). Odor sensitivity to geosmin enantiomers. *Chemical Senses*, *17*(1), 23–26. https://doi.org/10.1093/chemse/17.1.23

Recirculating aquaculture systems | Earth Sciences New Zealand | NIWA. (n.d.). Retrieved April 23, 2026, from https://niwa.co.nz/aquaculture/recirculating-aquaculture-systems

Rega, B., Fournier, N., & Guichard, E. (2003). Solid Phase Microextraction (SPME) of Orange Juice Flavor: Odor Representativeness by Direct Gas Chromatography Olfactometry (D-GC-O). *Journal of Agricultural and Food Chemistry*, *51*(24), 7092–7099. https://doi.org/10.1021/jf034384z

Rosenfeldt, E. J., Melcher, B., & Linden, K. G. (2005). UV and UV/H2O2 treatment of methylisoborneol (MIB) and geosmin in water. *Journal of Water Supply: Research and Technology-Aqua*, *54*(7), 423–434. https://doi.org/10.2166/aqua.2005.0040

Ruben, M. O., Akinsanola, A. B., Okon, M. E., Shitu, T., & Jagunna, I. I. (2025). Emerging challenges in aquaculture: Current perspectives and human health implications. *Veterinary World*, 15–28. https://doi.org/10.14202/vetworld.2025.15-28

References

Ruíz-Baltazar, Á. D. J. (2024). Advancements in nanoparticle-modified zeolites for sustainable water treatment: An interdisciplinary review. *Science of The Total Environment*, *946*, 174373. https://doi.org/10.1016/j.scitotenv.2024.174373

Sarker, P., Pilote, A., Auffret, M., Proulx, É., Villemur, R., Deschamps, M.-H., & Vandenberg, G. (2014). Reducing geosmin off-flavor compounds and waste outputs through dietary phosphorus management in rainbow trout aquaculture. *Aquaculture Environment Interactions*, *6*, 105–117. https://doi.org/10.3354/aei00119

Schrader, K. K., Davidson, J. W., Rimando, A. M., & Summerfelt, S. T. (2010). Evaluation of ozonation on levels of the off-flavor compounds geosmin and 2-methylisoborneol in water and rainbow trout Oncorhynchus mykiss from recirculating aquaculture systems. *Aquacultural Engineering*, *43*(2), 46–50. https://doi.org/10.1016/j.aquaeng.2010.05.003

Schrader, K. K., Davidson, J. W., & Summerfelt, S. T. (2013). Evaluation of the impact of nitrate-nitrogen levels in recirculating aquaculture systems on concentrations of the off-flavor compounds geosmin and 2-methylisoborneol in water and rainbow trout (*Oncorhynchus mykiss*). *Aquacultural Engineering*, *57*, 126–130. https://doi.org/10.1016/j.aquaeng.2013.07.002

(Sesha) Pochiraju, S., Hoppe-Jones, C., Adams, C., & Weinrich, L. (2021). Development and optimization of analytical methods for the detection of 18 taste and odor compounds in drinking water utilities. *Water Research X*, *11*, 100099. https://doi.org/10.1016/j.wroa.2021.100099

Shaw, R., Madan, S., Tiwari, S., & Tiwari, S. K. (2020). Creating Synergy of Microporous Hydrophilic–Organophilic Surfaces in Zeolite@Nano-Titania

Particles for Rapid Removal of Diverse Pollutants in Water. *Advanced Materials Interfaces*, *7*(23), 2001386. https://doi.org/10.1002/admi.202001386

Smith, J. L., Boyer, G. L., & Zimba, P. V. (2008). A review of cyanobacterial odorous and bioactive metabolites: Impacts and management alternatives in aquaculture. *Aquaculture*, *280*(1), 5–20. https://doi.org/10.1016/j.aquaculture.2008.05.007

Srinivasan, R., & Sorial, G. A. (2011). Treatment of taste and odor causing compounds 2-methyl isoborneol and geosmin in drinking water: A critical review. *Journal of Environmental Sciences*, *23*(1), 1–13. https://doi.org/10.1016/S1001-0742(10)60367-1

Suffet, I. H. (Mel), Khiari, D., & Bruchet, A. (1999). The Drinking Water Taste and Odor Wheel for the Millennium: Beyond Geosmin and 2-Methylisoborneol. *Water Science and Technology*, *40*(6), 1–13. https://doi.org/10.2166/wst.1999.0248

Summerfelt, S. T., & Vinci, B. J. (2008). Better Management Practices for Recirculating Aquaculture Systems. In *Environmental Best Management Practices for Aquaculture* (pp. 389–426). John Wiley & Sons, Ltd. https://doi.org/10.1002/9780813818672.ch10

Tang, S.-Z., Chen, Z.-X., Huang, L., Li, C.-H., Du, N.-N., Ren, J., Qin, D.-L., & Wang, P. (2025). Trace-level analysis of geosmin in aquaculture systems by Headspace SPME-GC-MS/MS. *MethodsX*, *14*, 103364. https://doi.org/10.1016/j.mex.2025.103364

Thomas, E. (2022, August 17). *How to create a Selected Ion Monitoring (SIM) method using Agilent 7000D GC/TQ and GCQQQ001 MassHunter Control Software*. The University of Waikato.

References

Tucker, C. S. (2000). Off-Flavor Problems in Aquaculture. *Reviews in Fisheries Science*, *8*(1), 45–88. https://doi.org/10.1080/10641260091129170

Tuduri, L., Desauziers, V., & Fanlo, J. L. (2002). Dynamic versus static sampling for the quantitative analysis of volatile organic compounds in air with polydimethylsiloxane–Carboxen solid-phase microextraction fibers. *Journal of Chromatography A, ExTech 2001 - Advances in Extraction Technologies*, *963*(1), 49–56. https://doi.org/10.1016/S0021-9673(02)00222-4

Validation of analytical procedures: Text and methodology Q2(R1). (2005). International Council for Harmonisation. https://database.ich.org/sites/default/files/ICH_Q2%28R2%29_Guideline_2023_1130_ErrorCorrection_2025.pdf

Wang, H. (2008). *Analysis of Geosmin and 2-Methylisoborneol (MIB) by Solid Phase Micro Extraction (SPME) and CI-MS-MS using the Varian 240 MS | LCGC International*. Chromatograophy Online. https://www.chromatographyonline.com/view/analysis-geosmin-and-2-methylisoborneol-mib-solid-phase-micro-extraction-spme-and-ci-ms-ms-using-var

Wang, L., Pearce, J., & Zhang, W. (2025). Detection of 2-methylisoborneol and Geosmin in drinking water: History and the current state-of-the-art. *Journal of Environmental Chemical Engineering*, *13*(3), 116834. https://doi.org/10.1016/j.jece.2025.116834

Wang, M., Xu, Y., Xie, Y., Yang, L., & Zhang, J. (2025). A Review of the Sources, Monitoring, Detection, and Removal of Typical Olfactory Substances Geosmin and 2-Methylisoborneol. *Water*, *17*(8), 1236. https://doi.org/10.3390/w17081236

References

Wang, Q., Zietzschmann, F., Yu, J., Hofman, R., An, W., Yang, M., & Rietveld, L. C. (2020). Projecting competition between 2-methylisoborneol and natural organic matter in adsorption onto activated carbon from ozonated source waters. *Water Research*, *173*, 115574. https://doi.org/10.1016/j.watres.2020.115574

Wee, L. H., Janssens, N., Vercammen, J., Tamaraschi, L., Thomassen, L. C. J., & Martens, J. A. (2015). Stable TiO_2 –USY zeolite composite coatings for efficient adsorptive and photocatalytic elimination of geosmin from water. *Journal of Materials Chemistry A*, *3*(5), 2258–2264. https://doi.org/10.1039/C4TA05941G

Wei, F., He, Y., Qu, X., Xu, Z., Zheng, S., Zhu, D., & Fu, H. (2019). *In situ* fabricated porous carbon coating derived from metal-organic frameworks for highly selective solid-phase microextraction. *Analytica Chimica Acta*, *1078*, 70–77. https://doi.org/10.1016/j.aca.2019.05.061

Yan, J. (2016). *Effect of activated carbon, oxidation and UV treatment on 2-methylisoborneol and geosmin removal from treated water* [The University of Waikato]. https://researchcommons.waikato.ac.nz/server/api/core/bitstreams/e5d701b9-a4c0-45ac-aad4-f59e70f7ef32/content

You, Y.-W. (2012). *Determination of Geosmin and 2- Methylisoborneol in water using Solid Phase Micro Extraction (SPME) and Gas Chromatography Mass Spectrometry (GC/MS*. Agilent. https://www.agilent.com/Library/applications/5991-1031EN.pdf

Young, W. F., Horth, H., Crane, R., Ogden, T., & Arnott, M. (1996). Taste and odour threshold concentrations of potential potable water contaminants. *Water Research*, *30*(2), 331–340. https://doi.org/10.1016/0043-1354(95)00173-5

References

Zhang, S.-Y., Li, G., Wu, H.-B., Liu, X.-G., Yao, Y.-H., Tao, L., & Liu, H. (2011). An integrated recirculating aquaculture system (RAS) for land-based fish farming: The effects on water quality and fish production. *Aquacultural Engineering*, *45*(3), 93–102. https://doi.org/10.1016/j.aquaeng.2011.08.001

Zhao, Y., Wang, T., Li, K., Pan, Y., & Liu, H. (2025). Research progress of analysis and control strategy of geosmin affecting the quality of freshwater fish. *Journal of Fisheries of China*, *48*(7), 079803–079811. https://doi.org/10.11964/jfc.20221013729

Zorzi, V., Bertini, A., Robertson, A., Berardinelli, A., Palmisano, L., & Parrino, F. (2023). The application of advanced oxidation processes including photocatalysis-based ones for the off-flavours removal (GSM and MIB) in recirculating aquaculture systems. *Molecular Catalysis*, *551*, 113616. https://doi.org/10.1016/j.mcat.2023.113616